JAAS

Accepted Manuscript

ROYAL SOCIETY OF CHEMISTRY

www.rsc.org/jaas

Table 1. Statistics obtained by the analysis of a 10 ng/g Nd-Sm solution using an Element XR sector-field ICPMS. A PFA µFlow pneumatic micronebuliser (Elemental Scientific) with a measured uptake rate of 123 µl/min (1.12 l/min sample Ar flow) was operated in the self-aspiration mode and coupled to a cooled cyclonic spray chamber. Nickel skimmer and skimmer cones (H-type, ~cylindrical orifice) were used. RF power was optimised at 1290 W, focus lens voltage - at -1175 V. The guard electrode of the torch was grounded. 300 sweeps were acquired in the low-resolution peak-hopping mode, the dwell time per isotope was set at 20 ms, the settle time - at 1 ms (electric scan). For raw data and calculus, see Electronic Appendix 2. The CeH$^+$/Ce$^+$ ratio was optimised to 0.007 %.

	single sweep					whole signal, estimated				
	^{143}Nd	^{145}Nd	^{146}Nd	^{147}Sm	^{149}Sm	^{143}Nd	^{145}Nd	^{146}Nd	^{147}Sm	^{149}Sm
mean count number per sweep	29845	20363	42016	35363	32514					
total count number (estimated total mean)						8953500	6108900	12604800	10608900	9754200
count number standard deviation ($s(N)$, full)	809	538	1143	958	941	14012	9318	19797	16593	16299
count number standard deviation ($s(N)=\sqrt{N}$, assuming ordinary Poisson statistics)	173	143	205	188	180	2992	2472	3550	3257	3123
Pearson's correlation coefficient (ρ)	0.307	0.285		0.354		same as for single sweeps				
RSD (%), ratio-of-means, eqn 19 (exact f-la valid for any statistics)	3.15	3.21		3.19		0.18	0.19		0.18	
RSD (%), ratio-of-means, eqn 24 (approx. f-la for strong double stochasticity)	3.28	3.32		3.27		0.19	0.19		0.19	
RSD (%), ratio-of-means, eqn 22 (minimum estimate assuming ordinary Poisson statistics)	0.91	0.85		0.77		0.05	0.05		0.04	
RSD (%), mean-of-ratios, eqn 25	3.17	3.22		3.19		0.18	0.19		0.18	
count number variance ($Var(N)$), full	654481	289444	1306449	917764	885481	196344300	86833200	391934700	275329200	265644300
excess variance ($p^2Var(M)$)	624636	269081	1264433	882401	852967	187390800	80724300	379329900	264720300	255890100
ratio of excess standard deviations ($s(M^x)/s(M^y)$) [&]	1.524	0.461		1.017		same as for single sweeps				
count number ratio (N^x/N^y), as measured	1.466	0.485		1.088		idem				
reference ratio for natural isotope abundances	1.47	0.48		1.08		idem				

[&] assuming the same ion transmission efficiency for the isotopes concerned.

Table 2. An implementation of the test of independent parallel sample introduction systems. A 10 ng/g Ba-Ce solution was analysed using an Element XR sector-field ICPMS. Two PFA µFlow pneumatic micronebuliser (Elemental Scientific) with measured uptake rates of 159 and 113 µl/min (0.58 and 0.54 l/min Ar flows, respectively[£]) were operated in the self-aspiration mode and coupled to cyclonic spray chambers. Nickel sampler and skimmer cones (H-type) were used. RF power was optimised at 1230 W, focus lens voltage - at -1201 V. The guard electrode was grounded. 350 sweeps were acquired in the low-resolution peak-hopping mode, the dwell time per isotope was set at 20 ms, the settle time - at 1 ms (electric scan). For raw data and calculus, see Electronic Appendix 7.

	1st nebuliser / spray chamber			2nd nebuliser / spray chamber			1st and 2nd nebulisers / spray chambers running in parallel		
	^{135}Ba	^{137}Ba	^{142}Ce	^{135}Ba	^{137}Ba	^{142}Ce	^{135}Ba	^{137}Ba	^{142}Ce
mean count number per sweep	5736	9867	9566	4066	6973	6803	10071	17248	16768
sum of the 1st and 2nd nebuliser count means							9803	16840	16369
count number standard deviation ($s(N)$, full)	214	349	361	159	251	236	338	610	578
count number standard deviation ($s(N)=\sqrt{N}$, assuming ordinary Poisson statistics)	76	99	98	64	84	82	100	131	129
count number variance ($Var(N)$), full	45787	121470	130118	25275	63099	55487	113932	371909	333674
Poisson variance, assuming ordinary Poisson statistics	5736	9867	9566	4066	6973	6803	10071	17248	16768
excess variance ($p^2Var(M)$), as measured	40051	111603	120552	21208	56126	48684	103862	354661	316906
sum of the 1st and 2nd nebuliser excess variances							61259	167729	169236
excess standard deviation ($ps(M)$), as measured	200.1	334.1	347.2	145.6	236.9	220.6	322.3	595.5	562.9
sum of the 1st and 2nd nebuliser excess standard deviations							345.8	571.0	567.8
excess standard deviation to mean ratio ($s(M^x)/M^x$)[&]	0.035	0.034	0.036	0.036	0.034	0.032	0.032	0.035	0.034
ratio of excess standard deviations ($s(M^{135Ba})/s(M^{137Ba})$)[&]	0.599			0.615			0.541		
count number ratio (N^{135Ba}/N^{137Ba}), as measured	0.581			0.583			0.584		
reference ratio for natural Ba isotope abundances	0.587			0.587			0.587		

[£] using higher argon flow rates per nebuliser results in an excessive total flow through the torch injector; this issue is easy to fix in a modification of this test intended for laser ablation; for pneumatic concentric nebulisers, compromises must unfortunately be made; a prefilming nebuliser capable of working at a low argon backpressure is preferable. [&] assuming the same ion transmission efficiency for ^{135}Ba and ^{137}Ba.

The ICPMS signal as a Poisson process: a review of basic concepts

Alex Ulianov[a],* Othmar Müntener[a] and Urs Schaltegger[b]

[a]Institute of Earth Sciences, University of Lausanne, Géopolis, 1015 Lausanne, Switzerland
[b]Section of Earth and Environmental Sciences, University of Geneva, Rue des Maraîchers 13, 1205 Geneva

Abstract

Understanding the structure of noise associated with a measurement process is interesting theoretically and has practical applications related to the quantification of detection capability, signal uncertainty and dead time. Here, we present and analyse arguments explaining the appearance of the Poisson process in the distribution of count numbers in inductively coupled plasma mass spectrometry (ICPMS) signals. We consider the Poisson distribution as a special case of the binomial distribution constrained by inefficient ion transmission from the ICP ion source to the detector. The universal form of the relevant Poisson process is doubly stochastic: the random nature of count numbers acquired per time unit is defined not only by the probabilistic selection of ions during their transport through the interface and ion channel, but also by fluctuations of the ion contents sampled by the spectrometer from the plasma and, more generally, by fluctuations of the rate of the Poisson process itself. Compared to an ordinary Poisson process, the doubly stochastic Poisson process has an excess variance that increases at higher analyte contents. The excess variance in the uncertainty of ICPMS signals is also known as flicker noise; it is an integral part of the doubly stochastic Poisson process and not a fully individual noise component. We review processes pertinent to its origin and formalisms used to describe it.

Introduction

The Poisson distribution is one of three main probability distributions in science (the other two being the Gaussian and the binomial distributions). It has been recognised for a while that Poisson, or counting, statistics play an important role in the interpretation of the ICPMS signal uncertainty. How do these statistics arise in ICPMS signals? How do they help to understand their structure and uncertainty? Trying to answer these questions, we usually recollect a well-known equation connecting count numbers and their variance. Is there anything else to recollect? Perhaps, with the outcome being not devoid of theoretical elegance and practical importance.

Let us consider an ICP mass spectrometer collecting counts during some predefined time interval T per isotope measurement. Let us assume for simplicity that the spectrometer detection system has a zero dead time, that it is operated in the counting detection regime and that its internal noise (e.g., due to thermionic and field emission from the dynodes of a secondary electron multiplier[1]) is negligible. Let us first imagine that an analyte is supplied to the interface of the mass spectrometer from the ICP ion source at a strictly constant rate [= number of ions supplied per time interval] and the spectrometer ion transmission is constant as well. Still, the observed ion count numbers will vary: our first measurement can yield N_1 counts, second measurement – N_2 counts, etc. (see section '*A binomial derivation of the Poisson process in ICPMS*'). If the number of measurements k is large, the mean value

$$\overline{N} = (N_1 + ... + N_k) / k \qquad (1)$$

is defined with a high precision. One can argue that the probability of obtaining exactly N_i counts as the outcome of a particular measurement is then defined by the law of Poisson characterised by a constant, time independent rate (intensity) I with a mean value of $\overline{N} / T$, and is as follows[1-6]:

$$p(N_i) = \frac{\overline{N}^{N_i} e^{-\overline{N}}}{N_i!} \qquad (2)$$

Besides, the variance

$$Var(N) = \overline{N} \qquad (3)$$

characterises the size of an interval, into which a particular value of N_i falls with some probability (that approaches the confidence interval of a Gauss distribution set at a mean value of $\overline{N}$ and standard deviation of $\sqrt{\overline{N}}$ at higher count numbers). The condition of a constant rate in formulae (1-3) can be relaxed: they are valid for any non-random count rate, where I is a deterministic function of time[2-5].

The obeyance of the counting results above to the Poisson law is important both theoretically and practically. In the field of detection capabilities quantification, at near zero count numbers, it allows applying the mathematical apparatus of tests for the equality of two Poisson means[7-9] to the background noise to get the critical value for detection decision in the 'paired measurements' framework[10]. Similarly, it allows using the cumulative probability of the Poisson distribution to compute the critical value if the background is 'well known'[10]. At higher count numbers, the square root dependence of the Poisson uncertainty from the mean count number enables computing the critical value and the detection limit based on the Poisson-Gauss approximation[10-12]. This powerful methodology, used for a while in radioactivity measurements, is slowly entering into the practice of the ICPMS analysis[13,14].

In the field of signal uncertainty calculations, the square root relationship between count numbers and their uncertainties allows easily calculating the uncertainty of the mean rate for any deterministic, non-transient (constant count rate) as well as transient (count rate is a deterministic function of time) Poisson signal. A derivation commonly used in such calculations is as follows[15-17]:

$$s(I_{ind.\ measurement}) = s\left(N/T\right) = \frac{s(N)}{T} = \frac{\sqrt{\overline{N}}}{T} = \sqrt{\frac{\overline{N}}{T^2}} = \sqrt{\frac{I_{mean}}{T}} \qquad (4)$$

where T is the total, precisely determined acquisition time for an analyte, of which the rate is discussed, and I is the count rate. It is common to use in this equation single measurement based estimates of $\overline{N}$, since the distribution of so-estimated uncertainties is known to be very precise:

$$s(\sqrt{N}) = \frac{\partial(\sqrt{N})}{\partial N} s(N) = \frac{1}{2\sqrt{N}}\sqrt{N} = 1/2 \qquad (5)$$

Finally, the adherence of counting results to the Poisson law with a constant rate allows estimating the detection system dead time (τ) and correcting raw counts according to the familiar formulae[1,6,18]:

$$N_{corrected} = \frac{TN_{measured}}{T - \tau N_{measured}};\ I_{corrected} = \frac{I_{measured}}{1 - \tau I_{measured}} \qquad (6)$$

The relevance of the Poisson process to the description of ICPMS signals has been recognised long ago. The early experience was related to and influenced by the description of noise in ICP atomic emission spectrometry (ICP-AES). Using the Fourier transform of the sequentially acquired intensity vs. time data into the frequency domain[19,20], several noise components were identified, of which the universally occurring were a white noise and a *1/f* noise[21-25]. The white noise, of which the amplitude is frequency independent, is interpreted as the Poisson (shot) noise[26,27]. The *1/f*, or flicker, noise, vanishing at high frequencies, is interpreted as an additional noise component independent of the Poisson noise; despite the same signal is discussed, it was postulated that the variance of the total number of counts N can be given, like a variance of the sum of two independent random variables, as follows[26,27]:

$$Var(N) = Var(Poisson\ term) + Var(1/f\ term) = mean\ count\ number + Var(1/f\ term) \qquad (7)$$

This equation also exists in a sensitivity based notation[28,29] almost forgotten in modern ICP literature. ICP-AES and later ICP-MS studies empirically demonstrated that, upon increasing the analyte concentration (intensity), *Var(1/f)* term increases faster than the Poisson term in the formula above, showing a quadratic dependence on the total number of counts N collected per given time interval[21,25-31].

Below we will show that eqn (7) and relationships between its terms find an elegant explanation in the theory of compound Poisson processes. But before it is necessary to consider why the Poisson counting process appears at all in the ICPMS technique. Representative opinions on this question are as follows: (i) 'as devices registering sums of counted ions, mass spectrometers yield Poisson distributed count numbers *per se (by itself)*'[13]; (ii) 'since MS deals with the detection of ions, it is subject to fundamental noise arising from the particulate nature of matter'[27]; (iii) 'all electron, ion and photon fluxes are subject to random variations in their rates described by Poisson statistics, for which the standard deviation of N counts received will be $\sqrt{N}$'[32]. Sadly, the ICPMS ion flow deviates from the last part of statement (iii), demonstrating an excess variance according to eqn (7). Besides, the opinions above are somewhat declarative. They can be developed in two directions, either by stating that the Poisson distribution appears in the ICPMS by heaven's decree, or by deriving it based on the binomial distribution and construction of ICP mass spectrometer - a perspective reviewed in this work.

It is worth noting that, despite the declarative understanding of the origin and mathematical form of the Poisson process currently prevailing in ICPMS, a wealth of experimental data regarding the ICPMS signal fluctuations is available in the literature. Perhaps, we deal with a case when 'practical techniques … evolve extensively to provide empirical solutions to real analytical problems before the basic research is completed'[33]. The prime aim of this contribution is to present the theory of the Poisson process in the context of the available data; when required, we present new experimental data.

A binomial derivation of the Poisson process in ICPMS

Let us give a traditional example from the field of telephone statistics, where the Poisson process is often encountered. Let us consider a call centre in a large city. We discuss the number of calls registered by the centre per time interval. We argue that such numbers are Poisson distributed. Why? Each person in the city is characterised by one of two potential states: either (s)he makes a call to the centre during the time interval of interest, or not. The total number of persons is M, the probability that a given person will make a call to the centre is p. What will be the probability of receiving exactly N calls during the dwell time? To answer this question, let us interpret M as the number of Bernoulli trials (making or not making a call). The probability of receiving exactly N calls is then defined by the binomial probability distribution function; generally, it depends on M and p:

$$probability\ (N|M,p)=\frac{M!}{(M-N)!N!}p^{N}(1-p)^{M-N} \quad (8)$$

The variance of the number of calls is as follows: $Var(N)=pM(1-p)$. Let us further suppose that M is very large (large population), while p is very small (how often do we call to a particular call centre?). At these conditions, the formula above can be reorganised. The corresponding derivation is classical. To preserve this text consistency, we present it here following a notation from Barrett and Myers[5] and Rainwater and Wu[6]. Substituting $p=\overline{N}/M$ yields:

$$probability\ (N|M,p)=\left[\frac{M(M-1)...(M-N+1)}{M^{N}}\left(1-\frac{\overline{N}}{M}\right)^{-N}\right]\left(1-\frac{\overline{N}}{M}\right)^{M}\frac{\overline{N}^{N}}{N!} \quad (9)$$

At $M\to+\infty$ and $\frac{\overline{N}}{M}=p\to 0$, the term in square brackets limits to 1. Besides,

$\lim_{M\to+\infty}\left(1-\frac{\overline{N}}{M}\right)^{M}=e^{-\overline{N}}$. Hence,

$$\lim_{M\to+\infty\ p\to 0}\left[probability\ (N|M,p)\right]=\frac{\overline{N}^{N}e^{-\overline{N}}}{N!} \quad (10)$$

i.e., the binomial distribution is approximated by a Poisson distribution with a mean of $\overline{N}=pM$ = the mean number of calls registered per time interval. The variance is also equal to $\overline{N}(=pM)$, since the (1-p) term in the formula $Var(N)=pM(1-p)$ is close to unity at small p and can be neglected.

Reworking this example in the context of ICPMS analysis is as follows. The call centre is the detector, while the population of call candidates is represented by ions in the torch. Let us first intentionally simplify the picture and assume that a large, constant number of ions M face the sampler orifice per given time interval. Facing the sampler orifice can be interpreted for an ion as facing a Bernoulli trial to be or not to be registered by the detection system. The probability p for each particular ion to get to the detector is very low: the ICP is an ion source operated at atmospheric pressure, as eddy currents maintaining the plasma by resistive heating cannot occur *in vacuo*. To transport ions from such a source inside the spectrometer ion channel, kept under vacuum, the principle of differential pumping[34,35] is used in all modern ICPMS. During the differential pumping, a large fraction of ions is lost between the sampler and the skimmer (in a conventional interface design, according to commonly used estimates, only ~1% of all ions passing through the sampler orifice then enter the skimmer orifice[36-39]). To these losses, incomplete extraction of the ions from the interface and their incomplete transmission inside the ion channel should be added, especially for light ions[27,39] and for ion beams analysed using quadrupole instruments[40] (especially of older designs[41]) and (sector field) instruments operated at a high resolution[40,42]. With older quadrupole ICPMS, only one ion is registered by the detection system for every 10^4-10^6 ions through the skimmer[43,44]; the quest for a more efficient extraction and transmission is still underway[39]. Finally, irrespective of the dead time related losses, the secondary electron multiplier is usually not 100% efficient in registering the arriving ions, as illustrated by the routine practice to optimise it - at the expense of its life time - by increasing inter-dynode voltages[45,46].

Thus, the whole probability p for an ion to get from the torch to the detector and be registered is low: the extreme versatility of the ICP ion source with respect to the sample introduction technique[47,48], connected with its operation at atmospheric pressure, is counterbalanced by an inefficient utilisation of ions obtained from the ICP. At high M and low p, the probabilities to register a particular number N of ion arrivals per time interval are approximated by a Poisson process with a mean of $\overline{N} = pM$. Similar considerations can be given regarding the noise generated inside the detector due to field and thermionic emission (e.g., a number of atoms is potentially subject to thermionic emission from the dynode surface, but the probability for a given atom to yield a free ion is small, at least at room temperature).

Henceforth, we will call p transmission efficiency and will strictly define it as the probability for an ion entering the orifice of the sampler cone to be registered by the detection system, adding a count to the total number of counts collected during an analysis of a given isotope.

In the sense of the above examples, the inefficiency of the ion transmission process in ICPMS and, consequently, the rarity of registered ions compared to the total number of ions generated in the ICP and facing the sampler orifice is the meaning of the statement ‘rarity begets poissonicity’, mentioned in the literature in a variety of forms (e.g., the ‘law of rare events’). A rich collection of further examples illustrating this statement can be found in refs. 2,3,5 and 49. Among these examples, binomial selection of photons emitted in a narrow sector from a spherical or cylindrical light source[5] could be mentioned, especially in the context of optical spectroscopic techniques, including ICP-AES.

An elementary introduction to doubly stochastic Poisson processes

Fluctuating M and p

In the simplified example above, M - the number of ions exposed to the sampler orifice for the whole duration of analysis - is constant: if we replicate the analysis, M remains the same, although the number N of counted ions is generally different from the first analysis. Besides, the transmission efficiency p remains constant from analysis to analysis. Consequently, $\overline{N}$ represents a constant value. A binomial selection from M at small p results in a Poisson distribution, of which the variance is $\overline{N} = pM(1-p) \approx pM$. The corresponding process can be called ordinary Poisson process.

Let us now consider a more general case when M and p randomly change from analysis to analysis. It could be imagined that a subset of N values is acquired at one M and p, an other subset – at an other M and p, etc., after which all subsets are mixed in proportions corresponding to the probability of occurrence of a given product pM (Fig.1). The corresponding process is called doubly stochastic Poisson process[2,5,50], compound or mixed Poisson process[4,49], or Cox process, in honour of its discoverer[51].

The mixing above results in the appearance of an excess variance in the distribution of count numbers that can be described quantitatively. Propagating errors in squares, we obtain:

$$Var(\overline{N}) = Var(pM) = \overline{p}^2 Var(M) + \overline{M}^2 Var(p) + 2\overline{p}\,\overline{M} Cov(p,M) \qquad (11)$$

However, $Var(\overline{N})$ describes the scatter of the mean count numbers $\overline{N}_i = p_i M_i$, while our purpose is to characterise the scatter in N, i.e. in the individual count numbers obtained from the analyses participating in our exercise (Fig. 1). To this purpose, we introduce the following substitution:

$$N = \varepsilon + \overline{N} \qquad (12)$$

where ε represents a Poisson error observed in a particular analysis relative to the mean count number value $\overline{N}$ associated with this analysis.
Assuming that $\overline{N}$ is not very small, we neglect covariance between ε and $\overline{N}$ and obtain:

$$Var(N) = Var(\varepsilon + \overline{N}) = Var(\varepsilon) + Var(\overline{N}) \qquad (13)$$

Let us consider the ε-term of this equation:

$$\begin{aligned} Var(\varepsilon) &= \frac{1}{n}\sum_{i=1}^{n}(\varepsilon_i - \overline{\varepsilon}_i)^2 = \frac{1}{n}\sum_{i=1}^{n}\varepsilon_i^2 = \frac{1}{n}\sum_{i=1}^{n}(N_i - \overline{N}_i)^2 = \frac{k_1}{n}\frac{\sum_{i=1}^{k_1}(N_{1\,i} - \overline{N}_1)^2}{k_1} + \ldots + \frac{k_m}{n}\frac{\sum_{i=1}^{k_m}(N_{m\,i} - \overline{N}_m)^2}{k_m} \\ &= \frac{k_1}{n}\overline{N}_1(1-\overline{p}_1) + \ldots + \frac{k_m}{n}\overline{N}_m(1-\overline{p}_m) = \overline{\overline{N}} - \left[\frac{k_1}{n}\overline{N}_1\overline{p}_1 + \ldots + \frac{k_m}{n}\overline{N}_m\overline{p}_m\right] \approx \overline{\overline{N}} \end{aligned}$$

(14)

Here, k_i is the number of Poisson outcomes scattered around a particular value of $\overline{N}_i$; consequently, $\frac{k_i}{n}$ is the probability to encounter an analysis associated with a particular $\overline{N}_i$ value. $\overline{p}_i$ is the mean transmission efficiency at each $\overline{N}_i$ value. $\overline{\overline{N}}$ is the mean count number obtained by averaging all individual counts collected at the different $\overline{N}_i$ values; hence the sign of double summation to designate it.

Combining eqn (11-14), we obtain:

$$\begin{aligned} Var(N) &= Var(\varepsilon) + \overline{p}^2 Var(M) + \overline{M}^2 Var(p) + 2\overline{p}\,\overline{M} Cov(p,M) \\ &\approx \overline{\overline{N}} + \overline{p}^2 Var(M) + \overline{M}^2 Var(p) + 2\overline{p}\,\overline{M} Cov(p,M) \end{aligned} \qquad (15)$$

The term $\overline{p}^2 Var(M) + \overline{M}^2 Var(p) + 2\overline{p}\,\overline{M} Cov(p,M)$ in the equation above can be called excess variance[5] to emphasize that the variance of a doubly stochastic Poisson process is higher compared to the variance of an ordinary Poisson distribution (cf. eqn 7). More generally, it is correct to think that the excess variance of a doubly stochastic Poisson process just represents variance of the Poisson means constituting this process (see eqn 12,13 and Fig. 1). For an ordinary Poisson process, the mean is fixed and the excess variance is zero.

Fluctuating M, constant p: single isotope

At a constant p, eqn (13,14) can be simplified:

$$Var(\varepsilon) = \frac{1}{n}\sum_{i=1}^{n}(\varepsilon_i - \overline{\varepsilon}_i)^2 = \frac{k_1}{n}\overline{N}_1(1-p) + \ldots + \frac{k_m}{n}\overline{N}_m(1-p) = \overline{\overline{N}}(1-p) \approx \overline{\overline{N}} \qquad (16)$$

$$Var(N) = Var(\varepsilon) + p^2 Var(M) = \overline{\overline{N}}(1-p) + p^2 Var(M) \approx \overline{\overline{N}} + p^2 Var(M) \qquad (17)$$

A derivation for eqn (16) employing integrals as the limiting form of sums can be found in Barrett and Myers[5]. Yet another derivation is given in section '*Fluctuating M, constant p: isotope ratio*' below.

The case of fluctuating *M* and constant *p* has important properties depending on the distribution of *M*. If, as a special case, it is Poissonian, then changes compared to the situation at a constant *M* are negligible: according to formula (17), the excess term $p^2 Var(M) = p^2\overline{M} = p\overline{\overline{N}}$ and $Var(N) = \overline{\overline{N}}$: a binomial selection from an ordinary Poisson distribution results in an ordinary Poisson distribution, a rule known as binomial selection theorem[5]. On increasing *Var(M)* further the excess variance term becomes more important. Let us consider an arbitrary example where a Poisson mean of 10^6 counts is obtained and the count number variance amounts to $2\text{x}10^6$ counts: this is twice as large as the variance predicted by the ordinary Poison statistics. Let us set p at 0.01%. Based on formula (17), we obtain:

$$\begin{aligned} &Var(N) = 2\times10^6 \approx 10^6 + (10^{-4})^2 Var(M) \Rightarrow Var(M) \approx 10^{14};\ s(M) \approx 10^7; \\ &\overline{M} = \overline{\overline{N}}/p = 10^6/10^{-4} = 10^{10};\ RSD\%(M) \approx \left[10^7/10^{10}\right]\times 100 = 0.1\% \end{aligned} \qquad (18)$$

It is instructive to compare this result with values obtained under the assumption that *M* is ordinary Poisson distributed, assuming that $\overline{\overline{N}}$ and *p* remain the same as in the example above:

$$Var(M) \approx \overline{M} = \overline{\overline{N}} / p = 10^6 / 10^{-4} = 10^{10};\; s(M) \approx 10^5;$$
$$RSD\%(M) \approx (10^5 / 10^{10}) \times 100 = 0.001\%;\; \overline{\overline{N}} = Var(N) = 10^6 \times 0.9999 + (10^{-4})^2 10^{10} = 10^6 \qquad (19)$$

Calculations (18,19) show that, for this particular setup, a twofold increase in the variance of count numbers collected, or otherwise a 1.4 times increase in their standard deviation, is caused by a 100-fold increase of the relative standard deviation of the number of ions in the primary ion population [*RSD%(M)*] - from *0.001* to *0.1%*. Still, even at *RSD%(M)*=0.1% the distribution of *M* remains rather precise: there is no need to have a very large scatter in *M* to observe consequences for *Var(N)*.

If both *M* and *p* are constant, formulae (15-17) converge to the variance formula for an ordinary binomial distribution: $Var(N) = \overline{N}(1-p)$, and further to the Poisson expression $Var(N) = \overline{N}$ by omitting the (1-*p*) term at small *p*.

Fluctuating M, constant p: isotope ratio

In applications, quantification of ICP signals usually requires handling count number (intensity) ratios and not only the individual count numbers[17,27,52-58]. The corresponding Poissonian formalism is briefly discussed below. First, let us generalise formula (17) using the property of bilinearity of covariance:

$$Cov(N^x, N^y) = \sum_{i=1}^{n} \frac{(N_i^x - \overline{\overline{N}}^x)(N_i^y - \overline{\overline{N}}^y)}{n} = \sum_{i=1}^{n} \frac{(\varepsilon_i^x + p^x M_i^x - p^x \overline{M}^x)(\varepsilon_i^y + p^y M_i^y - p^y \overline{M}^y)}{n}$$
$$= p^x p^y \sum_{i=1}^{n} \frac{(M_i^x - \overline{M}^x)(M_i^y - \overline{M}^y)}{n} + \sum_{i=1}^{n} \frac{\varepsilon_i^x \varepsilon_i^y}{n} + p^y \sum_{i=1}^{n} \frac{\varepsilon_i^x (M_i^y - \overline{M}^y)}{n} + p^x \sum_{i=1}^{n} \frac{\varepsilon_i^y (M_i^x - \overline{M}^x)}{n} \qquad (20)$$

Here, N^x and N^y are count numbers for isotopes *x* and *y* recorded by ICPMS, M^x and M^y are numbers of ions aspirated by the sampler orifice, p^x and p^y are transmission efficiencies, and ε□□□□□□ε^y are Poisson errors defined according to eqn (12,13). Since the mathematical expectation of a product of two independent random variables is equal to the product of their mathematical expectations, two last terms in eqn (20) equal zero. The second term also equals zero, if *x* and *y* are two different isotopes with independent Poisson errors in their count numbers; otherwise it is equal to $\overline{\overline{N}}(1-p)$ (eqn 16). We obtain:

$$Var(N) = Cov(N, N) = p^2 Var(M) + \overline{\overline{N}}(1-p) \;\Big|\, x = y \qquad (21a)$$

$$Cov(N^x, N^y) = p^x p^y \sum_{i=1}^{n} \frac{(M_i^x - \overline{M}^x)(M_i^y - \overline{M}^y)}{n} = p^x p^y Cov(M^x, M^y) \;\Big|\, x \neq y \qquad (21b)$$

Formula (21a), derived under the condition that *x* and *y* represent the same isotope, is identical to (17). Formula (21b), derived under the condition that *x* and *y* are two different isotopes, establishes correlation properties of the observed signal and of the ion population in the ICP ion source. At constant transmission efficiencies, a correlation in the source implies a correlation in the signal, and vice versa. The presence of such a correlation is desirable, as it reduces isotope ratio uncertainty[52-56]:

$$Var\left(\frac{N^x}{N^y}\right) = \left(\frac{1}{\overline{\overline{N}}^y}\right)^2 Var(N^x) + \frac{(\overline{\overline{N}}^x)^2}{(\overline{\overline{N}}^y)^4} Var(N^y) - 2\left(\frac{1}{\overline{\overline{N}}^y}\right)\left(\frac{\overline{\overline{N}}^x}{(\overline{\overline{N}}^y)^2}\right) Cov(N^x, N^y)$$
$$= \left(\frac{1}{\overline{\overline{N}}^y}\right)^2 Var(N^x) + \frac{(\overline{\overline{N}}^x)^2}{(\overline{\overline{N}}^y)^4} Var(N^y) - 2\left(\frac{1}{\overline{\overline{N}}^y}\right)\left(\frac{\overline{\overline{N}}^x}{(\overline{\overline{N}}^y)^2}\right) p^x p^y Cov(M^x, M^y) \qquad (22)$$

It is interesting to consider formula (22) as a function of the Pearson's correlation coefficient

$$\rho(M^x, M^y) = \frac{Cov(M^x, M^y)}{\left[Var(M^x) Var(M^y)\right]^{1/2}} \in [-1; +1] \qquad (23)$$

Introducing the correlation coefficient in eqn (22) results in an elementary but bulky derivation given in Electronic Appendix 1. This derivation can be reduced at the condition that standard deviation of *M* is proportional to *M* (*s(M)/M=Const*, see section '*Fluctuating M, sample introduction process'* and refs. 25-31 regarding the validity of this condition), yielding the following formula:

$$RSD\%\left(\frac{N^x}{N^y}\right)=\left[\frac{1}{\overline{\overline{N}}^x}+\frac{1}{\overline{\overline{N}}^y}+2\left[1-\rho(M^x,M^y)\right]\frac{s(M^x)}{\overline{M}^x}\frac{s(M^y)}{\overline{M}^y}\right]^{1/2}\times 100 \qquad (24)$$

In two cases - (i) primary ion populations fluctuate and perfectly correlate, simultaneously increasing or decreasing by the same fraction from analysis to analysis [$\rho(M^x,M^y)=1$] or (ii) primary ion populations are constant [$s(M^x),s(M^y)=0$], which corresponds to the ordinary Poisson process with variance equal to mean count number - this equation can be truncated and given in a more familiar form:

$$RSD\%\left(\frac{N^x}{N^y}\right)=\left[\frac{1}{N^x}+\frac{1}{N^y}\right]^{1/2}\times 100 \qquad (25)$$

Eqn (25) allows for a simple derivation based on the ordinary Poisson statistics only[27] and is often mentioned in the literature[27,57,58]. The coincidence between (i) and (ii) has a rigorous explanation: for perfectly correlating primary populations M^x and M^y, the excess variances of the individual isotope count numbers and the covariance term in eqn (19) cancel each other (see Electronic Appendix 1). The precision of isotope ratio analyses obtained at these conditions is limited, like for the ordinary Poisson distribution, by count numbers N^x and N^y. In all other cases, which include fluctuating primary populations that correlate only partly [$\rho(M^x,M^y)<1$], the relative standard deviation defined by the general equation (24) is higher compared to (25); in other words, the covariance term in eqn (19) decreases and the ratio uncertainty increases. Eqn (25) yields a minimum possible uncertainty in these cases. Strongly correlated signals are known to be the domain of multi-collector (MC-) ICPMS[52]. For count numbers in the order of 10^8, eqn (24,25) yield a minimum $RSD(N^x/N^y)$ of 0.005-0.02%, which falls within the range of isotope ratio uncertainties typically quoted for MC-ICPMS instruments[27,57,58].

Corroborating eqn (24) experimentally is hampered by the need to know the statistics of *M* that are not directly observable. For strong signals, simple approximations can still be made. Owing to the *s(M)~M* dependence, the excess variance can be the dominating variance component of such signals[28,29]:

$$Var(N)=Var(\varepsilon)+Var(\overline{N})=\overline{\overline{N}}+p^2Var(M)\approx p^2Var(M)=Var(\overline{N})\;\Big|\;p^2Var(M)>>\overline{\overline{N}} \qquad (26)$$

Combining eqn (24) and (26), we obtain (see Electronic Appendix 1):

$$RSD\%\left(\frac{N^x}{N^y}\right)=\left[\frac{1}{\overline{\overline{N}}^x}+\frac{1}{\overline{\overline{N}}^y}+2\left[1-\rho(N^x,N^y)\right]\frac{s(N^x)}{\overline{\overline{N}}^x}\frac{s(N^y)}{\overline{\overline{N}}^y}\right]^{1/2}\times 100 \qquad (27)$$

A practical comparison of count number relative standard deviations obtained from eqn (27) and (22) shows a good match. For example, measuring the ^{143}Nd/^{145}Nd count number ratio in the solution nebulisation regime at low resolution using an Element XR sector-field ICPMS, we obtained *RSDs* of 0.18 and 0.19%, respectively (see Table 1 for further details and examples, and Electronic Appendix 2 for raw data and calculus). These values also agree with uncertainty values obtained from the mean-of-ratios definition of the isotope ratio for a time-resolved signal[17,54-56] (Table 1, Electronic Appendix 2):

$$RSD\%\left(\frac{N^x}{N^y}\right)=\frac{s\left(\frac{N^x}{N^y}\right)_{ind.\ sweep}}{\sqrt{n_{sweeps}}\left(\frac{N^x}{N^y}\right)_{mean}}\times 100,\ \text{where}\ \left(\frac{N^x}{N^y}\right)_{mean}=\frac{\sum_{i=1}^{n_{sweeps}}\left(\frac{N^x}{N^y}\right)_{i\ ind.\ sweep}}{n_{sweeps}} \qquad (28)$$

Comparing ratio-of-means and mean-of-ratios uncertainties (eqn 22,27 vs. 28) is generally justified, at least at high count numbers (see refs. 54-56 and 59, as well as Electronic Appendix 3).

Noteworthy, a good match between the estimated $s(M^x)/s(M^y)$ ratio and the reference ratio of these isotopes supports the assumption *s(M)~M* underlying eqn (24,27) (Table 1). At this point, an elementary mathematical description of fluctuations in ion transmission efficiency and primary ion population in ICPMS signals is provided and a discussion of the sources of such fluctuations is due.

Sources of double stochasticity in ICPMS: experimental constraints

Fluctuations of ion transmission efficiency (*p*) and primary ion population in the torch (*M*) are two general sources of double stochasticity. In the existing ICP literature, their role has never been formalised and described theoretically using the mathematical apparatus of binomial selection or more advanced methods related to the mathematical description of double stochasticity (see section '*Double stochasticity and fluctuations of the rate*'). Still, experimentally their role has been recognised, (often) thoroughly described and much discussed, in the context of sample introduction by solution nebulisation especially; below we will refer to the corresponding literature when appropriate.

Fluctuating p?

In the *p,M*-convention used in this text, fluctuations in *p* depend on the performance of the spectrometer ion channel and on the performance of the sampler to skimmer ion transfer; the latter possibility will be reviewed in a subsequent section, along with other processes related to the analyte transfer through the ICP and interface. Here, we consider the ion channel only. Electric (magnetic) fields inside the channel should not be the subject of *random* changes during a measurement (should have a good repeatability between measurements); otherwise, the analyst is confronted with the statistics of *p*.

The possibility of such fluctuations and their role in compromising the precision of ICPMS data, especially when using early quadrupole ICPMS instruments operated in the peak-hopping mode, has been mentioned long ago [e.g., ref. 60]. This issue depends on the instrument and its mode of operation. Compromised isotope ratio uncertainties obtained at higher resolutions on sector-field instruments are sometimes also ascribed to this issue: narrow peaks observed at such conditions and scanned in the peak hopping regime require the highest mass calibration stability to avoid fluctuations in *p*[58]. Of course, ion transmission losses at a high resolution and, consequently, a reduction in the total number of counts collected per analysis are an additional explanation to these uncertainties (cf. eqn 24,25). High-resolution peak hopping analysis is unlikely a widespread practice in modern ICPMS. Low resolution peaks are wider and characterised by parabolic (quadrupole MS) or flat top trapezoidal (well maintained and tuned sector field MS) geometry that reduces the possibility of transmission efficiency fluctuations in the peak hopping regime. This feature helps stabilising the ion transmission efficiency and is recognised in the literature as one of key advantages of low resolution sector field ICPMS for high precision isotope ratio determinations[40,57,58,61]. Still, before deriving more definite conclusions regarding the role of fluctuations in *p*, the latter should be separated from fluctuations in *M*.

The role of fluctuations in *p* can be separately evaluated using a stable and sufficiently strong ion emitter placed at the beginning of the ion channel, which basically requires no sample introduction system to be interfaced to the ICPMS and minimises the role of random processes in the ICP torch. One such emitter that operates without modification to the spectrometer construction represents sampler and skimmer cones contaminated with lithium during the LA-ICPMS analysis of lithium tetraborate glass beads[62]. The associated pollution of the instrument belongs to canonical examples of contamination in ICPMS[63]. The cones seem to be the main source of this pollution: replacing the sampler and skimmer cones of our Element XR ICPMS reduces the ^{7}Li background intensity from c. 3-5x10^{5} to ~4x10^{3} cps in the laser ablation regime; cleaning the ablation cell and the torch and replacing the tubing further reduces these values down to ~2x10^{3} cps; the extraction lens was not replaced neither cleaned. Noteworthy, the role of the sampler in the lithium contamination budget is relatively insignificant compared to the skimmer; according to our experience, a contaminated skimmer accounts for more than 90% of the total background of lithium (few ions derived from the inner surface of the sampler orifice at the outermost boundary of the ion beam then pass through the skimmer).

We mounted contaminated sampler and skimmer cones on an Element XR otherwise cleaned as described above, and collected ^{7}Li background intensities using two different protocols (Fig. 2). Then, we replaced the both cones with uncontaminated ones and, without changing the tuning of the spectrometer, obtained signals of similar intensity by raster laser ablation of the NIST SRM 612 standard, which represent a soda-lime-silica glass doped with a range of trace elements, including lithium.

Sweep counts collected in the experiments with the contaminated cones closely follow the ordinary Poisson statistics. Sweep counts collected in the laser ablation experiments show uncertainties that are ~ 3 times higher than the uncertainties predicted by the ordinary Poisson distribution (Fig. 2). Although such results can be instrument dependent and, perhaps, less straightforward if very short mass discriminator settle times are applied, currently they do not allow suspecting that, for low-resolution work using modern ICP mass spectrometers, p perceivably fluctuates. Neither can this be suspected based on the main body of literature data acquired using modern ICPMS instruments.

Fluctuating M, sample introduction process?

The role of the sample introduction process in fluctuations of ICP signals was noticed in a number of studies. As early as 1980, Myers and Tracy demonstrated that the relative standard deviation of the carbon emission signal at 247.9 nm increases by a factor of ten if the sample is introduced in the ICP as an aerosol (sugar in water), compared to a gaseous mixture of carbon dioxide and argon[52,64]. They detected a strong correlation between the fluctuations of laser light scattered from the sample aerosol and simultaneously recorded emission signal, and noted that 'fluctuations in analyte emission are directly related to fluctuations in aerosol density', while the plasma itself 'is a very stable emission source'[52,65]. In the late 1980's, Antanavičius and co-workers studied ICP-AES signals for gaseous samples and aerosols obtained by solution nebulisation and injection of metal oxide powders in the ICP[66-68]. It was shown that the power spectral density of low frequency (flicker) noise obtained for aerosols increases by an order of magnitude compared to gaseous samples. Similar data (for helium ICP) were obtained by Montaser and co-workers[69]. Besides, ICP-AES signal fluctuations due to the passage of the individual droplets through the ICP were documented; besides, the role of the droplet desolvation process in the signal fluctuations was noticed[70,71]. Research from the 1990's, including papers by Olesik[71-73], Houk[74,75] and co-workers, proved that such fluctuations also occur in ICPMS signals and focussed on a detailed characterisation of the behaviour of droplet aerosols in the ICP, followed by studies of particles obtained by laser ablation in the 2000's[76-81]. Based on the investigation of ICPMS signals resolved on a tens of microsecond time scale that allowed detecting strong intensity peaks and dips connected with the passage of large individual droplets through the ICP, Hobbs and Olesik concluded: 'the behaviour of ICPMS signals is consistent with changes in ion number density in the plasma', and 'the sample introduction process is typically the main source of flicker noise in ICP spectrometry'[71]. An understanding was reached[52,64-73,82] that processes related to the introduction of aerosols in the ICP are essential in the appearance of 'what may be termed the ion distribution noise… caused by the inhomogeneous spatial distribution of analyte ions in the central channel of the plasma which carries the sample aerosol…'[83]. Also, there is a consensus that introducing a gaseous sample in the ICP, compared to the nebulisation of solutions, strongly reduces the excess variance of ICP-AES signals[52,64,66-69], confirming that the ICP is indeed a 'stable emission source'[52] (admittedly, nebulisers used in those studies were likely noisier than modern micronebulisers, making nebulisation uncertainties worse than they could be). Beyond solution nebulisation and laser ablation ICPMS, important data regarding the heterogeneity of the analyte spatial distribution can be found in the literature of atomic absorption spectrometry[84] and electrothermal vaporisation - ICPMS[85].

One could conclude that, for a sample introduction system supplying the analyte at a randomly changing rate because it 'produces noisy aerosols'[52,64-83,85,86], the statistics of M is essentially the statistics of this rate. How to model these statistics? ICP studies[69-75] show that the arrival of droplets in the ICP is a random process and emphasize the role of larger drop and particle sizes in signal fluctuations. It is also worth noting that some of the most precise single collector ICPMS data were acquired using tandem spray chambers especially efficient in removing large droplets[86-88]. Droplet (particle) transport processes are quantitatively complex, as are desolvation / vaporisation of larger droplets and particles in the ICP (given their potential to leave residues and influence the surrounding plasma properties[72-75]). Simplified statistical conclusions describing the role of drop size for the precision of ICPMS signals can still be given. Let us consider a solution nebulisation setup including a pneumatic nebuliser coupled to a double pass or cyclonic spray chamber[33,82,86]. The nebuliser produces tens, possibly hundreds of millions of droplets per second that enter the spray chamber with a velocity of several tens of meters per second[86]. The droplet size distribution is a key characteristic of the nebuliser[82,86,89]; however, to simplify the analysis, we will assume that the nebuliser is mono-dispersive (i.e., it produces droplets of the same size), that the number of droplets produced by the nebuliser per analysis is constant and that droplet alteration (evaporation, fragmentation, agglomeration) can be neglected. A significant part of the droplets is lost *en route* to the torch: in conventional setups run at a flow rate of 0.5-1.5 mL/min, gravitational settling, losses related to gas turbulences and inertial impact losses on the walls of the spray chamber reach 96-98% and more[82,86]. Let us define M^* as the total number of analyte atoms (dissolved ions) reaching the ICP in the form of droplets per analysis (per time interval), N^* as the total number of droplets reaching the ICP per analysis, p^* as droplet transport efficiency, or probability for a single droplet to pass through the spray chamber and reach the ICP, c^* as the number of analyte atoms (dissolved ions) in a droplet, and $\overline{M}^*$, $\overline{N}^*$ and $\overline{c}^*$ as the mean values of these parameters, respectively. We obtain:

$$M^* = \overline{c}^* N^* ;\ Var(M^*) = (\overline{c}^*)^2 Var(N^*) + (\overline{N}^*)^2 Var(\overline{c}^*) \qquad (29)$$

Using eqn (29) requires the individual variance terms to be determined. As N^* results from a binomial selection during droplet transportation to the ICP, we have:

$$Var(N^*) = \overline{N}^*(1-p^*) \qquad (30)$$

Explaining $Var(\overline{c}^*)$ might require referencing to classical literature of statistical physics to show that, in the strict sense, c^* and $\overline{c}^*$ are random parameters. Landau and Lifshitz[90] introduce the Poisson distribution as a distribution of gas molecule numbers in a small sub-volume of a main gas volume. As the number of molecules in the main volume is large and the probability for each molecule to occur in a small sub-volume of the system is small, the arising distribution is Poissonian (for two-dimensional examples of this kind, see refs. 3,91). Similarly, for the distribution of analyte particles in small droplets formed from a main volume of solution we obtain:

$$Var(\overline{c}^*) = Var(c^*)/\overline{N}^* = \overline{c}^*/\overline{N}^* \qquad (31)$$

Combining eqn (29-31) yields:

$$Var(M^*) = (\overline{c}^*)^2\overline{N}^*(1-p^*) + \overline{c}^*\overline{N}^* = \overline{M}^*\overline{c}^*(1-p^*) + \overline{M}^* \qquad (32)$$

Thus, inefficient pneumatic nebulisers indeed produce noisy tertiary aerosols, of which the noise only increases compared to eqn (32), provided various ‘non-idealities’ – renebulisation[86], (possibly) turbulences at the exit of the nebuliser[86], argon backpressure and uptake rate instabilities[92] - are considered.

According to eqn (32), the dependence between the analyte concentration and the variance of the primary ion population is almost exactly quadratic in a wide range of analyte contents (except for very low contents), well in accord with empirical observations[25-31]. At the same time, for a given M^*, increasing the number of droplets at the expense of the number of analyte atoms per droplet results in a linear decrease of *Var*(M^*) - which seems to be one of several reasons explaining the desire of the ICP community to reduce the size of droplets produced by solution nebulisation[82,86]. For a gaseous sample as a limiting case of aerosol ($c^* = 1,\ p^* = 1$), eqn (32) degenerates to $Var(M^*) = \overline{M}^*$ and the excess variance vanishes, provided the sample introduction process is its only source.

Still, the extent of influence of the analyte density fluctuations due to the droplet selection (eqn 32) on the signal uncertainty should not be overestimated. For example, for droplets with a diameter of 5 µm containing 1.22 n□/g of ^{143}Nd [=10 ng/g of Nd], for a droplet transport efficiency p^* close to zero and a mass spectrometer ion transmission efficiency p of 0.01%, the calculated excess variance amounts to 3.4% of the total number N of counted ions (i.e., of the ‘ordinary’ Poisson variance). For 10 µm droplets, it increases to 26.9%, which is still a moderate value (see Electronic Appendix 5). At the same time, solution nebulisation ICPMS signals roughly corresponding to the above setup show a marked excess variance (e.g., Table 1). Are there some other factors beyond the random analyte supply by the sample introduction system involved in the generation of the excess noise of ICPMS signals?

Here, we propose a test helping to estimate the relative contribution of the randomly changing sample introduction rate to the signal uncertainty. This test could be called *test of independent parallel sample introduction systems*; it is similar to the dual nebuliser test of Olesik and co-workers[70], but adapted for a mass spectrometer that does not allow a (quasi-) simultaneous data acquisition. Two nebuliser-spray chamber setups, possibly but not necessarily identical, are interfaced to the ICP torch injector through an Y-type connector (Fig. 3). Three signals are recorded. The first signal is obtained by aspirating a sample solution through the first nebuliser and spray chamber; in the meanwhile, the second nebuliser aspirates a high-purity nitric acid solution used for the dilution of the sample. To acquire the second signal, the roles of the nebulisers are reversed: the first nebuliser aspirates the high-purity nitric acid solution, while the second nebuliser – the sample. The third signal is obtained by the simultaneous aspiration of the sample using both nebulisers with their respective spray chambers. The purpose of the test is to compare the excess variances obtained from the above signals [$Var(M_1)$, $Var(M_2)$ and $Var(M_1+M_2)$, respectively]. The general expression for the variance of the sum of two random but (possibly) correlating variables is as follows:

$$Var(M_1+M_2)=Var(M_1)+Var(M_2)+2Cov(M_1,M_2) \qquad (33)$$

If these variables fluctuate independently of each other, then the covariance term of this equation vanishes and the relationship simplifies:

$$Var(M_1+M_2)=Var(M_1)+Var(M_2) \qquad (34)$$

If these variables are perfectly correlated, simultaneously increasing or decreasing by the same fraction in response to a common noise-generating process, then $\rho(M_1,M_2)=1$ and, consequently,

$$Cov(M_1,M_2)=\left[Var(M_1)Var(M_2)\right]^{1/2}=s(M_1)s(M_2) \qquad (35)$$

Therefore, in the case of a perfect correlation, eqn (30) can be rewritten as follows:

$$s(M_1+M_2)=s(M_1)+s(M_2) \qquad (36)$$

Eqn (34) and (36) describe two limiting cases. If we assume the rest of the measurement process to be a stable system introducing no further fluctuations in the primary ion statistics, then M_1 and M_2 fluctuations reflect the (in)stability of their respective sample introduction systems; since these systems are independent, there should be no correlation between their outputs [$Cov(M_1,M_2)=0$, eqn (34) hold true]. If we assume that the both sample introduction systems are stable and the source(s) of fluctuations in the primary ion statistics (and, more generally, sources of the excess variance of ICPMS signals) are hidden somewhere deeper in the ICPMS chain, then M_1 and M_2 have to respond to these fluctuations simultaneously and strongly co-vary [hence, eqn (36) holds true].

An implementation of this test is detailed in Table 2. Two pneumatic self-aspirating PFA μFlow micronebulisers (Elemental Scientific) with uptake rates of 159 and 113 μL/min interfaced to cyclonic spray chambers were employed. These nebulisers produce fine aerosols with a good transport efficiency; courtesy of the liquid prefilming in the nozzle, they operate at a low backpressure and allow using moderate argon flow rates[86,93]. For all isotopes studied (^{135}Ba, ^{137}Ba, ^{142}Ce; see Table 2), eqn (36) described the uncertainty budget of the test much better than eqn (34). Besides, the $s(M)$~M law was again confirmed, which highlights the close relationships between this law and the presence of internal correlation in the signal (for a discussion, see Electronic Appendix 6). The test is not very precise, however (as the $s(M_1)$, $s(M_2)$ and $s(M_1+M_2)$ values obtained from individual analyses are statistical estimates of uncertainty, these values have their own uncertainties; hence a scatter in the correlation coefficients computed from the covariance values derived from eqn (33), see Electronic Appendix 7).

Albeit specific to a given instrumentation, results of this test show that the randomised analyte supply from the sample introduction system is only one and, in the present case, not the main source of fluctuations in the primary ion statistics. We conclude that the evidence for noise associated with the aerosol introduction in the ICP is (i) generally unquestionable and well documented, although (ii) such noise cannot be the only reason to explain the appearance of excess uncertainty in ICPMS signals.

Fluctuating M, transfer of analyte inside the ICP and from the ICP to the mass spectrometer?

The result of the above test agrees with old ICP-AES data of Olesik and co-workers that demonstrated a good correlation between Ba and Ca emission signals at 8 mm above the load coil, despite each of these elements was supplied to the ICP through its own nebuliser / spray chamber[70]. This correlation vanished at 19 mm above the coil. The phenomenon was explained by the fluctuation of the plasma temperature caused by the desolvation of the droplets flying through the ICP; elements contained in the different droplets respond to such fluctuations similarly[70,71]. The relevant quantitative model remains to be constructed; still, it seems likely that the randomised solution supply to the ICP (as considered in the previous section) is, to some extent, a pre-requisite for the appearance of random noise of this type. Another question immediately arising is whether the random solution supply to the ICP and the desolvation-related fluctuations are the only sources of the excess variance of ICPMS signals.

It is appealing to consider this question in the context of data for gaseous samples, which - theoretically, as well as based on the ICP-AES data mentioned at the beginning of the previous section - ensure a more stable sample introduction process in the ICP and the absence of desolvation related fluctuations. Contrary to the ICP-AES archives, ICPMS experience does not contain fully compelling evidence in this direction. Gray and co-workers compared the precision of the ^{107}Ag/^{109}Ag ratio obtained by solution nebulisation with the precision of the ^{132}Xe/^{129}Xe ratio obtained by the addition of xenon to the sample gas[83]. Using a conventional sampler-skimmer interface, they obtained higher ^{107}Ag/^{109}Ag ratio uncertainties than expected from the ordinary Poisson distribution. On the contrary, the ^{132}Xe/^{129}Xe ratio uncertainty was as predicted by the ordinary Poisson distribution (cf. eqn (25) and (28), see ref. 83 for details). The corresponding xenon signals, integrated over ~70 channels with a dwell time of 100 µs per channel, reached $3.14\text{x}10^6$ cps[82]. Provided the integrated intensity is obtained by summation of the individual channel intensities, this amounts to 314 counts per peak. Given the quadratic dependence of the excess variance on signal intensity, the excess variance could vanish at these conditions (see refs. 17,77 for examples). Newer ICPMS experiments, albeit not specifically designed to handle uncertainties, do not reveal a large excess variance in ^{129}Xe fluctuations at intensities in the order of $1.5\text{-}1.6\text{x}10^5$ cps (1500-1600 counts / sweep collected in the peak hopping mode); a precise estimation of the variance from the presented data is, however, difficult.

Uncertainty data of varying level of detail can also be found in the rich, but metrologically non-specific literature of chemical vapour generation ICPMS. Some of such data show large excess uncertainties[95-97]. A conclusive analysis of their origin appears to be lacking. As the vapour generation devices can be quite complicated[98,99], the stability of the sample introduction process is sometimes questioned (e.g., pulsation of selenium hydride flow to the ICP[95], carbon monoxide flow rate fluctuations during nickel carbonyl generation[100],). In the ultimate case, solution nebulisation uncertainties are considered as the ‘gold standard’ for comparison with vapour generation ICPMS data![97]

Our ICPMS data on the introduction of xenon- and neon-argon mixtures in the ICP do show excess variance, especially at higher concentrations (Table 3, Electronic Appendix 8). Admittedly, these data are rather precise (compared to average solution nebulisation or laser ablation ICPMS data); but, compared to ordinary Poisson distributed data, they are over-dispersed. Combined with the lithium contaminated interface and the parallel sample introduction system tests described in the previous sections, this allows thinking that processes related to the analyte transfer through the ICP and analyte extraction from the ICP destabilise the primary ion population, thus broadening the statistics of M.

Firstly, there is some evidence that the statistics of M is related to turbulence inside the ICP: using a laminar flow torch seems to reduce the *1/f* noise component (although it is more efficient in the reduction of discrete frequency components)[22,23,101,102]. Laminar torches are one of the oldest inventions in ICP spectrometry[103]. However, commercial torches used in modern ICPMS are all designed for tangential auxiliary and cool gas injection[104]; thus, it is not excluded that ‘the rotating gas destabilises the injector channel’[23]. Besides, irrespective of the torch design, the ICP flame is thermally heterogeneous[105]: Faraday’s and Lenz’s laws constrain less change in the magnetic flux in the axial zone of the torch, which is consequently less heated by the eddy currents, a phenomenon called skin effect and found in any inductive heater. The injection of a sample aerosol carried by a relatively high velocity sample gas flow can further decrease its temperature. The intermediate, induction zone of the ICP flame is hotter. A turbulent mixing becomes possible inside the torch because of the density difference in the different plasma zones. Precisely evaluating the extent of influence of these processes is difficult at this time; overestimating their role appears inconsistent with the ICP-AES gas injection experiments mentioned in the previous section.

Secondly, instabilities at the boundary of the plasma in contact with the surrounding atmosphere and the ICPMS interface occur; the role of these instabilities was noted for the both laminar[23] and tangential[106] flow torches. In spite of the similarity of processes inside the ICP, the signal extraction mechanisms used in the ICP-AES and ICPMS techniques are different, and being a stable emission source does not *a priori* translate into a stable ion supply to the ion channel of the spectrometer. A100% ion extraction efficiency from the ICP into the sampler orifice is an optimistic estimate. Albeit dependent on the interface design and instrument tuning, it can be significantly less than 100%[107-110], at least for conventional interface pumps rated at 25-35 m^3/h. Photographs of the ICP at the boundary with the interface appear to show partial analyte escape[74,106]. Perhaps, more convincing are photographs of a sampler cone, of which the entire surface was heavily clogged during the analysis of relatively concentrated solutions.[111] At the same time, species from the surrounding atmosphere are present in the ICPMS signal, such as copper evaporated from the load coil (e.g., Elan 6000-series instruments), silver evaporated from the frontal plate surrounding the interface (e.g., Element 2-series instruments) and silicon derived from the walls of the torch and detectable irrespective of the spectral resolution, unless an alumina made torch is used[63,104]. This suggests that the surrounding analyte-free gas, is entrained into the sampler orifice. Besides, some polyatomic interferences, such as the $^{28}N_2^+$ interference on the major ^{28}Si isotope, can partially be explained by the entrainment of the surrounding atmosphere, including air, into the interface[110,112]. Thus, random (but also periodic[106,113]) losses in the ion population supplied by the sample introduction system become possible at the interface because of the mixing between the analyte-bearing and analyte-free gas, depending on how 'rough' the mixing process is (Fig. 4). A simplified way to describe the interface-related losses probabilistically is to divide the ICP channel into a number of incremental volumes containing the analyte, supposing that only a fraction of these volumes enters the sampler orifice, while the rest is lost. The corresponding binomial formalism is similar to the binomial description of the droplet selection in a nebuliser-spray chamber setup:

$$M' = \bar{c}' N' ; \; Var(M') = (\bar{c}')^2 \overline{N}'(1-p') + \bar{c}' \overline{N}' \qquad (37)$$

where *M'* is the number of ions aspirated by the sampler orifice per time interval (analysis), $\bar{c}'$ is the mean number of ions per incremental volume, *N'* is the number of such volumes aspirated by the sampler orifice per analysis, *p'* is the probability that an incremental volume will be aspirated by the sampler. The more homogeneous is the analyte flow to the sampler (smaller increments and, consequently, small $\bar{c}'$) and the higher is the extraction efficiency ($p' \to 1$), the 'smoother' is the signal. A diffusional mixing is thus harmless. A mixing controlled by gas flow dynamics, when the neighbour atoms in a given volume of analyte-bearing gas approaching the interface follow the same path and have the same fate - to enter or not to enter the sampler orifice, is not (see eqn 37).

Yet another, more general way to describe the analyte losses and the resulting uncertainty is to invoke the correlation properties of the resulting distribution. This way is also more canonical (see section '*Double stochasticity and fluctuations of the rate*'). To be consistent with mathematical texts, we present it here in the notation by Cox and Isham[50]. We divide the total value of *M* in small parts *dM*, each of which corresponding to the number of ions in an incremental volume of plasma aspirated by the sampler during time interval *Δt*. If we consider a large number of small incremental volumes sequentially arriving to the sampler orifice, it is reasonable to think that they are randomly diluted or concentrated in the studied analyte compared to the mean value. This can be due to the mixing in front of the sampler cone and also due to the sample introduction system instability. If the number of ions *dM(t, t+Δt)* in a particular volume observed during the period (*t, t*+Δ*t*) is a random value, the sum *M* of such numbers follows the randomness in *dM(t, t+Δt)* and is also random:

$$\begin{aligned} &Var(M) = Var\{M(0,T)\} \\ &= \sum_{t>0}^{t<T} Var\{dM(t,t+\Delta t)\} + 2\sum_{t>0}^{t<T}\sum_{u>0}^{u<T-t} Cov\{dM(t,t+\Delta t), dM(t+u,t+u+\Delta t')\} \end{aligned} \qquad (38)$$

If there is no mixing in front of the interface, then *dM* remains constant, provided the sample introduction process is stable. If *dM* is constant, the both variance and covariance terms in the right part of eqn (38) are equal to zero and the excess variance vanishes.

It should be noted that the ICPMS literature contains an additional explanation of the extraction related uncertainty. Gray and co-workers[83] admitted the role of sample introduction systems, but supposed that the origin of excess variance of the ICPMS signal can also be related to processes between the sampler and the skimmer[36-39,114]. They did not specify why the ion transmission efficiency inside the zone of silence in front of the skimmer tip is a randomly fluctuating parameter; otherwise, the analysis is reduced to the ordinary Poisson selection and the excess variance vanishes. Still, it is now documented by several independent studies that a disturbance, likely a standing shock wave, is indeed observed at the tip of the skimmer cone[44,115]; experimental or theoretical data explaining its action as a signal randomiser appear to be lacking. Perhaps, this problem merits further investigation (using a *strong* and *stable* ion emitter associated with the *sampler* cone?). Somewhat controversially, the data on gaseous samples provided by Gray and co-workers *themselves* were seemingly devoid of the excess variance, highlighting the role of the sample introduction system, not the interface, in its appearance. Besides, the small sampler orifice diameter (0.2 mm) used in the second series of their experiments allows supposing that the size of the incremental gas volume sampled from the ICP was defined by the sampler orifice, not by the inhomogeneity of the incoming ion flow; hence the dampening of the excess variance even in the presence of an 'aerosol' noise related to the nebulisation of liquid samples (a fairly unusual property!). The negative side of this approach is a huge instrument sensitivity loss[83].

Models reviewed above in this section - instability inside the ICP, destabilisation at the ICP - interface boundary, and fluctuations inside the interface - cover the whole operational sequence of the ICP ion source / first vacuum stage of the interface; they are all invoked to account for the appearance of the excess variance of ICPMS signals in the literature. From a personal standpoint, the authors of this text see fewer inconsistencies in the ICP - interface boundary model, but admit that further studies of the statistical role of the ICP and interface related processes are required.

To summarise, the double stochasticity of ICPMS signals has several potential sources (Table 4), of which noisy operation of the sample introduction system and, probably, the process of ion extraction from the ICP into the interface appear to be the most important at the present knowledge level. It is impressive for the ICP ion source to have two Achilles' heels - sample introduction at the entrance and ion extraction at the exit – and deservedly remain the most versatile and one of the most widely used ion sources in modern inorganic mass spectrometry.

Other *p,M*-conventions: changing the coordinates

The equation $\overline{N} = pM$ for the Poisson mean allows defining *p* and *M* arbitrarily. The definition used above in this text seem consistent with our understanding of the ICPMS noise and its sources as it follows from the literature and is reviewed in section '*Fluctuating M, sample introduction process*'. Still, other *p,M*-conventions are possible. For example, it is possible to define *M* as the number of atoms available for the sample introduction system per time interval (analysis), and *p* - as the probability for each of these atoms to be registered by the detection system as an ion count. For a homogeneous sample and for a sample introduction system with a constant uptake, *M* is constant (or, possibly, ordinary Poisson distributed); excess fluctuations during the measurement process are ascribed to *p*. According to eqn (15), the count number variance is then as follows:

$$Var(N) \approx \overline{\overline{N}} + M^2 Var(p) \qquad (39)$$

We do not see particular advantages of this convention. Below we review a more general representation of the doubly stochastic Poisson process, all particular *p,M*-conventions being its special cases.

Double stochasticity and fluctuations of the rate: an introduction to the existing formalisms

Considering the doubly stochastic Poisson process as a limiting form of the binomial selection complicated by fluctuations of primary ion population (*M*) and, possibly, transmission efficiency (*p*) is an elementary and understandable way to describe it. Still, mathematical literature tends to generalise the problem and rarely considers fluctuations in *p* and *M* separately[2,5,50]. Instead, it considers fluctuations of the rate $I(t) = pM / \Delta t$, i.e. considers the rate of the Poisson process as a random parameter, since product *pM* randomly changes. The corresponding formalism is not always intuitively understandable, but needs to be introduced here for two reasons: (i) the parameter observed in ICPMS measurements is the rate and not the individual statistics of *p* and *M*, (ii) a powerful mathematical apparatus describing connections between fluctuations and correlation of the rate is available. A disadvantage of introducing this formalism is that the individual uncertainty sources are, to some extent, obliterated.

A Poisson count rate can be defined for each time interval Δt. It is generally different for the different time intervals, though in the limit we will assume it constant within an interval:

$$I(t) = pdM(t,t+\Delta t)/\Delta t = \overline{dN(t,t+\Delta t)}/\Delta t \qquad (40)$$

Besides, a mean rate $\overline{I(t)}$ can be defined by averaging the individual rates above; for a non-transient signal, it corresponds to the mean rate for an individual interval, as it is calculated from a replicate series of such intervals. Using the same approach as in eqn (38), defining integral as the limit of a sum and applying the general formula for the variance of a sum of random variables, we obtain [ref. 50, sections 2.5 and 3.3]:

$$Var(N) = Var\{N(0,T)\} = \int_0^T Var\{dN(t,t+\Delta t)\} + 2\iint\limits_{\substack{0<t<T \\ 0<u\le T-t}} Cov\{dN(t,t+\Delta t), dN(t+u,t+u+\Delta t')\}$$

(41)

Henceforth, we assume that the studied signal is stationary (non-transient), simplifying the derivations. As $\Delta t \rightarrow 0$, $dN(t,t+\Delta t)$ can be considered as a variable taking only the values zero or one, with the probability to obtain one being equal to $\overline{I(t)}\Delta t$[5,50]. It then follows[50] from the variance definition that

$$Var\{dN(t,t+\Delta t)\} = \overline{I(t)}\Delta t \qquad (42)$$

Besides,

$$Cov\{dN(t,t+\Delta t), dN(t+u,t+u+\Delta t')\} = \left\{\overline{I(t)}h(u) - \overline{I(t)}^2\right\}\Delta t\Delta t' \qquad (43)$$

where *h(u)* is conditional intensity for the time interval $(t+u, t+u+\Delta t')$ equal to the probability to get one count during this interval, provided one count was already recorded in the interval $(t, t+\Delta t)$[50]. Reorganising formula (41), we obtain:

$$\begin{aligned} Var\{N(0,T)\} &= \int_0^T \overline{I(t)}\,dt + 2\int_0^T\int_0^{T-t}\left\{\overline{I(t)}h(u) - \overline{I(t)}^2\right\} du\, dt \\ &= \overline{I(t)}T + 2\overline{I(t)}\int_0^T (T-u)h(u)\,du - \overline{I(t)}^2 T^2 = \overline{\overline{N}} + 2\overline{I(t)}\int_0^T (T-u)h(u)\,du - \overline{\overline{N}}^2 \end{aligned} \qquad (44)$$

This equation can be re-written by expressing the conditional intensity *h(u)* via the autocovariance function $\gamma(u)$[50]:

$$h(u) = \overline{I(t)} + \gamma(u)/\overline{I(t)}\ ;\ Var\{N(0,T)\} = \overline{\overline{N}} + 2\int_0^T (T-u)\gamma(u)\,du \qquad (45)$$

Two other equivalent expressions for the total count variance can be given in terms of the autocorrelation function[2] and pair-correlation function[116], respectively. The autocovariance function $\gamma(u)$ is linked to the autocorrelation function $\rho(u)$ as follows[2]:

$$\gamma(u) = Var(I(t))\rho(u) \qquad (46)$$

Accordingly, introducing the autocorrelation function in equation (44) yields[2]:

$$Var\{N(0,T)\} = \overline{\overline{N}} + 2Var(I(t))\int_0^T (T-u)\rho(u)\,du \qquad (47)$$

The pair-correlation function $\eta(u)$ is linked to the conditional intensity *h(u)* as follows[116]:

$$h(u) = \overline{I(t)}(1+\eta(u)) \qquad (48)$$

Introducing the pair-correlation function in equation (44) yields[116]:

$$Var\{N(0,T)\} = \overline{\overline{N}} + 2\overline{I(t)}^2\int_0^T (T-u)\eta(u)\,du \qquad (49)$$

Formulae above for the description of the excess variance are all derived from formula (41) using three different but closely related tools (conditional intensity, autocovariance, autocorrelation and pair-correlation function) to describe correlation in the signal. If there is no such correlation, the autocorrelation function is zero and the excess variance vanishes (ordinary Poisson noise). In the presence of such a correlation, it could be interesting to track a link existing between the autocorrelation function and the spectral density of the power spectrum. It is described by the Wiener-Khinchin-Einstein theorem. Considering the corresponding mathematical apparatus in detail extends beyond the scope of this text. Still, here we will make some remarks. According to the Wiener-Khinchin-Einstein theorem[20],

$$S(f) = \int_{-\infty}^{+\infty} \rho(u)\cos(2\pi fu)\,du \qquad (50)$$

where $S(f)$ is the power spectral density of the signal, f is frequency, $\rho(u)$ is the autocorrelation function, and u is correlation time, as above. In one of the very first articles showing relationships between the low-frequency noise in ICP signals and the process of sample introduction, Antanavičius et al. argued: 'If the radiating particles are generated by droplet evaporation, they are correlated for some time'[68]. Indeed, if the rate of the Poisson process fluctuates, for example because more or less droplets (especially of a large size, see section '*Fluctuating M, sample introduction system*') reach the ICP per time interval, then a high count rate at the beginning of a period of high 'ion number density in the plasma'[70] means that somewhere within this period the rate will also be high, hence a rate correlation within this period. Time resolved ICP studies show that such periods are short and change rapidly (small u); beyond such a period, we can assume that $\rho(u)$ limits to zero. Thus, the integration interval in eqn (50) can be reduced from (-∞;+∞) to a narrow range around zero. In this range, at low frequencies, the product of angular frequency ($2\pi f$) and correlation time (u) is small, which maximises the cosine term in the integrated expression and, accordingly, increases the spectral density (see ref. 20, chapter I, for a similar example from the field of power engineering).

Concluding remarks and outlook

In ICPMS, 'transmission efficiency' and 'transport efficiency' are frequently used terms. It is important to recognise that a transmission efficiency is a probability by itself, which allows using the mathematical apparatus of the binomial selection for the interpretation of the signal uncertainty.

The ICPMS signal in its general form represents a doubly stochastic Poisson process, with an excess variance inherent to such processes. An excess variance often appears if a non-stationary random parameter is involved in the generation of a probability distribution. Analytical chemistry offers other examples illustrating this, such as the non-stationary blank (sample) and the non-stationary relative sensitivity factor. If the true mass of an analyte fluctuates in a series of blank solutions (e.g., vials containing them were variably contaminated), and the mass measurement technique is imprecise, then the total uncertainty of the measured analyte mass in a randomly selected blank is a combination of the both uncertainties above; it is higher than the mass measurement uncertainty alone[117]. The same applies to random changes of the sample mass consumed per measurement in a series of replicate analyses, especially if adding a controlled amount of internal standard does not seem feasible[94,118]. A more distant example concerns the determination of the relative sensitivity factor[119] (mass discrimination, 'mass bias') in LA-ICPMS[17,27,54,55,120] and secondary ion mass spectrometry[121-124]. This factor is often obtained by the (replicate) analysis of one single standard, the uncertainty of its mean value decreasing indefinitely with increasing the number of replicates. Then, it can happen that the relative sensitivity factor as determined from the standard yields inaccurate sample concentration ratios[125,126]. This situation can be considered from several standpoints. A statistician might argue that standards should represent a random selection of samples to be analysed and that the uncertainty of the above factor could be determined by the analysis of several standards and subsequent linear regression[127-130] of their concentration vs. intensity ratios. This uncertainty will generally be larger compared to a single-standard calibration, as the natural matrix-dependent variability of the relative sensitivity factor is accounted for. An 'inaccurate' sample concentration ratio becomes accurate, but less precise, once the total uncertainty of the relative sensitivity factor is propagated. In short, it is essential to recognise randomness in a statistics-generating parameter that, in the simplest form, is considered constant (refining the measurement technique in quest for its constancy being a parallel approach).

Understanding the ICPMS signal as a doubly stochastic Poisson process is causal and not symptomatic. For example, it is possible to apply a goodness-of-fit test to a distribution of sweep intensities and then to apply the Gauss confidence limits to the mean intensity obtained from this distribution, provided the distribution is approximately Gaussian according to the goodness-of-fit test[55]. An uncertainty value is the only result of this approach; we still do not understand why the signal fluctuates as it does. The doubly stochastic model reveals the source and propagation mechanism of the noise.

A qualitative understanding of the individual components of this model has been around for a while. It is appropriate here to return to the work by Gray *et al.*[83], who noted: (i) ‘It has long been accepted that the precision of isotope ratio measurements by inductively coupled plasma mass spectrometry (ICP-MS) is poorer than consideration of counting statistics would suggest is possible’; (ii) ‘One component of the random noise…is what may be termed the ion distribution noise. This is caused by the inhomogeneous spatial distribution of analyte ions in the central channel of the plasma which carries the sample aerosol…’. ‘The plasma actually fluctuates around the sampling orifice’, add Niu and Houk[38]. Important studies to this end by Olesik and co-workers were already given credit above in this text. It follows that a doubly stochastic Poisson distribution is encountered, with the precision *being in agreement* with the counting statistics constrained by this distribution, as discussed in this work.

It should be admitted that an analysis given in this work is conditional in several respects. For example, we assumed for simplicity that the detection is carried out in the counting regime. In the literature of mass spectrometry and its uncertainties, this assumption is handled as follows. For a Faraday cup, a potential difference between the ground and the cup is usually measured using a high ohmic resistor and then converted to current according to Ohm’s law. This electronic current compensates the current of positive ions incident on the Faraday cup. This current can be converted into count rate by dividing by $q_e=1.60210\text{x}10^{-19}$ C(=A x s)[27,46,131]. For a secondary electron multiplier operated in the analog mode, the current amplified by the analog stage of the multiplier is significantly higher than for a Faraday cup; it is converted into count rate using the detector cross calibration coefficient(s). From a statistical standpoint, this approach combines at least three types of uncertainties: (i) fluctuations in the number of ions arriving to the multiplier, (ii) fluctuations of the output current of the analog stage of the multiplier, (iii) measurement uncertainty of the current to voltage converter, the uncertainties (ii,iii) being superimposed on (i). We feel that the corresponding analysis lies beyond the scope of this text. Some relevant explanations and formulae can be found in ref. 46; further research is warranted.

Besides, we assumed that analyte *ions* and analyte *atoms* are statistically interchangeable terms, i.e. that ionisation process in the ICP does not randomise the population of analyte ions excessively. This point is not particularly important for elements that are ~100% ionised in the ICP; there are many of them[132,133]. For elements with a low degree of ionisation, this point invokes a binomial selection model: an ion in front of the sampler is considered as a result of binomial selection from the population of atoms supplied by the sample introduction system at a given probability of ionisation. If this probability is fixed (or deterministic, i.e., it does not change randomly with time), then the number of ions obtained from a fixed number of analyte atoms is binomially distributed. According to the binomial selection theorem, this does not introduce an excess variance in the distribution of counted ions[5]. At this time, we are unaware of data confirming a random behaviour of the probability of ionisation. Besides, neon injection experiments do no show systematically larger variances compared to xenon, in spite of the very different degree of ionisation of these elements (Table 3, Electronic Appendix 6).

We also postulated the same transmission efficiency p for all ions moving across the section of the sampler orifice. This is not exactly true: ions from the outer part of the ion beam have fewer chances to enter the skimmer orifice[134]. The same applies to droplets belonging the peripheral part of the aerosol cone inside a double pass spray chamber and removed from the aerosol flow through impacts with the inner barrel of the chamber[85]. It is possible to account for these effects by changing the p,M-convention, by defining $\overline{N} \equiv \int p(dM)\,dM$ or by deriving the excess variance through fluctuations of the rate (see previous section). Future research will assume increased complexity, but will benefit in terms of correctness, if deterministic changes in transmission (transport) efficiency are accounted for.

For uncertainty derivations, we assumed a zero dead time in the counting detection regime. The influence of the dead time related count losses on the Poisson distribution and its uncertainty has been discussed in the literature for a while; count numbers recorded in the presence of a dead time have somewhat less variance than predicted by the ordinary Poisson process[135-137]. Perhaps, this auxiliary aspect is worth a more thorough consideration in the ICPMS literature; nevertheless, it seems that a more general concern regarding the dead time correction of ICPMS signals exists. An interesting by-product of the double stochasticity is the compromised adequacy of formulae (6) for dead time correction. The derivation of these formulae[1,6,18] implies the same count rate during the period of actual counting and the period when the detection system is 'dead', thus restricting their application to the ordinary Poisson process. In a doubly stochastic Poisson process, periods of higher and lower rate change rapidly, and the first ion detected during a period of high rate prevents the registration of other ions arriving during this period (during a part of it covered by the dead time). The result is an intensity underestimation if formulae (6) are applied and the true dead time is used. The corresponding mathematical formalism can be found in refs. 116,138,139; it is not always easy to implement in practice. If formulae (6) are still employed[40,140-144], it is a good approach to avoid high intensity signals collection in the counting mode, since the double stochasticity is more marked at high intensities and the signal – less 'diluted' (higher chances for an ion or ions to fall within the dead time interval). This practice is encountered in some high accuracy isotope ratio ICPMS methods[55,145], where signals are collected in the 'forced' analog regime even if the upper intensity limit of the counting regime set by the instrument manufacturer is occasionally not reached (the analog signal does not have a dead time). A related approach is to set the upper intensity limit for the counting regime at a rather small value much lower than the counting saturation limit; ICPMS manufacturers usually implement this approach in their instruments. Yet another solution is to avoid applying the dead time correction to the mean intensity for the whole signal duration, or to the mean intensities of sweeps collected using a long dwell time; a very short dwell time, during which the rate does not change much, could be more adequate in this context. Finally, maintaining a sort of matching between the sample measurement setup (including intensities and their uncertainty) and that used to estimate the dead time during the instrument tuning can sometimes be feasible; on the contrary, determining the dead time based on relatively precise signals obtained using a 'smoothly' operating nebuliser and applying this dead time to significantly more disturbed data, such as some laser ablation ICPMS signals, might be imprudent. Approximately matching intensities of the analyte and the internal standard in an attempt to maintain a 1:1 ratio between them can also be recommended. A future study detailing the extent of the problem and providing a more thorough analysis of possible solutions seems to be warranted.

Finally, we decided to omit the problematics of very weak Poisson distributed ICPMS signals containing few counts per analysis. In the context of ideas reviewed above in this text, these problematics are trivial. The corresponding Poisson distributions show virtually no excess variance, since excess variance scales in quadrature with decreasing M, while the number of counts scales linearly. Nevertheless, such a triviality can be misleading. The mathematical apparatus required for the description and, particularly, for the comparison of two near-zero Poisson signals is not simple. The problem is related to the pronounced discreteness and skewness of the Poisson distribution for very small count numbers. Albeit the corresponding standard deviation values are still easy to estimate ($s(N)=\sqrt{N}$), assigning Gaussian confidence limits to these values is impossible. One analytically important aspect of this problem concerns the calculation of the critical value for detection decision ('detection limit' in the currently prevailing ICPMS terminology), especially in the framework of paired measurements (each sample acquisition is preceded by a background acquisition, e.g., in LA-ICPMS). *Is the analyte detected at a given confidence level, if the background contains one count and the signal - four counts?* And if that background would contain zero counts? Modern ICPMS instruments with their curved ion channels supress the photon noise[38,40]; setting a correct discriminator threshold minimises the internal noise of the secondary electron multiplier[40,45]; the gas blank is clean for most mass-to-charge ratios. Thus, obtaining a near-zero background reading in the context of our exercise is a common practice (uranium and the lanthanides being typical examples). Interestingly, the question posed above has for the first time been answered in 1940, in a - now canonical - article that, at first glance, belongs to agricultural research[7]. Much more has been done since then, including newer and more powerful tests for the equality of two Poisson means[8,9] and formulae for the detection limit with fast convergence to normality[10-12]. We refer the reader to the corresponding sources; this is an other case when a practically important question does not receive a straightforward empirical solution and invokes basic research.

Two obvious and complementary directions of further development in the area of the Poisson modelling of ICPMS signals are (i) study of the double stochasticity with the aim to minimise it by instrumental measures (sample introduction system and ICP-interface region, the randomising role of the latter being rather obscure at this time) to remove adverse effects associated with it, such as the precision loss due to excess variance and impact on the dead time determination and correction; (ii) mathematical description of the key parameters (rate and its correlation) associated with the double stochasticity to enable modelling the excess variance, if it is not removed by instrumental measures; the corresponding tools, such as the Kalman filter, will hopefully be considered in future ICPMS research.

Acknowledgements

A.U. thanks Olga Ulianova for her help during the preparation of the manuscript. We are grateful to an anonymous colleague who drove our attention to the role of the sample introduction system in the primary ion population statistics and to the rich experimental literature on these problematics. We thank two anonymous reviewers for their helpful and constructive comments. Thanks also go to Detlef Günther and Henry Longerich for discussions at an early stage of work on the manuscript and to Lothar Rottmann for consultations regarding the spectrometer construction. Besides, we gratefully acknowledge the editorial handling of the manuscript by Frank Vanhaecke. This contribution was presented during the Winter Conference on Plasma Spectrochemistry 2014. It was supported by grants Nr. 200021_138004/1 and 206021-117405 (R'EQUIP) from the Swiss National Science Foundation.

References

1 G.F. Knoll, *Radiation detection and measurement*, John Wiley & Sons, New York, 2nd edn, 1989, p. 754.
2 D.R. Cox and P.A.W. Lewis, *The statistical analysis of series of events*, Methuen&Co., London, 1968, p. 285.
3 W. Feller, *An introduction to the probability theory and its applications, volume I*, John Wiley & Sons, New York, 3rd edn, 1968, p. 528.
4 N.L. Johnson and S. Kotz, *Discrete distributions*, John Wiley & Sons, New York, 1969, p. 328.
5 H.H. Barrett and K.J. Myers, *Foundations of Image Science*, John Wiley & Sons, Hoboken, New Jersey, 2004, p. 1540.
6 L.J. Rainwater and C.S. Wu, Applications of probability theory to nuclear particle detection, Nucleonics, 1947, **1**, 60-69.
7 J. Przyborowski and H. Wilenski, Homogeneity of results in testing samples from Poisson series, *Biometrika*, 1940, **31**, 313-323.
8 K. Krishnamoorthy and J. Thomson, A more powerful test for comparing two Poisson means, *J. Stat. Plan. Inf.*, 2004, **119**, 23-35.
9 H.K.T. Ng, K. Gu and M.L. Tang, A comparative study of tests for the difference of two Poisson means, *Comp. Stat. Data Anal.*, 2007, **51**, 3085-3099.
10 L. Currie, On the detection of rare, and moderately rare, nuclear events, *J. Radioanal. Nucl. Chem.*, 2008, **276**, 285-297.
11 D.J. Strom and J.A. MacLellan, Evaluation of eight decision rules for low-level radioactivity counting, *Health Phys.*, 2001, **81**, 27-34.
12 MARLAP Multi-Agency Radiological Laboratory Analytical Protocol Manual, vol. 19-20, 2004.
13 M. Tanner, Shorter signals for improved signal to noise ratio, the influence of Poisson distribution, *J. Anal. At. Spectrom.*, 2010, **25**, 405–407.
14 T. Pettke, F. Oberli, A. Audétat, M. Guillong, A.C. Simon, J.J. Hanley and L.M. Klemm, Recent developments in element concentration and isotope ratio analysis of individual fluid inclusions by laser ablation single and multiple collector ICP-MS, *Ore Geol. Rev.*, 2012, **44**, 10-38.
15 W.L. Nicholson, Fixed time estimation of counting rates with background corrections. AEC R&D Report HW-76279, Hanford Works, Richland, Washington, 1963.
16 W.L. Nicholson, Statistics of net-counting-rate estimation with dominant background corrections, *Nucleonics*, 1966, **24**, 118-121.
17 Y. Luo, S. Gao, H.P. Longerich, D. Günther, S. Wunderli, H.L. Yuan and X.-M. Liu, The uncertainty budget of the multi-element analysis of glasses using LA-ICP-MS, *J. Anal. At. Spectrom.*, 2007, **22**, 122-130.
18 W.R. Leo, *Techniques for Nuclear and Particle Physics Experiments: A How-To Approach*, Springer-Verlag, Berlin-Heidelberg, 2nd edn, 1994, p. 378.

19 G.P. Tolstov, *Fourier series*, Dover Publications, 1976, p. 352.

20 G.M. Jenkins and D.G. Watts, *Spectral analysis and its applications*, Holden-Day, San Francisco, 1969, p. 525.

21 R.M. Belchamber and G. Horlick, Noise-power spectra of optical and acoustic emission signals from an inductively coupled plasma, *Spectrochim. Acta, Part B*, 1982, **37**, 17-27.

22 J. Davies and R.D. Snook, Studies of a low-noise laminar flow torch for inductively coupled plasma atomic emission spectrometry. Part 1. Fundamental characteristics, *J. Anal. At. Spectrom.*, 1986, **1**, 195-201.

23 J. Davies and R.D. Snook, Studies of a low-noise laminar flow torch for inductively coupled plasma atomic emission spectrometry. Part 2. Noise power studies and interference effects, *J. Anal. At. Spectrom.*, 1987, **2**, 27-31.

24 J.S. Crain, R.S. Houk and D.E. Eckels, Noise power spectral characteristics of an inductively coupled plasma-mass spectrometer, *Anal. Chem.*, 1989, **61**, 606-612.

25 N. Furuta, C.A. Monnig, P. Yang and G.M. Hieftje, Noise characteristics of an inductively coupled plasma-mass spectrometer, *Spectrochim. Acta, Part B*, 1989, **44**, 649-656.

26 P.K. Appelblad, I. Rodushkin and D.C. Baxter, Sources of uncertainty in isotope ratio measurements by inductively coupled plasma mass spectrometry, *Anal. Chem.*, 2001, **73**, 2911-2919.

27 D.C. Baxter, I. Rodushkin and E. Engström, Isotope abundance ratio measurements by inductively coupled plasma-sector field mass spectrometry, *J. Anal. At. Spectrom.*, 2012, **27**, 1355–1381.

28 E.D. Prudnikov and Y.S. Shapkina, Random errors in analytical methods, *Analyst*, 1984, **109**, 305-307.

29 E.D. Prudnikov and R.M. Barnes, Theoretical calculation of the standard deviation in inductively coupled plasma mass spectrometry, *J. Anal. At. Spectrom.*, 1999, **14**, 27-31.

30 E.D. Salin and G. Horlick, Signal-to-noise performance characteristics of an inductively coupled plasma, *Anal. Chem.*, 1980, **52**, 1578-1582.

31 M.P. Goudzwaard and M.T.C. de Loos-Vollebregt, Characterisation of noise in inductively coupled plasma – atomic emission spectrometry, *Spectrochim. Acta, Part B*, 1990, **45**, 887-901.

32 W. Compston, Geological age by instrumental analysis: The 29th Hallimond lecture, *Mineral. Mag.*, 1999, **63**, 297-311.

33 B.L. Sharp, Pneumatic nebulisers and spray chambers for inductively coupled plasma spectrometry. A review. Part 1. Nebulisers. *J. Anal. At. Spectrom.*, 1988, **3**, 613-652.

34 R. Campargue, High intensity supersonic molecular beam apparatus, *Rev. Sci. Instrum.*, 1964, **35**, 111–112.

35 J.H. Moore, C.C. Davis, M.A. Coplan and S.C. Greer, *Building Scientific Apparatus*, Cambridge University Press, 4th edn, 2009, p. 658.

36 D.J. Douglas, Fundamental aspects of inductively coupled plasma mass spectrometry, in *Inductively Coupled Plasmas in Analytical Atomic Spectrometry*, ed. A. Montaser and D.W. Golightly, VCH Publishers, New York, 2nd edn, 1992, pp. 613-650.

37 D.J. Douglas and J.B. French, Gas dynamics of the inductively coupled plasma mass spectrometry interface, *J. Anal. At. Spectrom.*, 1988, **3**, 743-747.

38 H. Niu and R.S. Houk, Fundamental aspects of ion extraction in inductively coupled plasma mass spectrometry, *Spectrochim. Acta, Part B*, 1996, **44**, 779-815.

39 M. Liezers, Sampling interface design and function, Ion extraction and focusing, in *ICP Mass Spectrometry Handbook*, ed. S.M. Nelms, Blackwell Publishing, Oxford UK, 2005, pp. 10-25.

40 N. Jakubowski, T. Prohaska, L. Rottmann and F. Vanhaecke, Inductively coupled plasma- and glow discharge plasma-sector field mass spectrometry, *J. Anal. At. Spectrom.*, 2011, **26**, 693-726.

41 G.M. Hieftje, Towards the next generation of plasma source mass spectrometers. Plenary lecture, *J. Anal. At. Spectrom.*, 1992, **7**, 783-790.

42 R. Thomas, Practical Guide to ICP-MS: A Tutorial for Beginners, CRC Press, 3rd edn, 2013, p. 446.

43 R.S. Houk, S.C.K. Shum and D.R. Wiederin, Frontiers in elemental analysis by mass spectrometry, *Anal. Chim. Acta*, 1991, 250, 61-70.

44 H. Niu and R.S. Houk, Langmuir probe measurements of the ion extraction process in inductively coupled plasma mass spectrometry – I. Spatially resolved determination of electron density and electron temperature. *Spectrochim. Acta, Part B*, 1994, **12-14**, 1283-1303.

45 H. Longerich, Laser ablation – inductively coupled plasma – mass spectrometry (LA-ICP-MS); An Introduction, in *Laser Ablation ICP-MS in the Earth Sciences: Current Practices and Out-*

standing Issues, ed. P. Sylvester, Mineralogical Association of Canada Short Course Series, Vancouver, BC, 2008, vol. 40, pp. 1-18.

46 K. Hunter and R. Stresau, Ion detection, in *ICP Mass Spectrometry Handbook*, ed. S.M. Nelms, Blackwell Publishing, Oxford UK, 2005, pp. 117-146.

47 A. Montaser, M.G. Minnich, J.A. McLean, H. Liu, J.A. Caruso and C.W. McLeod, Sample introduction in ICPMS, in *Inductively Coupled Plasma Mass Spectrometry*, ed. A. Montaser, Wiley-VCH, New York, 1998, pp. 83-264.

48 J.S. Becker and H.-J. Dietze, Inorganic trace analysis by mass spectrometry, *Spectrochim. Acta, Part B*, 1998, **53**, 1475–1506.

49 F.A. Haight, *Handbook of the Poisson distribution*, John Wiley & Sons, New York, 1967, p. 168.

50 D.R. Cox and V. Isham, *Point processes*, London-New York-Washington, Chapman & Hall, 1980, p. 188.

51 D.R. Cox, Some statistical methods connected with series of events, *J. R. Stat. Soc.*, *Series B*, 1955, **17**, 129-164.

52 S.A. Myers and D.H. Tracy, Improved performance using internal standardization in inductively-coupled plasma emission spectroscopy, *Spectrochim. Acta, Part B,* 1983, **38**, 1227-1253.

53 J. Meija and Z. Mester, Signal correlation in isotope ratio measurements with mass spectrometry: Effects on uncertainty propagation, *Spectrochim. Acta, Part B,* 2007, **62**, 1278-1284.

54 C.M. Fisher, H.P. Longerich, S.E. Jackson and J.M. Hanchar, Data acquisition and calculation of U–Pb isotopic analyses using laser ablation (single collector) inductively couple plasma mass spectrometry, *J. Anal. At. Spectrom.*, 2010, **25**, 1905-1920.

55 A. Ulianov, O. Müntener, U. Schaltegger and F. Bussy, The data treatment dependent variability of U-Pb zircon ages obtained using mono-collector, sector field, laser ablation ICPMS, *J. Anal. At. Spectrom.*, 2012, **27**, 663-676.

56 A. Ulianov and O. Müntener, Differencing as a method to estimate the uncertainty of a transient LA-ICPMS signal, *J. Anal. At. Spectrom.*, 2014, **29**, 934-940.

57 K.G. Heumann, S.M. Gallus, G. Rädlinger and J. Vogl, Precision and accuracy in isotope ratio measurements by plasma source mass spectrometry, *J. Anal. At. Spectrom.*, 1998, **13**, 1001-1008.

58 F. Vanhaecke, L. Balcaen and D. Malinovsky, Use of single-collector and multi-collector ICP-mass spectrometry for isotopic analysis, *J. Anal. At. Spectrom.*, 2009, **24**, 863-886.

59 R.C. Ogliore, G.R. Huss, and K. Nagashima, Ratio estimation in SIMS analysis, *Nucl. Instr. Meth. Phys. Res., Sect. B.*, 2011, **269**, 1910-1918.

60 I.S. Begley and B.L. Sharp, Occurrence and reduction of noise in inductively coupled plasma mass spectrometry for enhanced precision in isotope ratio measurement, *J. Anal. At. Spectrom.*, 1994, **9**, 171-176.

61 F. Vanhaecke, L. Moens, R. Dams and P. Taylor, Precise measurement of isotope ratios with a double-focusing magnetic sector ICP mass spectrometer, *Anal. Chem*., 1996, **68**, 567-569.

62 S.M. Eggins and J.M.G. Shelley, *Geostand. Geoanal. Res.*, 2002, **26**, 269-286.

63 D.C. Baxter, I. Rodushkin and E. Engström, Sources of contamination and remedial strategies in the multi-elemental trace analysis laboratory, *Anal. Bioanal. Chem.*, 2010, **396**, 365-377.

64 S.A. Myers and D.H. Tracy, Sources of noise and drift in ICP emission, *7th Annual Meeting FACSS*, Philadelphia, 1980, Abstract No. 5, *ICP Information Newslett*., 1980, **6**, 233.

65 S.A. Myers, D.H. Tracy and R.D. Ediger, Studies of cross-flow nebulisers, *International Winter Conference on Developments in Atomic Plasma Spectrochemical Analysis*, San Juan, Puerto Rico, 1980, Abstract No. 62, *ICP Information Newslett*., 1980, **6**, 366-368.

66 R. Antanavičius, P. Serapinas and P. Šimkus, Manifestation of the entering of a substance into an RF-discharge plasma in its radiation noise, *Opt. Spektrosk.* (USSR), 1987, **63**, 224-225.

67 R. Antanavičius, E. Nashlenas and P. Serapinas, Measurement of the radiation noise of an RF-discharge plasma with a disperse phase, *Opt. Spektrosk.* (USSR), 1989, **67**, 280-285.

68 R. Antanavičius, P. Serapinas and P. Šimkus, Observation of the frequency dependence of ICP radiation noise, *J. Phys. D: Appl. Phys.*, 1989, **22**, 254-257.

69 A. Montaser, I. Ishii, H. Tan, R.H. Clifford and D.W. Golightly, Noise power spectra comparing He and Ar ICP discharges, *Spectrochim. Acta, Part B*, 1989, **44**, 1163-1169.

70 J.W. Olesik, L.J. Smith and E.J. Williamsen, Signal fluctuations due to individual droplets in inductively coupled plasma atomic emission spectrometry. *Anal. Chem.*, 1989, **61**, 2002-2008.

71 S.E. Hobbs and J.W. Olesik, Inductively coupled plasma mass spectrometry signal fluctuations due to individual aerosol droplets and vaporizing particles, *Anal. Chem.*, 1992, **64**, 274-283.

72 J.W. Olesik, Investigating the fate of individual sample droplets in inductively coupled plasmas, *Appl. Spectrosc.*, 1997, **51**, 158A-175A.

73 J.W. Olesik, J.A. Kinzer and G.J. McGowan, Observation of atom and ion clouds produced from single droplets of sample in inductively coupled plasmas by optical emission and laser-induced fluorescence imaging, *Appl. Spectrosc.*, 1997, **51**, 607-616.

74 R.K. Winge, J.S. Crain and R.S. Houk, High speed photographic study of plasma fluctuations and intact aerosol particles in inductively coupled plasma mass spectrometry, *J. Anal. Atom. Spectrom.*, 1991, **6**, 601-604.

75 R.S. Houk, R.K. Winge and X. Chen, High speed photographic study of wet droplets and solid particles in the inductively coupled plasmas, *J. Anal. Atom. Spectrom.*, 1997, **12**, 1139-1148.

76 I. Horn and D. Günther, The influence of ablation carrier gases Ar, He and Ne on the particle size distribution and transport efficiencies of laser ablation-induced aerosols: implications for LA-ICP-MS, *Appl. Surf. Sci.*, 2003, **207**, 144-157.

77 D.B. Aeschliman, S.J. Bajic, D.P. Baldwin and R.S. Houk, High-speed digital photographic study of an inductively coupled plasma during ablation: comparison of dried solution aerosols from a microconcentric nebulizer and solid particles from laser ablation, *J. Anal. At. Spectrom.*, 2003, **18**, 1008-1014.

78 T. Hirata and Z. Miyazaki, High-speed camera imaging for laser ablation process: for further reliable elemental analysis using inductively coupled plasma-mass spectrometry, *Anal. Chem.*, 2007, **79**, 147-152.

79 D.C. Perdian, S.J. Bajic, D.P. Baldwin and R.S. Houk, Time-resolved studies of particle effects in laser ablation inductively coupled plasma-mass spectrometry. Part I. Investigation of nanosecond and femtosecond pulse width lasers and devices for particle size selection, *J. Anal. At. Spectrom.*, 2008, **23**, 325-335.

80 I. Horn, Comparison of femtosecond and nanosecond laser interactions with geological matrices and their influence on accuracy and precision of LA-ICP-MS data, in *Laser Ablation ICP-MS in the Earth Sciences: Current Practices and Outstanding Issues*, ed. P. Sylvester, Mineralogical Association of Canada Short Course Series, Vancouver, BC, 2008, vol. 40, pp. 53-65.

81 A. Tunheng and T. Hirata, Development of signal smoothing device for precise elemental analysis using laser ablation-ICP-mass spectrometry, *J. Anal. At. Spectrom*., 2004, **19**, 932-934.

82 A. Montaser, M.G. Minnich, H. Liu, A.G.T. Gustavsson and R.F. Browner, Fundamental aspects of sample introduction in ICP spectrometry, in *Inductively Coupled Plasma Mass Spectrometry*, ed. A. Montaser, Wiley-VCH, New York, 1998, pp. 335-420.

83 A.L. Gray, J.G. Williams, A.T. Ince and M. Liezers, Noise sources in inductively coupled plasma mass spectrometry: an investigation of their importance to the precision of isotope ratio measurements, *J. Anal. At. Spectrom.*, 1994, **9**, 1179-1181.

84 N.A. Panichev, Q. Ma, R.E. Sturgeon, C.L. Chakrabarti and V. Pavski, Condensation of analyte vapor species in graphite furnace atomic absorption spectrometry, *Spectrochimica Acta, Part B*, 1999, **54**, 719-731.

85 S. Okabayashi, S. Sakata and T. Hirata, Isotopic analysis of nano-gram amounts of tungsten using electrothermal vaporization (RTV)-MC-ICPMS technique, *44th Lunar and Planetary Science Conference*, The Woodlands, Texas, 2013, Abstract No. 1911.

86 J.-L. Todoli and J.-M. Mermet, Liquid sample introduction in ICP spectrometry: A practical guide, Elsevier, 2008, p. 300.

87 M. Hamester, D. Wiederin, J. Wills, W. Kerl and C.B. Douthitt, Strategies for isotope ratio measurements with a double focusing sector field ICP-MS, *Fresenius J. Anal. Chem.*, 1999, **364**, 495-497.

88 M. Krachler, N. Rausch, H. Feuerbacher and P. Klemens, A new HF-resistant tandem spray chamber for improved determination of trace elements and Pb isotopes using inductively coupled plasma-mass spectrometry. *Spectrochimica Acta, Part B*, 2005, **60**, 865-869.

89 J.A. McLean, M.G. Minnich, L.A. Iacone, H. Liu and A. Montaser, Nebulizer diagnostics: fundamental parameters, challenges, and techniques on the horizon, *J. Anal. At. Spectrom*., 1998, **13**, 829-842.

90 L.D. Landau and E.M. Lifshitz, *Course of theoretical physics, vol. 5, Statistical physics, part I*, Pergamon Press, 3rd edn, 1980, p. 387.

91 N.J. Johnson, A.W. Kemp and S. Kotz, *Univariate discrete distributions*, Wiley-Interscience, 3rd edn, 2005, p. 672.

92 W. Doherty, Non-linear signal response functions and their effects on the statistical and noise cancellation properties of isotope ratio measurements by multi-collector plasma mass spectrometry, *Spectrochim. Acta, Part B*, 2013, **85**, 78-92.

93 S.E. Maestre, J.L. Todolí and J.M. Mermet, Evaluation of several pneumatic micronebulizers with different designs for use in ICP–AES and ICP–MS. Future directions for further improvement, *Anal. Bioanal. Chem.*, 2004, **379**, 888-899.

94 M.J. Chang, J.D. Naworal, K. Walker and C.T. Connell, Investigations on the direct introduction of cigarette smoke for trace elements analysis by inductively coupled plasma mass spectrometry, *Spectrochim. Acta*, *Part B*, 2003, **58**, 1979-1996.

95 S.J. Christopher, S.E. Long, M.S. Rearick and J.D. Fassett, Development of isotope dilution cold vapour inductively coupled plasma mass spectrometry and its application to the certification of mercury in NIST standard reference materials, *Anal. Chem*., 2001, **73**, 2190-2199.

96 D. Layton-Matthews, M.I. Leybourne, J.M. Peterc and S.D. Scott, Determination of selenium isotopic ratios by continuous-hydridegeneration dynamic-reaction-cell inductively coupled plasma-mass spectrometry, *J. Anal. At. Spectrom*., 2006, **21**, 41–49.

97 C. Zheng, L. Yang, R.S. Sturgeon and X. Hou, UV photochemical vapour generation sample introduction for determination of Ni, Fe, and Se in biological tissue by isotope dilution ICPMS, Anal. Chem., 2010, **82**, 3899-3904.

98 P. Wu, L. He, C. Zheng, X. Hou and R.E. Sturgeon, Application of chemical vapour generation in non-tetrahydroborate media to analytical atomic spectrometry, *J. Anal. At. Spectrom*., 2010, **25**, 1217–1246.

99 Z. Long, Y. Luo, C. Zheng, P. Deng and X. Hou, Recent advance of hydride generation–analytical atomic spectrometry: Part I-technique development, *Appl. Spectrosc. Rev*., 2012, **47**, 382-413.

100 C.J. Park and S.A. Yim, Determination of nickel in water samples by isotope dilution inductively coupled plasma mass spectrometry with sample introduction by carbonyl vapor generation, *J. Anal. At. Spectrom*., 1999, **14**, 1061–1065.

101 J. Davies and R.D. Snook, Low-noise laminar flow torch for inductively coupled plasma atomic-emission spectrometry, *Analyst*, 1985, **110**, 887-888.

102 N.N. Sesi, P.J. Galley and G.M. Hieftje, Evaluation of a linear-flow torch for inductively coupled plasma atomic emission spectrometry, *J. Anal. At. Spectrom.*, 1993, **8**, 65-70.

103 R.H. Wendt and V.A. Fassel, Induction-coupled plasma spectrometric excitation source, *Anal. Chem.*, 1965, **37**, 920-922.

104 I.L. Turner and A. Montaser, Plasma generation in ICPMS, in *Inductively Coupled Plasma Mass Spectrometry*, ed. A. Montaser, Wiley-VCH, New York, 1998, pp. 265-334.

105 N. Furuta, Spatial profile measurement of ionization and excitation temperatures in an inductively coupled plasma, *Spectrochim. Acta, Part B*, 1985, **40**, 1013-1022.

106 A.T. Ince, J.G. Williams and A.L. Gray, Noise in inductively coupled plasma mass spectrometry: some preliminary measurements, *J. Anal. At. Spectrom.*, 1993, **8**, 899-903.

107 F. Vanhaecke, R. Dams and C. Vandecasteele, 'Zone model' as an explanation for signal behaviour and non-spectral interferences in inductively coupled plasma mass spectrometry, *J. Anal. At. Spectrom.*, 1993, **8**, 433-438.

108 L. Flamigni, J.Koch and D. Günther, Experimental and theoretical investigations about the vaporization of laser-produced aerosols and individual particles inside inductively-coupled plasmas - Implications for the extraction efficiency of ions prior to mass spectrometry, *Spectrochim. Acta, Part B,* 2012, **76**, 70-76.

109 M. Aghaei, L. Flamigni, H. Linder, D. Günther and A. Bogaerts, Occurrence of gas flow rotation motion inside the ICP torch: a computational and experimental study, *J. Anal. At. Spectrom.*, 2014, **29**, 249-261.

110 D. Günther, H.P. Longerich, S.E. Jackson and L. Forsythe, Effect of sampler orifice diameter on dry plasma inductively coupled plasma mass spectrometry (ICP-MS) backgrounds, sensitivities, and limits of detection using laser ablation sample introduction, *Fresenius J. Anal. Chem.*, 1996, **355**, 771-773.

111 Solution mode ICPMS, http://www.jsg.utexas.edu/icp-ms/solution, consulted on the 24th of August 2014.

112 N.M. Reed, R.O. Cairns, R.C. Hutton and Y. Takaku, Characterization of polyatomic ion interferences in inductively coupled plasma mass spectrometry using a high resolution mass spectrometer *J. Anal. At. Spectrom.*, 1994, **9**, 881-896.

113 R.K. Winge, D.E. Eckels, E.L. DeKalb and V.A. Fassel, Spatiotemporal characteristcs of the Inductively coupled plasma, *J. Anal. At. Spectrom.*, 1988, **3**, 849-855.

114 D.J. Douglas and S.D. Tanner, Fundamental considerations in ICPMS, in *Inductively Coupled Plasma Mass Spectrometry*, ed. A. Montaser, Wiley-VCH, New York, 1998, pp. 615-679.

115 N. Taylor and P.B. Farnsworth, Experimental characterization of the effect of skimmer cone design on shock formation and ion transmission efficiency in the vacuum interface of an inductively coupled plasma mass spectrometer, *Spectrochim. Acta*, *Part B*, 2012, **69**, 2-8.

116 M.L Larsen and A.B. Kostinski, Simple dead-time corrections for discrete time series of non-Poisson data, *Meas. Sci. Technol.*, 2009, **20**, paper 095101.

117 A. Ulianov, M. Honisch and O. Müntener, Calculating the net activity uncertainty if the background includes a nonstationary component, *Anal. Chem.*, 2013, **85**, 2589-2594.

118 M.J. Chang, J.D. Naworal and C.T. Connell J. Direct introduction of cigarette smoke for puff-by-puff trace metals analysis by inductively coupled plasma mass spectrometry, *J. Anal. At. Spectrom.*, 2006, **21**, 574–581.

119 F.L. King, J. Teng and R.E. Steiner, Glow discharge mass spectrometry: trace element determination in solid samples, *J. Mass. Spectrom.*, 1995, **30**, 1061-1075.

120 H.P. Longerich, S.E. Jackson and D. Günther, Laser ablation inductively coupled plasma mass spectrometric transient signal data acquisition and analyte concentration calculation, *J. Anal. At. Spectrom.*, 1996, **11**, 899-904.

121 A. Benninghoven, F.G. Rüdenauer and H.W. Werner, *Secondary ion mass spectrometry: basic concepts, instrumental aspects, applications and trends*, John Wiley & Sons, New York, 1987, p. 1227.

122 W. Compston, I.S. Williams and C. Meyer, U-Pb geochronology of zircon from lunar breccia 73217 using a sensitive high mass-resolution ion microprobe, *J. Geophys. Res.*, 1984, **89**, B525-B534.

123 J.M. Eiler, C.M. Graham and J.M. Valley, SIMS analysis of oxygen isotopes: matrix effects in complex minerals and glasses, *Chem. Geol.*, 1997, **138**, 221-244.

124 L.R. Riciputi, B.A. Paterson and R.L. Ripperdan, Measurement of light stable isotope ratios by SIMS: matrix effects for oxygen, carbon, and sulphur isotopes in minerals, *Int. J. Mass Spectrom.*, 1998, **178**, 81-112.

125 U. Klötzli, E. Klötzli, Z. Günes and Kosler, J. Accuracy of laser ablation U-Pb zircon dating: Results from a test using five different reference zircons. *Geostand. Geoanal. Res.*, 2009, **33**, 5-15.

126 E. Marillo-Sialer, J. Woodhead, J. Hergt, A. Greig, M. Guillong, A. Gleadow, E. Evans and C. Paton, The zircon 'matrix effect': evidence for an ablation rate control on the accuracy of U-Pb age determinations by LA-ICP-MS, *J. Anal. At. Spectrom.*, 2014, **29**, 981–989.

127 W.A. Fuller, *Measurement Error Models.* John Wiley & Sons, New York, 1987, p. 440.

128 D. Gujarati, *Basic Econometrics*, The McGraw-Hill Companies, 4th edn, 2004, p. 1002.

129 J.G. Eisenhauer, Regression through the origin, *Teaching Statistics* 2003, 76-80.

130 J.-M. Mermet, Quality of calibration in inductively coupled plasma atomic emission spectrometry, *Spectrochim. Acta, part B*, 1994, 49, 1313-1324.

131 K. Habfast, Advanced isotope ratio mass spectrometry I: Magnetic isotope ratio mass spectrometers, in *Modern isotope ratio mass spectrometry*, ed. I.T. Platzner, Wiley, New York, 1997, ch. 3, pp. 11-82.

132 R. S. Houk, Mass spectrometry of inductively coupled plasmas, *Anal. Chem.*, 1986, 58, 97A-105A.

133 A.A. Pupyshev, V.N. Muzgin and A.K. Lutsak, Thermochemical processes and ion transport in inductively coupled plasma mass spectrometry: theoretical description and experimental confirmation, *J. Anal. At. Spectrom.*, 1999, **14**, 1485–1492.

134 J.H. Macedone, D.J. Gammon and P.B. Farnsworth, Factors affecting the analyte transfer through the sampling orifice of an inductively coupled plasma mass spectrometer, *Spectrochim. Acta, Part B*, 2001, **56**, 1687-1695.

135 J.W. Müller, Counting statistics of a Poisson process with dead time, BIMP report 111, 1970, 14 p.

136 W.L. Smith, Renewal theory and its ramifications, *J.R. Stat. Soc., Series B*, 1958, **20**, 284-302.

137 G. Vannucci and M.C. Teich, Dead-time-modified photocount mean and variance for chaotic radiation, *J. Opt. Soc. Am.*, 1981, **71**, 164-170.

138 G. Vannucci and M.C. Teich, Effects of rate variations on the counting statistics of dead-time-modified Poisson processes, *Opt. Comm.*, 1978, **25**, 267-272.

139 M.D. Srinivas, Measurements and quantum probabilities, Universities Press (India) Ltd., Hyderabad, 2001, p. 272.

140 A. Held and P.D.P. Taylor, A calculation method based on isotope ratios for the determination of dead time and its uncertainty in ICP-MS and application of the method to investigating some features of a continuous dynode multiplier, *J. Anal. At. Spectrom.*, 1999, **14**, 1075-1079.

141 S.M. Nelms, C.R. Quétel, T. Prohaska, J. Vogl and P.D.P. Taylor, Evaluation of detector dead time calculation models for ICP-MS, *J. Anal. At. Spectrom.*, 2001, **16**, 333-338.

142 H. Rameбäck, M. Berglund, D. Vendelbo, R. Wellum and P.D.P. Taylor, On the determination of the true dead-time of a pulse-counting system in isotope ratio mass spectrometry, *J. Anal. At. Spectrom.*, 2001, **16**, 1271-1274.

143 J. Vogl, Calibration strategies and quality assurance, in *ICP Mass Spectrometry Handbook*, ed. S.M. Nelms, Blackwell Publishing, Oxford UK, 2005, pp. 147-181.

144 U. Nygren, H. Ramebäck, M. Berglund and D.C. Baxter, The importance of a correct dead time setting in isotope ratio mass spectrometry: implementation of an electronically determined dead time to reduce measurement uncertainty, *Int. J. Mass Spec.*, 2006, **257**, 12-15.

145 D. Frei and A. Gerdes, Precise and accurate *in situ* U–Pb dating of zircon with high sample throughput by automated LA-SF-ICP-MS, *Chem. Geol.*, 2008, **261**, 261-270.

Figure captions

Fig. 1. A schematic probability distribution of a doubly stochastic Poisson process as a blend of many individual Poisson processes, each of them having its own mean $\overline{N_i} = p_i M_i$ and variance $\sqrt{\overline{N}_i}$ and contributing a count number value, randomly positioned around $\overline{N}_i$, to the mixed probability distribution of the doubly stochastic process. Two statistics arise: (i) statistics of the random count number values, as measured; (ii) underlying statistics of the mean count number values, which are not directly accessible. In time-resolved ICPMS applications, this implies that a (hidden) mean count number vs. sweep pattern underlies the observed count number vs. sweep pattern. In strong signals, the two patterns almost coincide: in such signals, the ordinary Poisson scattering is insignificant compared to the scattering of the Poisson means (in other words, compared to the excess variance; see text for further explanations). In weak signals, the mean count number pattern is almost constant; the ordinary Poisson scattering dominates. There are at least two tools to reconstruct the hidden pattern - scaling the observed pattern of a strong signal obtained simultaneously with a weaker signal on a multi-collector spectrometer (to obtain the mean count number pattern of the weaker signal) and using the Kalman filter; discussing these tools in detail lies beyond the scope of this text.

Fig. 2. Count vs. sweep number statistics for lithium. (a-b) ^{7}Li background noise related to the contamination of the sampler and skimmer cones of an Element XR sector-field ICPMS. (c) ^{7}Li signal obtained by the raster laser ablation of a NIST SRM 612 glass using the same ICPMS equipped with clean sampler and skimmer cones [see Electronic Appendix 4 for experimental conditions and section '*Sources of double stochasticity, experimental constraints; Fluctuating p?*' for discussion].

Fig. 3. A schematic arrangement of the test of two independent parallel sample introduction systems; the droplet selection takes plays in the spray chambers only, no precipitates in the connecting tubing were observed [for details, see Table 2 and section '*Fluctuating M, sample introduction system*'].

Fig. 4. A schematic illustration of the mixing process in front of the sampler cone [for details, see section '*Fluctuating M, transfer of analyte inside the ICP and from the ICP to the mass spectrometer*'].

The ICPMS signal as a Poisson process: a review of basic concepts

Alex Ulianov[a],* Othmar Müntener[a] and Urs Schaltegger[b]

[a]Institute of Earth Sciences, University of Lausanne, Géopolis, 1015 Lausanne, Switzerland
[b]Section of Earth and Environmental Sciences, University of Geneva, Rue des Maraîchers 13, 1205 Geneva

Abstract

Understanding the structure of noise associated with a measurement process is interesting theoretically and has practical applications related to the quantification of detection capability, signal uncertainty and dead time. Here, we present and analyse arguments explaining the appearance of the Poisson process in the distribution of count numbers in inductively coupled plasma mass spectrometry (ICPMS) signals. We consider the Poisson distribution as a special case of the binomial distribution constrained by inefficient ion transmission from the ICP ion source to the detector. The universal form of the relevant Poisson process is doubly stochastic: the random nature of count numbers acquired per time unit is defined not only by the probabilistic selection of ions during their transport through the interface and ion channel, but also by fluctuations of the ion contents sampled by the spectrometer from the plasma and, more generally, by fluctuations of the rate of the Poisson process itself. Compared to an ordinary Poisson process, the doubly stochastic Poisson process has an excess variance that increases at higher analyte contents. The excess variance in the uncertainty of ICPMS signals is also known as flicker noise; it is an integral part of the doubly stochastic Poisson process and not a fully individual noise component. We review processes pertinent to its origin and formalisms used to describe it.

Introduction

The Poisson distribution is one of three main probability distributions in science (the other two being the Gaussian and the binomial distributions). It has been recognised for a while that Poisson, or counting, statistics play an important role in the interpretation of the ICPMS signal uncertainty. How do these statistics arise in ICPMS signals? How do they help to understand their structure and uncertainty? Trying to answer these questions, we usually recollect a well-known equation connecting count numbers and their variance. Is there anything else to recollect? Perhaps, with the outcome being not devoid of theoretical elegance and practical importance.

Let us consider an ICP mass spectrometer collecting counts during some predefined time interval T per isotope measurement. Let us assume for simplicity that the spectrometer detection system has a zero dead time, that it is operated in the counting detection regime and that its internal noise (e.g., due to thermionic and field emission from the dynodes of a secondary electron multiplier[1]) is negligible. Let us first imagine that an analyte is supplied to the interface of the mass spectrometer from the ICP ion source at a strictly constant rate [= number of ions supplied per time interval] and the spectrometer ion transmission is constant as well. Still, the observed ion count numbers will vary: our first measurement can yield N_1 counts, second measurement – N_2 counts, etc. (see section '*A binomial derivation of the Poisson process in ICPMS*'). If the number of measurements k is large, the mean value

$$\overline{N} = (N_1 + ... + N_k) / k \qquad (1)$$

is defined with a high precision. One can argue that the probability of obtaining exactly N_i counts as the outcome of a particular measurement is then defined by the law of Poisson characterised by a constant, time independent rate (intensity) I with a mean value of $\overline{N}/T$, and is as follows[1-6]:

$$p(N_i) = \frac{\overline{N}^{N_i} e^{-\overline{N}}}{N_i!} \qquad (2)$$

Besides, the variance

$$Var(N) = \overline{N} \qquad (3)$$

characterises the size of an interval, into which a particular value of N_i falls with some probability (that approaches the confidence interval of a Gauss distribution set at a mean value of $\overline{N}$ and standard deviation of $\sqrt{\overline{N}}$ at higher count numbers). The condition of a constant rate in formulae (1-3) can be relaxed: they are valid for any non-random count rate, where I is a deterministic function of time[2-5].

The obeyance of the counting results above to the Poisson law is important both theoretically and practically. In the field of detection capabilities quantification, at near zero count numbers, it allows applying the mathematical apparatus of tests for the equality of two Poisson means[7-9] to the background noise to get the critical value for detection decision in the ‘paired measurements’ framework[10]. Similarly, it allows using the cumulative probability of the Poisson distribution to compute the critical value if the background is ‘well known’[10]. At higher count numbers, the square root dependence of the Poisson uncertainty from the mean count number enables computing the critical value and the detection limit based on the Poisson-Gauss approximation[10-12]. This powerful methodology, used for a while in radioactivity measurements, is slowly entering into the practice of the ICPMS analysis[13,14].

In the field of signal uncertainty calculations, the square root relationship between count numbers and their uncertainties allows easily calculating the uncertainty of the mean rate for any deterministic, non-transient (constant count rate) as well as transient (count rate is a deterministic function of time) Poisson signal. A derivation commonly used in such calculations is as follows[15-17]:

$$s(I_{ind.\ measurement}) = s\left(N/T\right) = \frac{s(N)}{T} = \frac{\sqrt{\overline{N}}}{T} = \sqrt{\frac{\overline{N}}{T^2}} = \sqrt{\frac{I_{mean}}{T}} \qquad (4)$$

where T is the total, precisely determined acquisition time for an analyte, of which the rate is discussed, and I is the count rate. It is common to use in this equation single measurement based estimates of $\overline{N}$, since the distribution of so-estimated uncertainties is known to be very precise:

$$s(\sqrt{N}) = \frac{\partial(\sqrt{N})}{\partial N} s(N) = \frac{1}{2\sqrt{N}}\sqrt{N} = 1/2 \qquad (5)$$

Finally, the adherence of counting results to the Poisson law with a constant rate allows estimating the detection system dead time (τ) and correcting raw counts according to the familiar formulae[1,6,18]:

$$N_{corrected} = \frac{TN_{measured}}{T - \tau N_{measured}};\ I_{corrected} = \frac{I_{measured}}{1 - \tau I_{measured}} \qquad (6)$$

The relevance of the Poisson process to the description of ICPMS signals has been recognised long ago. The early experience was related to and influenced by the description of noise in ICP atomic emission spectrometry (ICP-AES). Using the Fourier transform of the sequentially acquired intensity vs. time data into the frequency domain[19,20], several noise components were identified, of which the universally occurring were a white noise and a *1/f* noise[21-25]. The white noise, of which the amplitude is frequency independent, is interpreted as the Poisson (shot) noise[26,27]. The *1/f*, or flicker, noise, vanishing at high frequencies, is interpreted as an additional noise component independent of the Poisson noise; despite the same signal is discussed, it was postulated that the variance of the total number of counts N can be given, like a variance of the sum of two independent random variables, as follows[26,27]:

$$Var(N) = Var(Poisson\ term) + Var(1/f\ term) = mean\ count\ number + Var(1/f\ term) \qquad (7)$$

This equation also exists in a sensitivity based notation[28,29] almost forgotten in modern ICP literature. ICP-AES and later ICP-MS studies empirically demonstrated that, upon increasing the analyte concentration (intensity), *Var(1/f)* term increases faster than the Poisson term in the formula above, showing a quadratic dependence on the total number of counts N collected per given time interval[21,25-31].

Below we will show that eqn (7) and relationships between its terms find an elegant explanation in the theory of compound Poisson processes. But before it is necessary to consider why the Poisson counting process appears at all in the ICPMS technique. Representative opinions on this question are as follows: (i) ‘as devices registering sums of counted ions, mass spectrometers yield Poisson distributed count numbers *per se (by itself)*’[13]; (ii) ‘since MS deals with the detection of ions, it is subject to fundamental noise arising from the particulate nature of matter’[27]; (iii) ‘all electron, ion and photon fluxes are subject to random variations in their rates described by Poisson statistics, for which the standard deviation of N counts received will be $\sqrt{N}$’[32]. Sadly, the ICPMS ion flow deviates from the last part of statement (iii), demonstrating an excess variance according to eqn (7). Besides, the opinions above are somewhat declarative. They can be developed in two directions, either by stating that the Poisson distribution appears in the ICPMS by heaven’s decree, or by deriving it based on the binomial distribution and construction of ICP mass spectrometer - a perspective reviewed in this work.

It is worth noting that, despite the declarative understanding of the origin and mathematical form of the Poisson process currently prevailing in ICPMS, a wealth of experimental data regarding the ICPMS signal fluctuations is available in the literature. Perhaps, we deal with a case when 'practical techniques … evolve extensively to provide empirical solutions to real analytical problems before the basic research is completed'[33]. The prime aim of this contribution is to present the theory of the Poisson process in the context of the available data; when required, we present new experimental data.

A binomial derivation of the Poisson process in ICPMS

Let us give a traditional example from the field of telephone statistics, where the Poisson process is often encountered. Let us consider a call centre in a large city. We discuss the number of calls registered by the centre per time interval. We argue that such numbers are Poisson distributed. Why? Each person in the city is characterised by one of two potential states: either (s)he makes a call to the centre during the time interval of interest, or not. The total number of persons is M, the probability that a given person will make a call to the centre is p. What will be the probability of receiving exactly N calls during the dwell time? To answer this question, let us interpret M as the number of Bernoulli trials (making or not making a call). The probability of receiving exactly N calls is then defined by the binomial probability distribution function; generally, it depends on M and p:

$$probability\ (N|M,p)=\frac{M!}{(M-N)!\,N!}p^{N}(1-p)^{M-N} \qquad (8)$$

The variance of the number of calls is as follows: $Var(N)=pM(1-p)$. Let us further suppose that M is very large (large population), while p is very small (how often do we call to a particular call centre?). At these conditions, the formula above can be reorganised. The corresponding derivation is classical. To preserve this text consistency, we present it here following a notation from Barrett and Myers[5] and Rainwater and Wu[6]. Substituting $p=\overline{N}/M$ yields:

$$probability\ (N|M,p)=\left[\frac{M(M-1)...(M-N+1)}{M^{N}}\left(1-\frac{\overline{N}}{M}\right)^{-N}\right]\left(1-\frac{\overline{N}}{M}\right)^{M}\frac{\overline{N}^{N}}{N!} \qquad (9)$$

At $M\rightarrow+\infty$ and $\frac{\overline{N}}{M}=p\rightarrow 0$, the term in square brackets limits to 1. Besides, $\lim_{M\rightarrow+\infty}\left(1-\frac{\overline{N}}{M}\right)^{M}=e^{-\overline{N}}$. Hence,

$$\lim_{M\rightarrow+\infty\ p\rightarrow 0}\left[probability\ (N|M,p)\right]=\frac{\overline{N}^{N}e^{-\overline{N}}}{N!} \qquad (10)$$

i.e., the binomial distribution is approximated by a Poisson distribution with a mean of $\overline{N}=pM$ = the mean number of calls registered per time interval. The variance is also equal to $\overline{N}(=pM)$, since the (1-p) term in the formula $Var(N)=pM(1-p)$ is close to unity at small p and can be neglected.

Reworking this example in the context of ICPMS analysis is as follows. The call centre is the detector, while the population of call candidates is represented by ions in the torch. Let us first intentionally simplify the picture and assume that a large, constant number of ions M face the sampler orifice per given time interval. Facing the sampler orifice can be interpreted for an ion as facing a Bernoulli trial to be or not to be registered by the detection system. The probability p for each particular ion to get to the detector is very low: the ICP is an ion source operated at atmospheric pressure, as eddy currents maintaining the plasma by resistive heating cannot occur *in vacuo*. To transport ions from such a source inside the spectrometer ion channel, kept under vacuum, the principle of differential pumping[34,35] is used in all modern ICPMS. During the differential pumping, a large fraction of ions is lost between the sampler and the skimmer (in a conventional interface design, according to commonly used estimates, only ~1% of all ions passing through the sampler orifice then enter the skimmer orifice[36-39]). To these losses, incomplete extraction of the ions from the interface and their incomplete transmission inside the ion channel should be added, especially for light ions[27,39] and for ion beams analysed using quadrupole instruments[40] (especially of older designs[41]) and (sector field) instruments operated at a high resolution[40,42]. With older quadrupole ICPMS, only one ion is registered by the detection system for every 10^4-10^6 ions through the skimmer[43,44]; the quest for a more efficient extraction and transmission is still underway[39]. Finally, irrespective of the dead time related losses, the secondary electron multiplier is usually not 100% efficient in registering the arriving ions, as illustrated by the routine practice to optimise it - at the expense of its life time - by increasing inter-dynode voltages[45,46].

Thus, the whole probability p for an ion to get from the torch to the detector and be registered is low: the extreme versatility of the ICP ion source with respect to the sample introduction technique[47,48], connected with its operation at atmospheric pressure, is counterbalanced by an inefficient utilisation of ions obtained from the ICP. At high M and low p, the probabilities to register a particular number N of ion arrivals per time interval are approximated by a Poisson process with a mean of $\overline{N} = pM$. Similar considerations can be given regarding the noise generated inside the detector due to field and thermionic emission (e.g., a number of atoms is potentially subject to thermionic emission from the dynode surface, but the probability for a given atom to yield a free ion is small, at least at room temperature).

Henceforth, we will call p transmission efficiency and will strictly define it as the probability for an ion entering the orifice of the sampler cone to be registered by the detection system, adding a count to the total number of counts collected during an analysis of a given isotope.

In the sense of the above examples, the inefficiency of the ion transmission process in ICPMS and, consequently, the rarity of registered ions compared to the total number of ions generated in the ICP and facing the sampler orifice is the meaning of the statement ‘rarity begets poissonicity’, mentioned in the literature in a variety of forms (e.g., the ‘law of rare events’). A rich collection of further examples illustrating this statement can be found in refs. 2,3,5 and 49. Among these examples, binomial selection of photons emitted in a narrow sector from a spherical or cylindrical light source[5] could be mentioned, especially in the context of optical spectroscopic techniques, including ICP-AES.

An elementary introduction to doubly stochastic Poisson processes

Fluctuating M and p

In the simplified example above, M - the number of ions exposed to the sampler orifice for the whole duration of analysis - is constant: if we replicate the analysis, M remains the same, although the number N of counted ions is generally different from the first analysis. Besides, the transmission efficiency p remains constant from analysis to analysis. Consequently, $\overline{N}$ represents a constant value. A binomial selection from M at small p results in a Poisson distribution, of which the variance is $\overline{N} = pM(1-p) \approx pM$. The corresponding process can be called ordinary Poisson process.

Let us now consider a more general case when M and p randomly change from analysis to analysis. It could be imagined that a subset of N values is acquired at one M and p, an other subset – at an other M and p, etc., after which all subsets are mixed in proportions corresponding to the probability of occurrence of a given product pM (Fig.1). The corresponding process is called doubly stochastic Poisson process[2,5,50], compound or mixed Poisson process[4,49], or Cox process, in honour of its discoverer[51].

The mixing above results in the appearance of an excess variance in the distribution of count numbers that can be described quantitatively. Propagating errors in squares, we obtain:

$$Var(\overline{N}) = Var(pM) = \overline{p}^2 Var(M) + \overline{M}^2 Var(p) + 2\overline{p}\,\overline{M}Cov(p,M) \qquad (11)$$

However, $Var(\overline{N})$ describes the scatter of the mean count numbers $\overline{N}_i = p_i M_i$, while our purpose is to characterise the scatter in N, i.e. in the individual count numbers obtained from the analyses participating in our exercise (Fig. 1). To this purpose, we introduce the following substitution:

$$N = \varepsilon + \overline{N} \qquad (12)$$

where ε represents a Poisson error observed in a particular analysis relative to the mean count number value $\overline{N}$ associated with this analysis.

Assuming that $\overline{N}$ is not very small, we neglect covariance between ε and $\overline{N}$ and obtain:

$$Var(N) = Var(\varepsilon + \overline{N}) = Var(\varepsilon) + Var(\overline{N}) \qquad (13)$$

Let us consider the ε-term of this equation:

$$Var(\varepsilon) = \frac{1}{n}\sum_{i=1}^{n}(\varepsilon_i - \overline{\varepsilon}_i)^2 = \frac{1}{n}\sum_{i=1}^{n}\varepsilon_i^2 = \frac{1}{n}\sum_{i=1}^{n}(N_i - \overline{N}_i)^2 = \frac{k_1}{n}\frac{\sum_{i=1}^{k_1}(N_{1\,i} - \overline{N}_1)^2}{k_1} + \ldots + \frac{k_m}{n}\frac{\sum_{i=1}^{k_m}(N_{m\,i} - \overline{N}_m)^2}{k_m}$$
$$= \frac{k_1}{n}\overline{N}_1(1-\overline{p}_1) + \ldots + \frac{k_m}{n}\overline{N}_m(1-\overline{p}_m) = \overline{\overline{N}} - \left[\frac{k_1}{n}\overline{N}_1\overline{p}_1 + \ldots + \frac{k_m}{n}\overline{N}_m\overline{p}_m\right] \approx \overline{\overline{N}}$$
$$(14)$$

Here, k_i is the number of Poisson outcomes scattered around a particular value of $\overline{N}_i$; consequently, $\frac{k_i}{n}$ is the probability to encounter an analysis associated with a particular $\overline{N}_i$ value. $\overline{p}_i$ is the mean transmission efficiency at each $\overline{N}_i$ value. $\overline{\overline{N}}$ is the mean count number obtained by averaging all individual counts collected at the different $\overline{N}_i$ values; hence the sign of double summation to designate it.

Combining eqn (11-14), we obtain:

$$\begin{aligned} Var(N) &= Var(\varepsilon) + \overline{p}^2 Var(M) + \overline{M}^2 Var(p) + 2\overline{p}\,\overline{M}Cov(p,M) \\ &\approx \overline{\overline{N}} + \overline{p}^2 Var(M) + \overline{M}^2 Var(p) + 2\overline{p}\,\overline{M}Cov(p,M) \end{aligned} \qquad (15)$$

The term $\overline{p}^2 Var(M) + \overline{M}^2 Var(p) + 2\overline{p}\,\overline{M}Cov(p,M)$ in the equation above can be called excess variance[5] to emphasize that the variance of a doubly stochastic Poisson process is higher compared to the variance of an ordinary Poisson distribution (cf. eqn 7). More generally, it is correct to think that the excess variance of a doubly stochastic Poisson process just represents variance of the Poisson means constituting this process (see eqn 12,13 and Fig. 1). For an ordinary Poisson process, the mean is fixed and the excess variance is zero.

Fluctuating M, constant p: single isotope

At a constant p, eqn (13,14) can be simplified:

$$Var(\varepsilon) = \frac{1}{n}\sum_{i=1}^{n}(\varepsilon_i - \overline{\varepsilon}_i)^2 = \frac{k_1}{n}\overline{N}_1(1-p) + \ldots + \frac{k_m}{n}\overline{N}_m(1-p) = \overline{\overline{N}}(1-p) \approx \overline{\overline{N}} \qquad (16)$$

$$Var(N) = Var(\varepsilon) + p^2 Var(M) = \overline{\overline{N}}(1-p) + p^2 Var(M) \approx \overline{\overline{N}} + p^2 Var(M) \qquad (17)$$

A derivation for eqn (16) employing integrals as the limiting form of sums can be found in Barrett and Myers[5]. Yet another derivation is given in section '*Fluctuating M, constant p: isotope ratio*' below.

The case of fluctuating M and constant p has important properties depending on the distribution of M. If, as a special case, it is Poissonian, then changes compared to the situation at a constant M are negligible: according to formula (17), the excess term $p^2 Var(M) = p^2\overline{M} = p\overline{\overline{N}}$ and $Var(N) = \overline{\overline{N}}$: a binomial selection from an ordinary Poisson distribution results in an ordinary Poisson distribution, a rule known as binomial selection theorem[5]. On increasing *Var(M)* further the excess variance term becomes more important. Let us consider an arbitrary example where a Poisson mean of 10^6 counts is obtained and the count number variance amounts to 2x10^6 counts: this is twice as large as the variance predicted by the ordinary Poison statistics. Let us set p at 0.01%. Based on formula (17), we obtain:

$$\begin{gathered}Var(N)=2\times10^{6}\approx10^{6}+(10^{-4})^{2}\,Var(M)\Rightarrow Var(M)\approx10^{14};\;\; s(M)\approx10^{7};\\ \overline{M}=\overline{\overline{N}}\,/\,p=10^{6}\,/\,10^{-4}=10^{10};\;\; RSD\%(M)\approx\left[10^{7}\,/\,10^{10}\right]\times100=0.1\%\end{gathered}\tag{18}$$

It is instructive to compare this result with values obtained under the assumption that M is ordinary Poisson distributed, assuming that $\overline{\overline{N}}$ and p remain the same as in the example above:

$$\begin{gathered}Var(M)\approx\overline{M}=\overline{\overline{N}}\,/\,p=10^{6}\,/\,10^{-4}=10^{10};\;\; s(M)\approx10^{5};\\ RSD\%(M)\approx(10^{5}\,/\,10^{10})\times100=0.001\%;\;\; \overline{\overline{N}}=Var(N)=10^{6}\times0.9999+(10^{-4})^{2}10^{10}=10^{6}\end{gathered}\tag{19}$$

Calculations (18,19) show that, for this particular setup, a twofold increase in the variance of count numbers collected, or otherwise a 1.4 times increase in their standard deviation, is caused by a 100-fold increase of the relative standard deviation of the number of ions in the primary ion population [*RSD%(M)*] - from *0.001* to *0.1%*. Still, even at *RSD%(M)*=0.1% the distribution of M remains rather precise: there is no need to have a very large scatter in M to observe consequences for *Var(N)*.

If both M and p are constant, formulae (15-17) converge to the variance formula for an ordinary binomial distribution: $Var(N)=\overline{N}(1-p)$, and further to the Poisson expression $Var(N)=\overline{N}$ by omitting the (1-p) term at small p.

Fluctuating M, constant p: isotope ratio

In applications, quantification of ICP signals usually requires handling count number (intensity) ratios and not only the individual count numbers[17,27,52-58]. The corresponding Poissonian formalism is briefly discussed below. First, let us generalise formula (17) using the property of bilinearity of covariance:

$$\begin{aligned}Cov(N^{x},N^{y})&=\sum_{i=1}^{n}\frac{(N_i^{x}-\overline{\overline{N}}^{x})(N_i^{y}-\overline{\overline{N}}^{y})}{n}=\sum_{i=1}^{n}\frac{(\varepsilon_i^{x}+p^{x}M_i^{x}-p^{x}\overline{M}^{x})(\varepsilon_i^{y}+p^{y}M_i^{y}-p^{y}\overline{M}^{y})}{n}\\ &=p^{x}p^{y}\sum_{i=1}^{n}\frac{(M_i^{x}-\overline{M}^{x})(M_i^{y}-\overline{M}^{y})}{n}+\sum_{i=1}^{n}\frac{\varepsilon_i^{x}\varepsilon_i^{y}}{n}+p^{y}\sum_{i=1}^{n}\frac{\varepsilon_i^{x}(M_i^{y}-\overline{M}^{y})}{n}+p^{x}\sum_{i=1}^{n}\frac{\varepsilon_i^{y}(M_i^{x}-\overline{M}^{x})}{n}\end{aligned}\tag{20}$$

Here, N^x and N^y are count numbers for isotopes x and y recorded by ICPMS, M^x and M^y are numbers of ions aspirated by the sampler orifice, p^x and p^y are transmission efficiencies, and ε□□□□□□ε^y are Poisson errors defined according to eqn (12,13). Since the mathematical expectation of a product of two independent random variables is equal to the product of their mathematical expectations, two last terms in eqn (20) equal zero. The second term also equals zero, if x and y are two different isotopes with independent Poisson errors in their count numbers; otherwise it is equal to $\overline{\overline{N}}(1-p)$ (eqn 16). We obtain:

$$Var(N)=Cov(N,N)=p^{2}Var(M)+\overline{\overline{N}}(1-p)\;\;\big|x=y\tag{21a}$$

$$Cov(N^{x},N^{y})=p^{x}p^{y}\sum_{i=1}^{n}\frac{(M_i^{x}-\overline{M}^{x})(M_i^{y}-\overline{M}^{y})}{n}=p^{x}p^{y}Cov(M^{x},M^{y})\;\;\big|x\neq y\tag{21b}$$

Formula (21a), derived under the condition that x and y represent the same isotope, is identical to (17). Formula (21b), derived under the condition that x and y are two different isotopes, establishes correlation properties of the observed signal and of the ion population in the ICP ion source. At constant transmission efficiencies, a correlation in the source implies a correlation in the signal, and vice versa. The presence of such a correlation is desirable, as it reduces isotope ratio uncertainty[52-56]:

$$\begin{aligned}Var\left(\frac{N^{x}}{N^{y}}\right)&=\left(\frac{1}{\overline{\overline{N}}^{y}}\right)^{2}Var(N^{x})+\frac{(\overline{\overline{N}}^{x})^{2}}{(\overline{\overline{N}}^{y})^{4}}Var(N^{y})-2\left(\frac{1}{\overline{\overline{N}}^{y}}\right)\left(\frac{\overline{\overline{N}}^{x}}{(\overline{\overline{N}}^{y})^{2}}\right)Cov(N^{x},N^{y})\\ &=\left(\frac{1}{\overline{\overline{N}}^{y}}\right)^{2}Var(N^{x})+\frac{(\overline{\overline{N}}^{x})^{2}}{(\overline{\overline{N}}^{y})^{4}}Var(N^{y})-2\left(\frac{1}{\overline{\overline{N}}^{y}}\right)\left(\frac{\overline{\overline{N}}^{x}}{(\overline{\overline{N}}^{y})^{2}}\right)p^{x}p^{y}Cov(M^{x},M^{y})\end{aligned}\tag{22}$$

It is interesting to consider formula (22) as a function of the Pearson's correlation coefficient

$$\rho(M^x,M^y)=\frac{Cov(M^x,M^y)}{\left[Var(M^x)Var(M^y)\right]^{1/2}}\in\left[-1;+1\right]\qquad(23)$$

Introducing the correlation coefficient in eqn (22) results in an elementary but bulky derivation given in Electronic Appendix 1. This derivation can be reduced at the condition that standard deviation of *M* is proportional to *M* (*s(M)/M=Const*, see section '*Fluctuating M, sample introduction process*' and refs. 25-31 regarding the validity of this condition), yielding the following formula:

$$RSD\%\left(\frac{N^x}{N^y}\right)=\left[\frac{1}{\overline{\overline{N}}^x}+\frac{1}{\overline{\overline{N}}^y}+2\left[1-\rho(M^x,M^y)\right]\frac{s(M^x)}{\overline{M}^x}\frac{s(M^y)}{\overline{M}^y}\right]^{1/2}\times100\qquad(24)$$

In two cases - (i) primary ion populations fluctuate and perfectly correlate, simultaneously increasing or decreasing by the same fraction from analysis to analysis [$\rho(M^x,M^y)=1$] or (ii) primary ion populations are constant [$s(M^x),s(M^y)=0$], which corresponds to the ordinary Poisson process with variance equal to mean count number - this equation can be truncated and given in a more familiar form:

$$RSD\%\left(\frac{N^x}{N^y}\right)=\left[\frac{1}{N^x}+\frac{1}{N^y}\right]^{1/2}\times100\qquad(25)$$

Eqn (25) allows for a simple derivation based on the ordinary Poisson statistics only[27] and is often mentioned in the literature[27,57,58]. The coincidence between (i) and (ii) has a rigorous explanation: for perfectly correlating primary populations M^x and M^y, the excess variances of the individual isotope count numbers and the covariance term in eqn (19) cancel each other (see Electronic Appendix 1). The precision of isotope ratio analyses obtained at these conditions is limited, like for the ordinary Poisson distribution, by count numbers N^x and N^y. In all other cases, which include fluctuating primary populations that correlate only partly [$\rho(M^x,M^y)<1$], the relative standard deviation defined by the general equation (24) is higher compared to (25); in other words, the covariance term in eqn (19) decreases and the ratio uncertainty increases. Eqn (25) yields a minimum possible uncertainty in these cases. Strongly correlated signals are known to be the domain of multi-collector (MC-) ICPMS[52]. For count numbers in the order of 10^8, eqn (24,25) yield a minimum $RSD(N^x/N^y)$ of 0.005-0.02%, which falls within the range of isotope ratio uncertainties typically quoted for MC-ICPMS instruments[27,57,58].

Corroborating eqn (24) experimentally is hampered by the need to know the statistics of *M* that are not directly observable. For strong signals, simple approximations can still be made. Owing to the *s(M)~M* dependence, the excess variance can be the dominating variance component of such signals[28,29]:

$$Var(N)=Var(\varepsilon)+Var(\overline{N})=\overline{\overline{N}}+p^2Var(M)\approx p^2Var(M)=Var(\overline{N})\;\Big|\;p^2Var(M)>>\overline{\overline{N}}\qquad(26)$$

Combining eqn (24) and (26), we obtain (see Electronic Appendix 1):

$$RSD\%\left(\frac{N^x}{N^y}\right)=\left[\frac{1}{\overline{\overline{N}}^x}+\frac{1}{\overline{\overline{N}}^y}+2\left[1-\rho(N^x,N^y)\right]\frac{s(N^x)}{\overline{\overline{N}}^x}\frac{s(N^y)}{\overline{\overline{N}}^y}\right]^{1/2}\times100\qquad(27)$$

A practical comparison of count number relative standard deviations obtained from eqn (27) and (22) shows a good match. For example, measuring the ^{143}Nd/^{145}Nd count number ratio in the solution nebulisation regime at low resolution using an Element XR sector-field ICPMS, we obtained *RSDs* of 0.18 and 0.19%, respectively (see Table 1 for further details and examples, and Electronic Appendix 2 for raw data and calculus). These values also agree with uncertainty values obtained from the mean-of-ratios definition of the isotope ratio for a time-resolved signal[17,54-56] (Table 1, Electronic Appendix 2):

$$RSD\%\left(\frac{N^x}{N^y}\right)=\frac{s\left(\frac{N^x}{N^y}\right)_{ind.\ sweep}}{\sqrt{n_{sweeps}}\left(\frac{N^x}{N^y}\right)_{mean}}\times100,\ \text{where}\ \left(\frac{N^x}{N^y}\right)_{mean}=\frac{\sum_{i=1}^{n_{sweeps}}\left(\frac{N^x}{N^y}\right)_{i\ ind.\ sweep}}{n_{sweeps}}\qquad(28)$$

Comparing ratio-of-means and mean-of-ratios uncertainties (eqn 22,27 vs. 28) is generally justified, at least at high count numbers (see refs. 54-56 and 59, as well as Electronic Appendix 3).

Noteworthy, a good match between the estimated $s(M^x)/s(M^y)$ ratio and the reference ratio of these isotopes supports the assumption $s(M)\sim M$ underlying eqn (24,27) (Table 1). At this point, an elementary mathematical description of fluctuations in ion transmission efficiency and primary ion population in ICPMS signals is provided and a discussion of the sources of such fluctuations is due.

Sources of double stochasticity in ICPMS: experimental constraints

Fluctuations of ion transmission efficiency (p) and primary ion population in the torch (M) are two general sources of double stochasticity. In the existing ICP literature, their role has never been formalised and described theoretically using the mathematical apparatus of binomial selection or more advanced methods related to the mathematical description of double stochasticity (see section '*Double stochasticity and fluctuations of the rate*'). Still, experimentally their role has been recognised, (often) thoroughly described and much discussed, in the context of sample introduction by solution nebulisation especially; below we will refer to the corresponding literature when appropriate.

Fluctuating p?

In the p,M-convention used in this text, fluctuations in p depend on the performance of the spectrometer ion channel and on the performance of the sampler to skimmer ion transfer; the latter possibility will be reviewed in a subsequent section, along with other processes related to the analyte transfer through the ICP and interface. Here, we consider the ion channel only. Electric (magnetic) fields inside the channel should not be the subject of *random* changes during a measurement (should have a good repeatability between measurements); otherwise, the analyst is confronted with the statistics of p.

The possibility of such fluctuations and their role in compromising the precision of ICPMS data, especially when using early quadrupole ICPMS instruments operated in the peak-hopping mode, has been mentioned long ago [e.g., ref. 60]. This issue depends on the instrument and its mode of operation. Compromised isotope ratio uncertainties obtained at higher resolutions on sector-field instruments are sometimes also ascribed to this issue: narrow peaks observed at such conditions and scanned in the peak hopping regime require the highest mass calibration stability to avoid fluctuations in p[58]. Of course, ion transmission losses at a high resolution and, consequently, a reduction in the total number of counts collected per analysis are an additional explanation to these uncertainties (cf. eqn 24,25). High-resolution peak hopping analysis is unlikely a widespread practice in modern ICPMS. Low resolution peaks are wider and characterised by parabolic (quadrupole MS) or flat top trapezoidal (well maintained and tuned sector field MS) geometry that reduces the possibility of transmission efficiency fluctuations in the peak hopping regime. This feature helps stabilising the ion transmission efficiency and is recognised in the literature as one of key advantages of low resolution sector field ICPMS for high precision isotope ratio determinations[40,57,58,61]. Still, before deriving more definite conclusions regarding the role of fluctuations in p, the latter should be separated from fluctuations in M.

The role of fluctuations in p can be separately evaluated using a stable and sufficiently strong ion emitter placed at the beginning of the ion channel, which basically requires no sample introduction system to be interfaced to the ICPMS and minimises the role of random processes in the ICP torch. One such emitter that operates without modification to the spectrometer construction represents sampler and skimmer cones contaminated with lithium during the LA-ICPMS analysis of lithium tetraborate glass beads[62]. The associated pollution of the instrument belongs to canonical examples of contamination in ICPMS[63]. The cones seem to be the main source of this pollution: replacing the sampler and skimmer cones of our Element XR ICPMS reduces the ^{7}Li background intensity from c. 3-5x10^5 to ~4x10^3 cps in the laser ablation regime; cleaning the ablation cell and the torch and replacing the tubing further reduces these values down to ~2x10^3 cps; the extraction lens was not replaced neither cleaned. Noteworthy, the role of the sampler in the lithium contamination budget is relatively insignificant compared to the skimmer; according to our experience, a contaminated skimmer accounts for more than 90% of the total background of lithium (few ions derived from the inner surface of the sampler orifice at the outermost boundary of the ion beam then pass through the skimmer).

We mounted contaminated sampler and skimmer cones on an Element XR otherwise cleaned as described above, and collected ^{7}Li background intensities using two different protocols (Fig. 2). Then, we replaced the both cones with uncontaminated ones and, without changing the tuning of the spectrometer, obtained signals of similar intensity by raster laser ablation of the NIST SRM 612 standard, which represent a soda-lime-silica glass doped with a range of trace elements, including lithium.

Sweep counts collected in the experiments with the contaminated cones closely follow the ordinary Poisson statistics. Sweep counts collected in the laser ablation experiments show uncertainties that are ~ 3 times higher than the uncertainties predicted by the ordinary Poisson distribution (Fig. 2). Although such results can be instrument dependent and, perhaps, less straightforward if very short mass discriminator settle times are applied, currently they do not allow suspecting that, for low-resolution work using modern ICP mass spectrometers, p perceivably fluctuates. Neither can this be suspected based on the main body of literature data acquired using modern ICPMS instruments.

Fluctuating M, sample introduction process?

The role of the sample introduction process in fluctuations of ICP signals was noticed in a number of studies. As early as 1980, Myers and Tracy demonstrated that the relative standard deviation of the carbon emission signal at 247.9 nm increases by a factor of ten if the sample is introduced in the ICP as an aerosol (sugar in water), compared to a gaseous mixture of carbon dioxide and argon[52,64]. They detected a strong correlation between the fluctuations of laser light scattered from the sample aerosol and simultaneously recorded emission signal, and noted that 'fluctuations in analyte emission are directly related to fluctuations in aerosol density', while the plasma itself 'is a very stable emission source'[52,65]. In the late 1980's, Antanavičius and co-workers studied ICP-AES signals for gaseous samples and aerosols obtained by solution nebulisation and injection of metal oxide powders in the ICP[66-68]. It was shown that the power spectral density of low frequency (flicker) noise obtained for aerosols increases by an order of magnitude compared to gaseous samples. Similar data (for helium ICP) were obtained by Montaser and co-workers[69]. Besides, ICP-AES signal fluctuations due to the passage of the individual droplets through the ICP were documented; besides, the role of the droplet desolvation process in the signal fluctuations was noticed[70,71]. Research from the 1990's, including papers by Olesik[71-73], Houk[74,75] and co-workers, proved that such fluctuations also occur in ICPMS signals and focussed on a detailed characterisation of the behaviour of droplet aerosols in the ICP, followed by studies of particles obtained by laser ablation in the 2000's[76-81]. Based on the investigation of ICPMS signals resolved on a tens of microsecond time scale that allowed detecting strong intensity peaks and dips connected with the passage of large individual droplets through the ICP, Hobbs and Olesik concluded: 'the behaviour of ICPMS signals is consistent with changes in ion number density in the plasma', and 'the sample introduction process is typically the main source of flicker noise in ICP spectrometry'[71]. An understanding was reached[52,64-73,82] that processes related to the introduction of aerosols in the ICP are essential in the appearance of 'what may be termed the ion distribution noise… caused by the inhomogeneous spatial distribution of analyte ions in the central channel of the plasma which carries the sample aerosol…'[83]. Also, there is a consensus that introducing a gaseous sample in the ICP, compared to the nebulisation of solutions, strongly reduces the excess variance of ICP-AES signals[52,64,66-69], confirming that the ICP is indeed a 'stable emission source'[52] (admittedly, nebulisers used in those studies were likely noisier than modern micronebulisers, making nebulisation uncertainties worse than they could be). Beyond solution nebulisation and laser ablation ICPMS, important data regarding the heterogeneity of the analyte spatial distribution can be found in the literature of atomic absorption spectrometry[84] and electrothermal vaporisation - ICPMS[85].

One could conclude that, for a sample introduction system supplying the analyte at a randomly changing rate because it 'produces noisy aerosols'[52,64-83,85,86], the statistics of M is essentially the statistics of this rate. How to model these statistics? ICP studies[69-75] show that the arrival of droplets in the ICP is a random process and emphasize the role of larger drop and particle sizes in signal fluctuations. It is also worth noting that some of the most precise single collector ICPMS data were acquired using tandem spray chambers especially efficient in removing large droplets[86-88]. Droplet (particle) transport processes are quantitatively complex, as are desolvation / vaporisation of larger droplets and particles in the ICP (given their potential to leave residues and influence the surrounding plasma properties[72-75]). Simplified statistical conclusions describing the role of drop size for the precision of ICPMS signals can still be given. Let us consider a solution nebulisation setup including a pneumatic nebuliser coupled to a double pass or cyclonic spray chamber[33,82,86]. The nebuliser produces tens, possibly hundreds of millions of droplets per second that enter the spray chamber with a velocity of several tens of meters per second[86]. The droplet size distribution is a key characteristic of the nebuliser[82,86,89]; however, to simplify the analysis, we will assume that the nebuliser is mono-dispersive (i.e., it produces droplets of the same size), that the number of droplets produced by the nebuliser per analysis is constant and that droplet alteration (evaporation, fragmentation, agglomeration) can be neglected. A significant part of the droplets is lost *en route* to the torch: in conventional setups run at a flow rate of 0.5-1.5 mL/min, gravitational settling, losses related to gas turbulences and inertial impact losses on the walls of the spray chamber reach 96-98% and more[82,86]. Let us define M^* as the total number of analyte atoms (dissolved ions) reaching the ICP in the form of droplets per analysis (per time interval), N^* as the total number of droplets reaching the ICP per analysis, p^* as droplet transport efficiency, or probability for a single droplet to pass through the spray chamber and reach the ICP, c^* as the number of analyte atoms (dissolved ions) in a droplet, and $\overline{M}^*$, $\overline{N}^*$ and $\bar{c}^*$ as the mean values of these parameters, respectively. We obtain:

$$M^* = \bar{c}^* N^*;\ Var(M^*) = (\bar{c}^*)^2 Var(N^*) + (\overline{N}^*)^2 Var(\bar{c}^*) \qquad (29)$$

Using eqn (29) requires the individual variance terms to be determined. As N^* results from a binomial selection during droplet transportation to the ICP, we have:

$$Var(N^*) = \overline{N}^*(1 - p^*) \qquad (30)$$

Explaining $Var(\bar{c}^*)$ might require referencing to classical literature of statistical physics to show that, in the strict sense, c^* and $\bar{c}^*$ are random parameters. Landau and Lifshitz[90] introduce the Poisson distribution as a distribution of gas molecule numbers in a small sub-volume of a main gas volume. As the number of molecules in the main volume is large and the probability for each molecule to occur in a small sub-volume of the system is small, the arising distribution is Poissonian (for two-dimensional examples of this kind, see refs. 3,91). Similarly, for the distribution of analyte particles in small droplets formed from a main volume of solution we obtain:

$$Var(\bar{c}^*) = Var(c^*)/\overline{N}^* = \bar{c}^*/\overline{N}^* \qquad (31)$$

Combining eqn (29-31) yields:

$$Var(M^*) = (\bar{c}^*)^2 \overline{N}^*(1 - p^*) + \bar{c}^* \overline{N}^* = \overline{M}^* \bar{c}^*(1 - p^*) + \overline{M}^* \qquad (32)$$

Thus, inefficient pneumatic nebulisers indeed produce noisy tertiary aerosols, of which the noise only increases compared to eqn (32), provided various ‘non-idealities’ – renebulisation[86], (possibly) turbulences at the exit of the nebuliser[86], argon backpressure and uptake rate instabilities[92] - are considered.

According to eqn (32), the dependence between the analyte concentration and the variance of the primary ion population is almost exactly quadratic in a wide range of analyte contents (except for very low contents), well in accord with empirical observations[25-31]. At the same time, for a given M^*, increasing the number of droplets at the expense of the number of analyte atoms per droplet results in a linear decrease of *Var(*M^**)* - which seems to be one of several reasons explaining the desire of the ICP community to reduce the size of droplets produced by solution nebulisation[82,86]. For a gaseous sample as a limiting case of aerosol ($c^* = 1,\ p^* = 1$), eqn (32) degenerates to $Var(M^*) = \overline{M}^*$ and the excess variance vanishes, provided the sample introduction process is its only source.

Still, the extent of influence of the analyte density fluctuations due to the droplet selection (eqn 32) on the signal uncertainty should not be overestimated. For example, for droplets with a diameter of 5 µm containing 1.22 n□/g of ^{143}Nd [=10 ng/g of Nd], for a droplet transport efficiency p^* close to zero and a mass spectrometer ion transmission efficiency p of 0.01%, the calculated excess variance amounts to 3.4% of the total number N of counted ions (i.e., of the ‘ordinary’ Poisson variance). For 10 µm droplets, it increases to 26.9%, which is still a moderate value (see Electronic Appendix 5). At the same time, solution nebulisation ICPMS signals roughly corresponding to the above setup show a marked excess variance (e.g., Table 1). Are there some other factors beyond the random analyte supply by the sample introduction system involved in the generation of the excess noise of ICPMS signals?

Here, we propose a test helping to estimate the relative contribution of the randomly changing sample introduction rate to the signal uncertainty. This test could be called *test of independent parallel sample* *introduction systems*; it is similar to the dual nebuliser test of Olesik and co-workers[70], but adapted for a mass spectrometer that does not allow a (quasi-) simultaneous data acquisition. Two nebuliser-spray chamber setups, possibly but not necessarily identical, are interfaced to the ICP torch injector through an Y-type connector (Fig. 3). Three signals are recorded. The first signal is obtained by aspirating a sample solution through the first nebuliser and spray chamber; in the meanwhile, the second nebuliser aspirates a high-purity nitric acid solution used for the dilution of the sample. To acquire the second signal, the roles of the nebulisers are reversed: the first nebuliser aspirates the high-purity nitric acid solution, while the second nebuliser – the sample. The third signal is obtained by the simultaneous aspiration of the sample using both nebulisers with their respective spray chambers. The purpose of the test is to compare the excess variances obtained from the above signals [$Var(M_1)$, $Var(M_2)$ and $Var(M_1+M_2)$, respectively]. The general expression for the variance of the sum of two random but (possibly) correlating variables is as follows:

$$Var(M_1+M_2)=Var(M_1)+Var(M_2)+2Cov(M_1,M_2) \qquad (33)$$

If these variables fluctuate independently of each other, then the covariance term of this equation vanishes and the relationship simplifies:

$$Var(M_1+M_2)=Var(M_1)+Var(M_2) \qquad (34)$$

If these variables are perfectly correlated, simultaneously increasing or decreasing by the same fraction in response to a common noise-generating process, then $\rho(M_1,M_2)=1$ and, consequently,

$$Cov(M_1,M_2)=\left[Var(M_1)Var(M_2)\right]^{1/2}=s(M_1)s(M_2) \qquad (35)$$

Therefore, in the case of a perfect correlation, eqn (30) can be rewritten as follows:

$$s(M_1+M_2)=s(M_1)+s(M_2) \qquad (36)$$

Eqn (34) and (36) describe two limiting cases. If we assume the rest of the measurement process to be a stable system introducing no further fluctuations in the primary ion statistics, then M_1 and M_2 fluctuations reflect the (in)stability of their respective sample introduction systems; since these systems are independent, there should be no correlation between their outputs [$Cov(M_1,M_2)=0$, eqn (34) hold true]. If we assume that the both sample introduction systems are stable and the source(s) of fluctuations in the primary ion statistics (and, more generally, sources of the excess variance of ICPMS signals) are hidden somewhere deeper in the ICPMS chain, then M_1 and M_2 have to respond to these fluctuations simultaneously and strongly co-vary [hence, eqn (36) holds true].

An implementation of this test is detailed in Table 2. Two pneumatic self-aspirating PFA µFlow micronebulisers (Elemental Scientific) with uptake rates of 159 and 113 µL/min interfaced to cyclonic spray chambers were employed. These nebulisers produce fine aerosols with a good transport efficiency; courtesy of the liquid prefilming in the nozzle, they operate at a low backpressure and allow using moderate argon flow rates[86,93]. For all isotopes studied (^{135}Ba, ^{137}Ba, ^{142}Ce; see Table 2), eqn (36) described the uncertainty budget of the test much better than eqn (34). Besides, the $s(M)$~M law was again confirmed, which highlights the close relationships between this law and the presence of internal correlation in the signal (for a discussion, see Electronic Appendix 6). The test is not very precise, however (as the $s(M_1)$, $s(M_2)$ and $s(M_1+M_2)$ values obtained from individual analyses are statistical estimates of uncertainty, these values have their own uncertainties; hence a scatter in the correlation coefficients computed from the covariance values derived from eqn (33), see Electronic Appendix 7).

Albeit specific to a given instrumentation, results of this test show that the randomised analyte supply from the sample introduction system is only one and, in the present case, not the main source of fluctuations in the primary ion statistics. We conclude that the evidence for noise associated with the aerosol introduction in the ICP is (i) generally unquestionable and well documented, although (ii) such noise cannot be the only reason to explain the appearance of excess uncertainty in ICPMS signals.

Fluctuating M, transfer of analyte inside the ICP and from the ICP to the mass spectrometer?

The result of the above test agrees with old ICP-AES data of Olesik and co-workers that demonstrated a good correlation between Ba and Ca emission signals at 8 mm above the load coil, despite each of these elements was supplied to the ICP through its own nebuliser / spray chamber[70]. This correlation vanished at 19 mm above the coil. The phenomenon was explained by the fluctuation of the plasma temperature caused by the desolvation of the droplets flying through the ICP; elements contained in the different droplets respond to such fluctuations similarly[70,71]. The relevant quantitative model remains to be constructed; still, it seems likely that the randomised solution supply to the ICP (as considered in the previous section) is, to some extent, a pre-requisite for the appearance of random noise of this type. Another question immediately arising is whether the random solution supply to the ICP and the desolvation-related fluctuations are the only sources of the excess variance of ICPMS signals.

It is appealing to consider this question in the context of data for gaseous samples, which - theoretically, as well as based on the ICP-AES data mentioned at the beginning of the previous section - ensure a more stable sample introduction process in the ICP and the absence of desolvation related fluctuations. Contrary to the ICP-AES archives, ICPMS experience does not contain fully compelling evidence in this direction. Gray and co-workers compared the precision of the ^{107}Ag/^{109}Ag ratio obtained by solution nebulisation with the precision of the ^{132}Xe/^{129}Xe ratio obtained by the addition of xenon to the sample gas[83]. Using a conventional sampler-skimmer interface, they obtained higher ^{107}Ag/^{109}Ag ratio uncertainties than expected from the ordinary Poisson distribution. On the contrary, the ^{132}Xe/^{129}Xe ratio uncertainty was as predicted by the ordinary Poisson distribution (cf. eqn (25) and (28), see ref. 83 for details). The corresponding xenon signals, integrated over ~70 channels with a dwell time of 100 μs per channel, reached 3.14×10^6 cps[82]. Provided the integrated intensity is obtained by summation of the individual channel intensities, this amounts to 314 counts per peak. Given the quadratic dependence of the excess variance on signal intensity, the excess variance could vanish at these conditions (see refs. 17,77 for examples). Newer ICPMS experiments, albeit not specifically designed to handle uncertainties, do not reveal a large excess variance in ^{129}Xe fluctuations at intensities in the order of $1.5\text{-}1.6\times10^5$ cps (1500-1600 counts / sweep collected in the peak hopping mode); a precise estimation of the variance from the presented data is, however, difficult.

Uncertainty data of varying level of detail can also be found in the rich, but metrologically non-specific literature of chemical vapour generation ICPMS. Some of such data show large excess uncertainties[95-97]. A conclusive analysis of their origin appears to be lacking. As the vapour generation devices can be quite complicated[98,99], the stability of the sample introduction process is sometimes questioned (e.g., pulsation of selenium hydride flow to the ICP[95], carbon monoxide flow rate fluctuations during nickel carbonyl generation[100],). In the ultimate case, solution nebulisation uncertainties are considered as the ‘gold standard’ for comparison with vapour generation ICPMS data![97]

Our ICPMS data on the introduction of xenon- and neon-argon mixtures in the ICP do show excess variance, especially at higher concentrations (Table 3, Electronic Appendix 8). Admittedly, these data are rather precise (compared to average solution nebulisation or laser ablation ICPMS data); but, compared to ordinary Poisson distributed data, they are over-dispersed. Combined with the lithium contaminated interface and the parallel sample introduction system tests described in the previous sections, this allows thinking that processes related to the analyte transfer through the ICP and analyte extraction from the ICP destabilise the primary ion population, thus broadening the statistics of M.

Firstly, there is some evidence that the statistics of M is related to turbulence inside the ICP: using a laminar flow torch seems to reduce the $1/f$ noise component (although it is more efficient in the reduction of discrete frequency components)[22,23,101,102]. Laminar torches are one of the oldest inventions in ICP spectrometry[103]. However, commercial torches used in modern ICPMS are all designed for tangential auxiliary and cool gas injection[104]; thus, it is not excluded that ‘the rotating gas destabilises the injector channel’[23]. Besides, irrespective of the torch design, the ICP flame is thermally heterogeneous[105]: Faraday’s and Lenz’s laws constrain less change in the magnetic flux in the axial zone of the torch, which is consequently less heated by the eddy currents, a phenomenon called skin effect and found in any inductive heater. The injection of a sample aerosol carried by a relatively high velocity sample gas flow can further decrease its temperature. The intermediate, induction zone of the ICP flame is hotter. A turbulent mixing becomes possible inside the torch because of the density difference in the different plasma zones. Precisely evaluating the extent of influence of these processes is difficult at this time; overestimating their role appears inconsistent with the ICP-AES gas injection experiments mentioned in the previous section.

Secondly, instabilities at the boundary of the plasma in contact with the surrounding atmosphere and the ICPMS interface occur; the role of these instabilities was noted for the both laminar[23] and tangential[106] flow torches. In spite of the similarity of processes inside the ICP, the signal extraction mechanisms used in the ICP-AES and ICPMS techniques are different, and being a stable emission source does not *a priori* translate into a stable ion supply to the ion channel of the spectrometer. A100% ion extraction efficiency from the ICP into the sampler orifice is an optimistic estimate. Albeit dependent on the interface design and instrument tuning, it can be significantly less than 100%[107-110], at least for conventional interface pumps rated at 25-35 m^3/h. Photographs of the ICP at the boundary with the interface appear to show partial analyte escape[74,106]. Perhaps, more convincing are photographs of a sampler cone, of which the entire surface was heavily clogged during the analysis of relatively concentrated solutions.[111] At the same time, species from the surrounding atmosphere are present in the ICPMS signal, such as copper evaporated from the load coil (e.g., Elan 6000-series instruments), silver evaporated from the frontal plate surrounding the interface (e.g., Element 2-series instruments) and silicon derived from the walls of the torch and detectable irrespective of the spectral resolution, unless an alumina made torch is used[63,104]. This suggests that the surrounding analyte-free gas, is entrained into the sampler orifice. Besides, some polyatomic interferences, such as the $^{28}N_2^+$ interference on the major ^{28}Si isotope, can partially be explained by the entrainment of the surrounding atmosphere, including air, into the interface[110,112]. Thus, random (but also periodic[106,113]) losses in the ion population supplied by the sample introduction system become possible at the interface because of the mixing between the analyte-bearing and analyte-free gas, depending on how ‘rough’ the mixing process is (Fig. 4). A simplified way to describe the interface-related losses probabilistically is to divide the ICP channel into a number of incremental volumes containing the analyte, supposing that only a fraction of these volumes enters the sampler orifice, while the rest is lost. The corresponding binomial formalism is similar to the binomial description of the droplet selection in a nebuliser-spray chamber setup:

$$M' = \bar{c}' N' ;\ Var(M') = (\bar{c}')^2 \overline{N}' (1 - p') + \bar{c}' \overline{N}' \qquad (37)$$

where *M’* is the number of ions aspirated by the sampler orifice per time interval (analysis), $\bar{c}'$ is the mean number of ions per incremental volume, *N’* is the number of such volumes aspirated by the sampler orifice per analysis, *p’* is the probability that an incremental volume will be aspirated by the sampler. The more homogeneous is the analyte flow to the sampler (smaller increments and, consequently, small $\bar{c}'$) and the higher is the extraction efficiency ($p' \to 1$), the ‘smoother’ is the signal. A diffusional mixing is thus harmless. A mixing controlled by gas flow dynamics, when the neighbour atoms in a given volume of analyte-bearing gas approaching the interface follow the same path and have the same fate - to enter or not to enter the sampler orifice, is not (see eqn 37).

Yet another, more general way to describe the analyte losses and the resulting uncertainty is to invoke the correlation properties of the resulting distribution. This way is also more canonical (see section ‘*Double stochasticity and fluctuations of the rate*’). To be consistent with mathematical texts, we present it here in the notation by Cox and Isham[50]. We divide the total value of *M* in small parts *dM*, each of which corresponding to the number of ions in an incremental volume of plasma aspirated by the sampler during time interval *Δt*. If we consider a large number of small incremental volumes sequentially arriving to the sampler orifice, it is reasonable to think that they are randomly diluted or concentrated in the studied analyte compared to the mean value. This can be due to the mixing in front of the sampler cone and also due to the sample introduction system instability. If the number of ions *dM(t, t+Δt)* in a particular volume observed during the period (*t, t*+Δ*t*) is a random value, the sum *M* of such numbers follows the randomness in *dM(t, t+Δt)* and is also random:

$$\begin{aligned} &Var(M) = Var\{M(0,T)\} \\ &= \sum_{t>0}^{t<T} Var\{dM(t, t+\Delta t)\} + 2\sum_{t>0}^{t<T}\sum_{u>0}^{u<T-t} Cov\{dM(t,t+\Delta t), dM(t+u, t+u+\Delta t')\} \end{aligned} \qquad (38)$$

If there is no mixing in front of the interface, then *dM* remains constant, provided the sample introduction process is stable. If *dM* is constant, the both variance and covariance terms in the right part of eqn (38) are equal to zero and the excess variance vanishes.

It should be noted that the ICPMS literature contains an additional explanation of the extraction related uncertainty. Gray and co-workers[83] admitted the role of sample introduction systems, but supposed that the origin of excess variance of the ICPMS signal can also be related to processes between the sampler and the skimmer[36-39,114]. They did not specify why the ion transmission efficiency inside the zone of silence in front of the skimmer tip is a randomly fluctuating parameter; otherwise, the analysis is reduced to the ordinary Poisson selection and the excess variance vanishes. Still, it is now documented by several independent studies that a disturbance, likely a standing shock wave, is indeed observed at the tip of the skimmer cone[44,115]; experimental or theoretical data explaining its action as a signal randomiser appear to be lacking. Perhaps, this problem merits further investigation (using a *strong* and *stable* ion emitter associated with the *sampler* cone?). Somewhat controversially, the data on gaseous samples provided by Gray and co-workers *themselves* were seemingly devoid of the excess variance, highlighting the role of the sample introduction system, not the interface, in its appearance. Besides, the small sampler orifice diameter (0.2 mm) used in the second series of their experiments allows supposing that the size of the incremental gas volume sampled from the ICP was defined by the sampler orifice, not by the inhomogeneity of the incoming ion flow; hence the dampening of the excess variance even in the presence of an 'aerosol' noise related to the nebulisation of liquid samples (a fairly unusual property!). The negative side of this approach is a huge instrument sensitivity loss[83].

Models reviewed above in this section - instability inside the ICP, destabilisation at the ICP - interface boundary, and fluctuations inside the interface - cover the whole operational sequence of the ICP ion source / first vacuum stage of the interface; they are all invoked to account for the appearance of the excess variance of ICPMS signals in the literature. From a personal standpoint, the authors of this text see fewer inconsistencies in the ICP - interface boundary model, but admit that further studies of the statistical role of the ICP and interface related processes are required.

To summarise, the double stochasticity of ICPMS signals has several potential sources (Table 4), of which noisy operation of the sample introduction system and, probably, the process of ion extraction from the ICP into the interface appear to be the most important at the present knowledge level. It is impressive for the ICP ion source to have two Achilles' heels - sample introduction at the entrance and ion extraction at the exit – and deservedly remain the most versatile and one of the most widely used ion sources in modern inorganic mass spectrometry.

Other *p,M*-conventions: changing the coordinates

The equation $\overline{N} = pM$ for the Poisson mean allows defining p and M arbitrarily. The definition used above in this text seem consistent with our understanding of the ICPMS noise and its sources as it follows from the literature and is reviewed in section '*Fluctuating M, sample introduction process*'. Still, other *p,M*-conventions are possible. For example, it is possible to define M as the number of atoms available for the sample introduction system per time interval (analysis), and p - as the probability for each of these atoms to be registered by the detection system as an ion count. For a homogeneous sample and for a sample introduction system with a constant uptake, M is constant (or, possibly, ordinary Poisson distributed); excess fluctuations during the measurement process are ascribed to p. According to eqn (15), the count number variance is then as follows:

$$Var(N) \approx \overline{\overline{N}} + M^2 Var(p) \qquad (39)$$

We do not see particular advantages of this convention. Below we review a more general representation of the doubly stochastic Poisson process, all particular *p,M*-conventions being its special cases.

Double stochasticity and fluctuations of the rate: an introduction to the existing formalisms

Considering the doubly stochastic Poisson process as a limiting form of the binomial selection complicated by fluctuations of primary ion population (M) and, possibly, transmission efficiency (p) is an elementary and understandable way to describe it. Still, mathematical literature tends to generalise the problem and rarely considers fluctuations in p and M separately[2,5,50]. Instead, it considers fluctuations of the rate $I(t) = pM / \Delta t$, i.e. considers the rate of the Poisson process as a random parameter, since product pM randomly changes. The corresponding formalism is not always intuitively understandable, but needs to be introduced here for two reasons: (i) the parameter observed in ICPMS measurements is the rate and not the individual statistics of p and M, (ii) a powerful mathematical apparatus describing connections between fluctuations and correlation of the rate is available. A disadvantage of introducing this formalism is that the individual uncertainty sources are, to some extent, obliterated.

A Poisson count rate can be defined for each time interval Δt. It is generally different for the different time intervals, though in the limit we will assume it constant within an interval:

$$I(t) = pdM(t,t+\Delta t)/\Delta t = \overline{dN(t,t+\Delta t)}/\Delta t \qquad (40)$$

Besides, a mean rate $\overline{I(t)}$ can be defined by averaging the individual rates above; for a non-transient signal, it corresponds to the mean rate for an individual interval, as it is calculated from a replicate series of such intervals. Using the same approach as in eqn (38), defining integral as the limit of a sum and applying the general formula for the variance of a sum of random variables, we obtain [ref. 50, sections 2.5 and 3.3]:

$$Var(N) = Var\{N(0,T)\} = \int_0^T Var\{dN(t,t+\Delta t)\} + 2 \iint\limits_{\substack{0<t<T \\ 0<u\le T-t}} Cov\{dN(t,t+\Delta t), dN(t+u,t+u+\Delta t')\}$$

(41)

Henceforth, we assume that the studied signal is stationary (non-transient), simplifying the derivations. As $\Delta t \to 0$, $dN(t,t+\Delta t)$ can be considered as a variable taking only the values zero or one, with the probability to obtain one being equal to $\overline{I(t)}\Delta t$ [5,50]. It then follows[50] from the variance definition that

$$Var\{dN(t,t+\Delta t)\} = \overline{I(t)}\Delta t \qquad (42)$$

Besides,

$$Cov\{dN(t,t+\Delta t), dN(t+u,t+u+\Delta t')\} = \left\{\overline{I(t)}h(u) - \overline{I(t)}^2\right\}\Delta t\Delta t' \qquad (43)$$

where *h(u)* is conditional intensity for the time interval $(t+u, t+u+\Delta t')$ equal to the probability to get one count during this interval, provided one count was already recorded in the interval $(t, t+\Delta t)$[50]. Reorganising formula (41), we obtain:

$$\begin{aligned} Var\{N(0,T)\} &= \int_0^T \overline{I(t)}\,dt + 2\int_0^T\int_0^{T-t} \left\{\overline{I(t)}h(u) - \overline{I(t)}^2\right\} du\,dt \\ &= \overline{I(t)}T + 2\overline{I(t)}\int_0^T (T-u)h(u)\,du - \overline{I(t)}^2T^2 = \overline{\overline{N}} + 2\overline{I(t)}\int_0^T (T-u)h(u)\,du - \overline{\overline{N}}^2 \end{aligned} \qquad (44)$$

This equation can be re-written by expressing the conditional intensity *h(u)* via the autocovariance function $\gamma(u)$[50]:

$$h(u) = \overline{I(t)} + \gamma(u)/\overline{I(t)}\ ;\ Var\{N(0,T)\} = \overline{\overline{N}} + 2\int_0^T (T-u)\gamma(u)\,du \qquad (45)$$

Two other equivalent expressions for the total count variance can be given in terms of the autocorrelation function[2] and pair-correlation function[116], respectively. The autocovariance function $\gamma(u)$ is linked to the autocorrelation function $\rho(u)$ as follows[2]:

$$\gamma(u) = Var(I(t))\rho(u) \qquad (46)$$

Accordingly, introducing the autocorrelation function in equation (44) yields[2]:

$$Var\{N(0,T)\} = \overline{\overline{N}} + 2Var(I(t))\int_0^T (T-u)\rho(u)\,du \qquad (47)$$

The pair-correlation function $\eta(u)$ is linked to the conditional intensity *h(u)* as follows[116]:

$$h(u) = \overline{I(t)}(1+\eta(u)) \qquad (48)$$

Introducing the pair-correlation function in equation (44) yields[116]:

$$Var\{N(0,T)\} = \overline{\overline{N}} + 2\overline{I(t)}^2\int_0^T (T-u)\eta(u)\,du \qquad (49)$$

Formulae above for the description of the excess variance are all derived from formula (41) using three different but closely related tools (conditional intensity, autocovariance, autocorrelation and pair-correlation function) to describe correlation in the signal. If there is no such correlation, the autocorrelation function is zero and the excess variance vanishes (ordinary Poisson noise). In the presence of such a correlation, it could be interesting to track a link existing between the autocorrelation function and the spectral density of the power spectrum. It is described by the Wiener-Khinchin-Einstein theorem. Considering the corresponding mathematical apparatus in detail extends beyond the scope of this text. Still, here we will make some remarks. According to the Wiener-Khinchin-Einstein theorem[20],

$$S(f)=\int_{-\infty}^{+\infty}\rho(u)\cos(2\pi fu)\,du \qquad (50)$$

where $S(f)$ is the power spectral density of the signal, f is frequency, $\rho(u)$ is the autocorrelation function, and u is correlation time, as above. In one of the very first articles showing relationships between the low-frequency noise in ICP signals and the process of sample introduction, Antanavičius et al. argued: ‘If the radiating particles are generated by droplet evaporation, they are correlated for some time’[68]. Indeed, if the rate of the Poisson process fluctuates, for example because more or less droplets (especially of a large size, see section ‘*Fluctuating M, sample introduction system*’) reach the ICP per time interval, then a high count rate at the beginning of a period of high ‘ion number density in the plasma’[70] means that somewhere within this period the rate will also be high, hence a rate correlation within this period. Time resolved ICP studies show that such periods are short and change rapidly (small u); beyond such a period, we can assume that $\rho(u)$ limits to zero. Thus, the integration interval in eqn (50) can be reduced from (-∞;+∞) to a narrow range around zero. In this range, at low frequencies, the product of angular frequency ($2\pi f$) and correlation time (u) is small, which maximises the cosine term in the integrated expression and, accordingly, increases the spectral density (see ref. 20, chapter I, for a similar example from the field of power engineering).

Concluding remarks and outlook

In ICPMS, ‘transmission efficiency‘ and ‘transport efficiency’ are frequently used terms. It is important to recognise that a transmission efficiency is a probability by itself, which allows using the mathematical apparatus of the binomial selection for the interpretation of the signal uncertainty.

The ICPMS signal in its general form represents a doubly stochastic Poisson process, with an excess variance inherent to such processes. An excess variance often appears if a non-stationary random parameter is involved in the generation of a probability distribution. Analytical chemistry offers other examples illustrating this, such as the non-stationary blank (sample) and the non-stationary relative sensitivity factor. If the true mass of an analyte fluctuates in a series of blank solutions (e.g., vials containing them were variably contaminated), and the mass measurement technique is imprecise, then the total uncertainty of the measured analyte mass in a randomly selected blank is a combination of the both uncertainties above; it is higher than the mass measurement uncertainty alone[117]. The same applies to random changes of the sample mass consumed per measurement in a series of replicate analyses, especially if adding a controlled amount of internal standard does not seem feasible[94,118]. A more distant example concerns the determination of the relative sensitivity factor[119] (mass discrimination, ‘mass bias’) in LA-ICPMS[17,27,54,55,120] and secondary ion mass spectrometry[121-124]. This factor is often obtained by the (replicate) analysis of one single standard, the uncertainty of its mean value decreasing indefinitely with increasing the number of replicates. Then, it can happen that the relative sensitivity factor as determined from the standard yields inaccurate sample concentration ratios[125,126]. This situation can be considered from several standpoints. A statistician might argue that standards should represent a random selection of samples to be analysed and that the uncertainty of the above factor could be determined by the analysis of several standards and subsequent linear regression[127-130] of their concentration vs. intensity ratios. This uncertainty will generally be larger compared to a single-standard calibration, as the natural matrix-dependent variability of the relative sensitivity factor is accounted for. An ‘inaccurate’ sample concentration ratio becomes accurate, but less precise, once the total uncertainty of the relative sensitivity factor is propagated. In short, it is essential to recognise randomness in a statistics-generating parameter that, in the simplest form, is considered constant (refining the measurement technique in quest for its constancy being a parallel approach).

Understanding the ICPMS signal as a doubly stochastic Poisson process is causal and not symptomatic. For example, it is possible to apply a goodness-of-fit test to a distribution of sweep intensities and then to apply the Gauss confidence limits to the mean intensity obtained from this distribution, provided the distribution is approximately Gaussian according to the goodness-of-fit test[55]. An uncertainty value is the only result of this approach; we still do not understand why the signal fluctuates as it does. The doubly stochastic model reveals the source and propagation mechanism of the noise.

A qualitative understanding of the individual components of this model has been around for a while. It is appropriate here to return to the work by Gray *et al.*[83], who noted: (i) 'It has long been accepted that the precision of isotope ratio measurements by inductively coupled plasma mass spectrometry (ICP-MS) is poorer than consideration of counting statistics would suggest is possible'; (ii) 'One component of the random noise…is what may be termed the ion distribution noise. This is caused by the inhomogeneous spatial distribution of analyte ions in the central channel of the plasma which carries the sample aerosol…'. 'The plasma actually fluctuates around the sampling orifice', add Niu and Houk[38]. Important studies to this end by Olesik and co-workers were already given credit above in this text. It follows that a doubly stochastic Poisson distribution is encountered, with the precision *being in agreement* with the counting statistics constrained by this distribution, as discussed in this work.

It should be admitted that an analysis given in this work is conditional in several respects. For example, we assumed for simplicity that the detection is carried out in the counting regime. In the literature of mass spectrometry and its uncertainties, this assumption is handled as follows. For a Faraday cup, a potential difference between the ground and the cup is usually measured using a high ohmic resistor and then converted to current according to Ohm's law. This electronic current compensates the current of positive ions incident on the Faraday cup. This current can be converted into count rate by dividing by q_e=1.60210x10^{-19} C(=A x s)[27,46,131]. For a secondary electron multiplier operated in the analog mode, the current amplified by the analog stage of the multiplier is significantly higher than for a Faraday cup; it is converted into count rate using the detector cross calibration coefficient(s). From a statistical standpoint, this approach combines at least three types of uncertainties: (i) fluctuations in the number of ions arriving to the multiplier, (ii) fluctuations of the output current of the analog stage of the multiplier, (iii) measurement uncertainty of the current to voltage converter, the uncertainties (ii,iii) being superimposed on (i). We feel that the corresponding analysis lies beyond the scope of this text. Some relevant explanations and formulae can be found in ref. 46; further research is warranted.

Besides, we assumed that analyte *ions* and analyte *atoms* are statistically interchangeable terms, i.e. that ionisation process in the ICP does not randomise the population of analyte ions excessively. This point is not particularly important for elements that are ~100% ionised in the ICP; there are many of them[132,133]. For elements with a low degree of ionisation, this point invokes a binomial selection model: an ion in front of the sampler is considered as a result of binomial selection from the population of atoms supplied by the sample introduction system at a given probability of ionisation. If this probability is fixed (or deterministic, i.e., it does not change randomly with time), then the number of ions obtained from a fixed number of analyte atoms is binomially distributed. According to the binomial selection theorem, this does not introduce an excess variance in the distribution of counted ions[5]. At this time, we are unaware of data confirming a random behaviour of the probability of ionisation. Besides, neon injection experiments do no show systematically larger variances compared to xenon, in spite of the very different degree of ionisation of these elements (Table 3, Electronic Appendix 6).

We also postulated the same transmission efficiency p for all ions moving across the section of the sampler orifice. This is not exactly true: ions from the outer part of the ion beam have fewer chances to enter the skimmer orifice[134]. The same applies to droplets belonging the peripheral part of the aerosol cone inside a double pass spray chamber and removed from the aerosol flow through impacts with the inner barrel of the chamber[85]. It is possible to account for these effects by changing the *p,M*-convention, by defining $\overline{N} \equiv \int p(dM)\,dM$ or by deriving the excess variance through fluctuations of the rate (see previous section). Future research will assume increased complexity, but will benefit in terms of correctness, if deterministic changes in transmission (transport) efficiency are accounted for.

For uncertainty derivations, we assumed a zero dead time in the counting detection regime. The influence of the dead time related count losses on the Poisson distribution and its uncertainty has been discussed in the literature for a while; count numbers recorded in the presence of a dead time have somewhat less variance than predicted by the ordinary Poisson process[135-137]. Perhaps, this auxiliary aspect is worth a more thorough consideration in the ICPMS literature; nevertheless, it seems that a more general concern regarding the dead time correction of ICPMS signals exists. An interesting by-product of the double stochasticity is the compromised adequacy of formulae (6) for dead time correction. The derivation of these formulae[1,6,18] implies the same count rate during the period of actual counting and the period when the detection system is 'dead', thus restricting their application to the ordinary Poisson process. In a doubly stochastic Poisson process, periods of higher and lower rate change rapidly, and the first ion detected during a period of high rate prevents the registration of other ions arriving during this period (during a part of it covered by the dead time). The result is an intensity underestimation if formulae (6) are applied and the true dead time is used. The corresponding mathematical formalism can be found in refs. 116,138,139; it is not always easy to implement in practice. If formulae (6) are still employed[40,140-144], it is a good approach to avoid high intensity signals collection in the counting mode, since the double stochasticity is more marked at high intensities and the signal – less 'diluted' (higher chances for an ion or ions to fall within the dead time interval). This practice is encountered in some high accuracy isotope ratio ICPMS methods[55,145], where signals are collected in the 'forced' analog regime even if the upper intensity limit of the counting regime set by the instrument manufacturer is occasionally not reached (the analog signal does not have a dead time). A related approach is to set the upper intensity limit for the counting regime at a rather small value much lower than the counting saturation limit; ICPMS manufacturers usually implement this approach in their instruments. Yet another solution is to avoid applying the dead time correction to the mean intensity for the whole signal duration, or to the mean intensities of sweeps collected using a long dwell time; a very short dwell time, during which the rate does not change much, could be more adequate in this context. Finally, maintaining a sort of matching between the sample measurement setup (including intensities and their uncertainty) and that used to estimate the dead time during the instrument tuning can sometimes be feasible; on the contrary, determining the dead time based on relatively precise signals obtained using a 'smoothly' operating nebuliser and applying this dead time to significantly more disturbed data, such as some laser ablation ICPMS signals, might be imprudent. Approximately matching intensities of the analyte and the internal standard in an attempt to maintain a 1:1 ratio between them can also be recommended. A future study detailing the extent of the problem and providing a more thorough analysis of possible solutions seems to be warranted.

Finally, we decided to omit the problematics of very weak Poisson distributed ICPMS signals containing few counts per analysis. In the context of ideas reviewed above in this text, these problematics are trivial. The corresponding Poisson distributions show virtually no excess variance, since excess variance scales in quadrature with decreasing M, while the number of counts scales linearly. Nevertheless, such a triviality can be misleading. The mathematical apparatus required for the description and, particularly, for the comparison of two near-zero Poisson signals is not simple. The problem is related to the pronounced discreteness and skewness of the Poisson distribution for very small count numbers. Albeit the corresponding standard deviation values are still easy to estimate ($s(N)=\sqrt{N}$), assigning Gaussian confidence limits to these values is impossible. One analytically important aspect of this problem concerns the calculation of the critical value for detection decision ('detection limit' in the currently prevailing ICPMS terminology), especially in the framework of paired measurements (each sample acquisition is preceded by a background acquisition, e.g., in LA-ICPMS). *Is the analyte detected at a given confidence level, if the background contains one count and the signal - four counts?* And if that background would contain zero counts? Modern ICPMS instruments with their curved ion channels supress the photon noise[38,40]; setting a correct discriminator threshold minimises the internal noise of the secondary electron multiplier[40,45]; the gas blank is clean for most mass-to-charge ratios. Thus, obtaining a near-zero background reading in the context of our exercise is a common practice (uranium and the lanthanides being typical examples). Interestingly, the question posed above has for the first time been answered in 1940, in a - now canonical - article that, at first glance, belongs to agricultural research[7]. Much more has been done since then, including newer and more powerful tests for the equality of two Poisson means[8,9] and formulae for the detection limit with fast convergence to normality[10-12]. We refer the reader to the corresponding sources; this is an other case when a practically important question does not receive a straightforward empirical solution and invokes basic research.

Two obvious and complementary directions of further development in the area of the Poisson modelling of ICPMS signals are (i) study of the double stochasticity with the aim to minimise it by instrumental measures (sample introduction system and ICP-interface region, the randomising role of the latter being rather obscure at this time) to remove adverse effects associated with it, such as the precision loss due to excess variance and impact on the dead time determination and correction; (ii) mathematical description of the key parameters (rate and its correlation) associated with the double stochasticity to enable modelling the excess variance, if it is not removed by instrumental measures; the corresponding tools, such as the Kalman filter, will hopefully be considered in future ICPMS research.

Acknowledgements

A.U. thanks Olga Ulianova for her help during the preparation of the manuscript. We are grateful to an anonymous colleague who drove our attention to the role of the sample introduction system in the primary ion population statistics and to the rich experimental literature on these problematics. We thank two anonymous reviewers for their helpful and constructive comments. Thanks also go to Detlef Günther and Henry Longerich for discussions at an early stage of work on the manuscript and to Lothar Rottmann for consultations regarding the spectrometer construction. Besides, we gratefully acknowledge the editorial handling of the manuscript by Frank Vanhaecke. This contribution was presented during the Winter Conference on Plasma Spectrochemistry 2014. It was supported by grants Nr. 200021_138004/1 and 206021-117405 (R'EQUIP) from the Swiss National Science Foundation.

References

1 G.F. Knoll, *Radiation detection and measurement*, John Wiley & Sons, New York, 2nd edn, 1989, p. 754.
2 D.R. Cox and P.A.W. Lewis, *The statistical analysis of series of events*, Methuen&Co., London, 1968, p. 285.
3 W. Feller, *An introduction to the probability theory and its applications, volume I*, John Wiley & Sons, New York, 3rd edn, 1968, p. 528.
4 N.L. Johnson and S. Kotz, *Discrete distributions*, John Wiley & Sons, New York, 1969, p. 328.
5 H.H. Barrett and K.J. Myers, *Foundations of Image Science*, John Wiley & Sons, Hoboken, New Jersey, 2004, p. 1540.
6 L.J. Rainwater and C.S. Wu, Applications of probability theory to nuclear particle detection, Nucleonics, 1947, **1**, 60-69.
7 J. Przyborowski and H. Wilenski, Homogeneity of results in testing samples from Poisson series, *Biometrika*, 1940, **31**, 313-323.
8 K. Krishnamoorthy and J. Thomson, A more powerful test for comparing two Poisson means, *J. Stat. Plan. Inf.*, 2004, **119**, 23-35.
9 H.K.T. Ng, K. Gu and M.L. Tang, A comparative study of tests for the difference of two Poisson means, *Comp. Stat. Data Anal.*, 2007, **51**, 3085-3099.
10 L. Currie, On the detection of rare, and moderately rare, nuclear events, *J. Radioanal. Nucl. Chem.*, 2008, **276**, 285-297.
11 D.J. Strom and J.A. MacLellan, Evaluation of eight decision rules for low-level radioactivity counting, *Health Phys.*, 2001, **81**, 27-34.
12 MARLAP Multi-Agency Radiological Laboratory Analytical Protocol Manual, vol. 19-20, 2004.
13 M. Tanner, Shorter signals for improved signal to noise ratio, the influence of Poisson distribution, *J. Anal. At. Spectrom.*, 2010, **25**, 405–407.
14 T. Pettke, F. Oberli, A. Audétat, M. Guillong, A.C. Simon, J.J. Hanley and L.M. Klemm, Recent developments in element concentration and isotope ratio analysis of individual fluid inclusions by laser ablation single and multiple collector ICP-MS, *Ore Geol. Rev.*, 2012, **44**, 10-38.
15 W.L. Nicholson, Fixed time estimation of counting rates with background corrections. AEC R&D Report HW-76279, Hanford Works, Richland, Washington, 1963.
16 W.L. Nicholson, Statistics of net-counting-rate estimation with dominant background corrections, *Nucleonics*, 1966, **24**, 118-121.
17 Y. Luo, S. Gao, H.P. Longerich, D. Günther, S. Wunderli, H.L. Yuan and X.-M. Liu, The uncertainty budget of the multi-element analysis of glasses using LA-ICP-MS, *J. Anal. At. Spectrom.*, 2007, **22**, 122-130.
18 W.R. Leo, *Techniques for Nuclear and Particle Physics Experiments: A How-To Approach*, Springer-Verlag, Berlin-Heidelberg, 2nd edn, 1994, p. 378.

19 G.P. Tolstov, *Fourier series*, Dover Publications, 1976, p. 352.

20 G.M. Jenkins and D.G. Watts, *Spectral analysis and its applications*, Holden-Day, San Francisco, 1969, p. 525.

21 R.M. Belchamber and G. Horlick, Noise-power spectra of optical and acoustic emission signals from an inductively coupled plasma, *Spectrochim. Acta, Part B*, 1982, **37**, 17-27.

22 J. Davies and R.D. Snook, Studies of a low-noise laminar flow torch for inductively coupled plasma atomic emission spectrometry. Part 1. Fundamental characteristics, *J. Anal. At. Spectrom.*, 1986, **1**, 195-201.

23 J. Davies and R.D. Snook, Studies of a low-noise laminar flow torch for inductively coupled plasma atomic emission spectrometry. Part 2. Noise power studies and interference effects, *J. Anal. At. Spectrom.*, 1987, **2**, 27-31.

24 J.S. Crain, R.S. Houk and D.E. Eckels, Noise power spectral characteristics of an inductively coupled plasma-mass spectrometer, *Anal. Chem.*, 1989, **61**, 606-612.

25 N. Furuta, C.A. Monnig, P. Yang and G.M. Hieftje, Noise characteristics of an inductively coupled plasma-mass spectrometer, *Spectrochim. Acta, Part B*, 1989, **44**, 649-656.

26 P.K. Appelblad, I. Rodushkin and D.C. Baxter, Sources of uncertainty in isotope ratio measurements by inductively coupled plasma mass spectrometry, *Anal. Chem.*, 2001, **73**, 2911-2919.

27 D.C. Baxter, I. Rodushkin and E. Engström, Isotope abundance ratio measurements by inductively coupled plasma-sector field mass spectrometry, *J. Anal. At. Spectrom.*, 2012, **27**, 1355–1381.

28 E.D. Prudnikov and Y.S. Shapkina, Random errors in analytical methods, *Analyst*, 1984, **109**, 305-307.

29 E.D. Prudnikov and R.M. Barnes, Theoretical calculation of the standard deviation in inductively coupled plasma mass spectrometry, *J. Anal. At. Spectrom.*, 1999, **14**, 27-31.

30 E.D. Salin and G. Horlick, Signal-to-noise performance characteristics of an inductively coupled plasma, *Anal. Chem.*, 1980, **52**, 1578-1582.

31 M.P. Goudzwaard and M.T.C. de Loos-Vollebregt, Characterisation of noise in inductively coupled plasma – atomic emission spectrometry, *Spectrochim. Acta, Part B*, 1990, **45**, 887-901.

32 W. Compston, Geological age by instrumental analysis: The 29th Hallimond lecture, *Mineral. Mag.*, 1999, **63**, 297-311.

33 B.L. Sharp, Pneumatic nebulisers and spray chambers for inductively coupled plasma spectrometry. A review. Part 1. Nebulisers. *J. Anal. At. Spectrom.*, 1988, **3**, 613-652.

34 R. Campargue, High intensity supersonic molecular beam apparatus, *Rev. Sci. Instrum.*, 1964, **35**, 111–112.

35 J.H. Moore, C.C. Davis, M.A. Coplan and S.C. Greer, *Building Scientific Apparatus*, Cambridge University Press, 4th edn, 2009, p. 658.

36 D.J. Douglas, Fundamental aspects of inductively coupled plasma mass spectrometry, in *Inductively Coupled Plasmas in Analytical Atomic Spectrometry*, ed. A. Montaser and D.W. Golightly, VCH Publishers, New York, 2nd edn, 1992, pp. 613-650.

37 D.J. Douglas and J.B. French, Gas dynamics of the inductively coupled plasma mass spectrometry interface, *J. Anal. At. Spectrom.*, 1988, **3**, 743-747.

38 H. Niu and R.S. Houk, Fundamental aspects of ion extraction in inductively coupled plasma mass spectrometry, *Spectrochim. Acta, Part B*, 1996, **44**, 779-815.

39 M. Liezers, Sampling interface design and function, Ion extraction and focusing, in *ICP Mass Spectrometry Handbook*, ed. S.M. Nelms, Blackwell Publishing, Oxford UK, 2005, pp. 10-25.

40 N. Jakubowski, T. Prohaska, L. Rottmann and F. Vanhaecke, Inductively coupled plasma- and glow discharge plasma-sector field mass spectrometry, *J. Anal. At. Spectrom.*, 2011, **26**, 693-726.

41 G.M. Hieftje, Towards the next generation of plasma source mass spectrometers. Plenary lecture, *J. Anal. At. Spectrom.*, 1992, **7**, 783-790.

42 R. Thomas, Practical Guide to ICP-MS: A Tutorial for Beginners, CRC Press, 3rd edn, 2013, p. 446.

43 R.S. Houk, S.C.K. Shum and D.R. Wiederin, Frontiers in elemental analysis by mass spectrometry, *Anal. Chim. Acta*, 1991, 250, 61-70.

44 H. Niu and R.S. Houk, Langmuir probe measurements of the ion extraction process in inductively coupled plasma mass spectrometry – I. Spatially resolved determination of electron density and electron temperature. *Spectrochim. Acta, Part B*, 1994, **12-14**, 1283-1303.

45 H. Longerich, Laser ablation – inductively coupled plasma – mass spectrometry (LA-ICP-MS); An Introduction, in *Laser Ablation ICP-MS in the Earth Sciences: Current Practices and Out-*

standing Issues, ed. P. Sylvester, Mineralogical Association of Canada Short Course Series, Vancouver, BC, 2008, vol. 40, pp. 1-18.

46 K. Hunter and R. Stresau, Ion detection, in *ICP Mass Spectrometry Handbook*, ed. S.M. Nelms, Blackwell Publishing, Oxford UK, 2005, pp. 117-146.

47 A. Montaser, M.G. Minnich, J.A. McLean, H. Liu, J.A. Caruso and C.W. McLeod, Sample introduction in ICPMS, in *Inductively Coupled Plasma Mass Spectrometry*, ed. A. Montaser, Wiley-VCH, New York, 1998, pp. 83-264.

48 J.S. Becker and H.-J. Dietze, Inorganic trace analysis by mass spectrometry, *Spectrochim. Acta, Part B*, 1998, **53**, 1475–1506.

49 F.A. Haight, *Handbook of the Poisson distribution*, John Wiley & Sons, New York, 1967, p. 168.

50 D.R. Cox and V. Isham, *Point processes*, London-New York-Washington, Chapman & Hall, 1980, p. 188.

51 D.R. Cox, Some statistical methods connected with series of events, *J. R. Stat. Soc.*, *Series B*, 1955, **17**, 129-164.

52 S.A. Myers and D.H. Tracy, Improved performance using internal standardization in inductively-coupled plasma emission spectroscopy, *Spectrochim. Acta, Part B,* 1983, **38**, 1227-1253.

53 J. Meija and Z. Mester, Signal correlation in isotope ratio measurements with mass spectrometry: Effects on uncertainty propagation, *Spectrochim. Acta, Part B,* 2007, **62**, 1278-1284.

54 C.M. Fisher, H.P. Longerich, S.E. Jackson and J.M. Hanchar, Data acquisition and calculation of U–Pb isotopic analyses using laser ablation (single collector) inductively couple plasma mass spectrometry, *J. Anal. At. Spectrom.*, 2010, **25**, 1905-1920.

55 A. Ulianov, O. Müntener, U. Schaltegger and F. Bussy, The data treatment dependent variability of U-Pb zircon ages obtained using mono-collector, sector field, laser ablation ICPMS, *J. Anal. At. Spectrom.*, 2012, **27**, 663-676.

56 A. Ulianov and O. Müntener, Differencing as a method to estimate the uncertainty of a transient LA-ICPMS signal, *J. Anal. At. Spectrom.*, 2014, **29**, 934-940.

57 K.G. Heumann, S.M. Gallus, G. Rädlinger and J. Vogl, Precision and accuracy in isotope ratio measurements by plasma source mass spectrometry, *J. Anal. At. Spectrom.*, 1998, **13**, 1001-1008.

58 F. Vanhaecke, L. Balcaen and D. Malinovsky, Use of single-collector and multi-collector ICP-mass spectrometry for isotopic analysis, *J. Anal. At. Spectrom.*, 2009, **24**, 863-886.

59 R.C. Ogliore, G.R. Huss, and K. Nagashima, Ratio estimation in SIMS analysis, *Nucl. Instr. Meth. Phys. Res., Sect. B.*, 2011, **269**, 1910-1918.

60 I.S. Begley and B.L. Sharp, Occurrence and reduction of noise in inductively coupled plasma mass spectrometry for enhanced precision in isotope ratio measurement, *J. Anal. At. Spectrom.*, 1994, **9**, 171-176.

61 F. Vanhaecke, L. Moens, R. Dams and P. Taylor, Precise measurement of isotope ratios with a double-focusing magnetic sector ICP mass spectrometer, *Anal. Chem*., 1996, **68**, 567-569.

62 S.M. Eggins and J.M.G. Shelley, *Geostand. Geoanal. Res.*, 2002, **26**, 269-286.

63 D.C. Baxter, I. Rodushkin and E. Engström, Sources of contamination and remedial strategies in the multi-elemental trace analysis laboratory, *Anal. Bioanal. Chem.*, 2010, **396**, 365-377.

64 S.A. Myers and D.H. Tracy, Sources of noise and drift in ICP emission, *7th Annual Meeting FACSS*, Philadelphia, 1980, Abstract No. 5, *ICP Information Newslett*., 1980, **6**, 233.

65 S.A. Myers, D.H. Tracy and R.D. Ediger, Studies of cross-flow nebulisers, *International Winter Conference on Developments in Atomic Plasma Spectrochemical Analysis*, San Juan, Puerto Rico, 1980, Abstract No. 62, *ICP Information Newslett*., 1980, **6**, 366-368.

66 R. Antanavičius, P. Serapinas and P. Šimkus, Manifestation of the entering of a substance into an RF-discharge plasma in its radiation noise, *Opt. Spektrosk.* (USSR), 1987, **63**, 224-225.

67 R. Antanavičius, E. Nashlenas and P. Serapinas, Measurement of the radiation noise of an RF-discharge plasma with a disperse phase, *Opt. Spektrosk.* (USSR), 1989, **67**, 280-285.

68 R. Antanavičius, P. Serapinas and P. Šimkus, Observation of the frequency dependence of ICP radiation noise, *J. Phys. D: Appl. Phys.*, 1989, **22**, 254-257.

69 A. Montaser, I. Ishii, H. Tan, R.H. Clifford and D.W. Golightly, Noise power spectra comparing He and Ar ICP discharges, *Spectrochim. Acta, Part B*, 1989, **44**, 1163-1169.

70 J.W. Olesik, L.J. Smith and E.J. Williamsen, Signal fluctuations due to individual droplets in inductively coupled plasma atomic emission spectrometry. *Anal. Chem.*, 1989, **61**, 2002-2008.

71 S.E. Hobbs and J.W. Olesik, Inductively coupled plasma mass spectrometry signal fluctuations due to individual aerosol droplets and vaporizing particles, *Anal. Chem.*, 1992, **64**, 274-283.

72 J.W. Olesik, Investigating the fate of individual sample droplets in inductively coupled plasmas, *Appl. Spectrosc.*, 1997, **51**, 158A-175A.

73 J.W. Olesik, J.A. Kinzer and G.J. McGowan, Observation of atom and ion clouds produced from single droplets of sample in inductively coupled plasmas by optical emission and laser-induced fluorescence imaging, *Appl. Spectrosc.*, 1997, **51**, 607-616.

74 R.K. Winge, J.S. Crain and R.S. Houk, High speed photographic study of plasma fluctuations and intact aerosol particles in inductively coupled plasma mass spectrometry, *J. Anal. Atom. Spectrom.*, 1991, **6**, 601-604.

75 R.S. Houk, R.K. Winge and X. Chen, High speed photographic study of wet droplets and solid particles in the inductively coupled plasmas, *J. Anal. Atom. Spectrom.*, 1997, **12**, 1139-1148.

76 I. Horn and D. Günther, The influence of ablation carrier gases Ar, He and Ne on the particle size distribution and transport efficiencies of laser ablation-induced aerosols: implications for LA-ICP-MS, *Appl. Surf. Sci.*, 2003, **207**, 144-157.

77 D.B. Aeschliman, S.J. Bajic, D.P. Baldwin and R.S. Houk, High-speed digital photographic study of an inductively coupled plasma during ablation: comparison of dried solution aerosols from a microconcentric nebulizer and solid particles from laser ablation, *J. Anal. At. Spectrom.*, 2003, **18**, 1008-1014.

78 T. Hirata and Z. Miyazaki, High-speed camera imaging for laser ablation process: for further reliable elemental analysis using inductively coupled plasma-mass spectrometry, *Anal. Chem.*, 2007, **79**, 147-152.

79 D.C. Perdian, S.J. Bajic, D.P. Baldwin and R.S. Houk, Time-resolved studies of particle effects in laser ablation inductively coupled plasma-mass spectrometry. Part I. Investigation of nanosecond and femtosecond pulse width lasers and devices for particle size selection, *J. Anal. At. Spectrom.*, 2008, **23**, 325-335.

80 I. Horn, Comparison of femtosecond and nanosecond laser interactions with geological matrices and their influence on accuracy and precision of LA-ICP-MS data, in *Laser Ablation ICP-MS in the Earth Sciences: Current Practices and Outstanding Issues*, ed. P. Sylvester, Mineralogical Association of Canada Short Course Series, Vancouver, BC, 2008, vol. 40, pp. 53-65.

81 A. Tunheng and T. Hirata, Development of signal smoothing device for precise elemental analysis using laser ablation-ICP-mass spectrometry, *J. Anal. At. Spectrom.*, 2004, **19**, 932-934.

82 A. Montaser, M.G. Minnich, H. Liu, A.G.T. Gustavsson and R.F. Browner, Fundamental aspects of sample introduction in ICP spectrometry, in *Inductively Coupled Plasma Mass Spectrometry*, ed. A. Montaser, Wiley-VCH, New York, 1998, pp. 335-420.

83 A.L. Gray, J.G. Williams, A.T. Ince and M. Liezers, Noise sources in inductively coupled plasma mass spectrometry: an investigation of their importance to the precision of isotope ratio measurements, *J. Anal. At. Spectrom.*, 1994, **9**, 1179-1181.

84 N.A. Panichev, Q. Ma, R.E. Sturgeon, C.L. Chakrabarti and V. Pavski, Condensation of analyte vapor species in graphite furnace atomic absorption spectrometry, *Spectrochimica Acta, Part B*, 1999, **54**, 719-731.

85 S. Okabayashi, S. Sakata and T. Hirata, Isotopic analysis of nano-gram amounts of tungsten using electrothermal vaporization (RTV)-MC-ICPMS technique, *44th Lunar and Planetary Science Conference*, The Woodlands, Texas, 2013, Abstract No. 1911.

86 J.-L. Todoli and J.-M. Mermet, Liquid sample introduction in ICP spectrometry: A practical guide, Elsevier, 2008, p. 300.

87 M. Hamester, D. Wiederin, J. Wills, W. Kerl and C.B. Douthitt, Strategies for isotope ratio measurements with a double focusing sector field ICP-MS, *Fresenius J. Anal. Chem.*, 1999, **364**, 495-497.

88 M. Krachler, N. Rausch, H. Feuerbacher and P. Klemens, A new HF-resistant tandem spray chamber for improved determination of trace elements and Pb isotopes using inductively coupled plasma-mass spectrometry. *Spectrochimica Acta, Part B*, 2005, **60**, 865-869.

89 J.A. McLean, M.G. Minnich, L.A. Iacone, H. Liu and A. Montaser, Nebulizer diagnostics: fundamental parameters, challenges, and techniques on the horizon, *J. Anal. At. Spectrom.*, 1998, **13**, 829-842.

90 L.D. Landau and E.M. Lifshitz, *Course of theoretical physics, vol. 5, Statistical physics, part I*, Pergamon Press, 3rd edn, 1980, p. 387.

91 N.J. Johnson, A.W. Kemp and S. Kotz, *Univariate discrete distributions*, Wiley-Interscience, 3rd edn, 2005, p. 672.

92 W. Doherty, Non-linear signal response functions and their effects on the statistical and noise cancellation properties of isotope ratio measurements by multi-collector plasma mass spectrometry, *Spectrochim. Acta, Part B*, 2013, **85**, 78-92.

93 S.E. Maestre, J.L. Todolí and J.M. Mermet, Evaluation of several pneumatic micronebulizers with different designs for use in ICP–AES and ICP–MS. Future directions for further improvement, *Anal. Bioanal. Chem.*, 2004, **379**, 888-899.

94 M.J. Chang, J.D. Naworal, K. Walker and C.T. Connell, Investigations on the direct introduction of cigarette smoke for trace elements analysis by inductively coupled plasma mass spectrometry, *Spectrochim. Acta*, *Part B*, 2003, **58**, 1979-1996.

95 S.J. Christopher, S.E. Long, M.S. Rearick and J.D. Fassett, Development of isotope dilution cold vapour inductively coupled plasma mass spectrometry and its application to the certification of mercury in NIST standard reference materials, *Anal. Chem.*, 2001, **73**, 2190-2199.

96 D. Layton-Matthews, M.I. Leybourne, J.M. Peterc and S.D. Scott, Determination of selenium isotopic ratios by continuous-hydridegeneration dynamic-reaction-cell inductively coupled plasma-mass spectrometry, *J. Anal. At. Spectrom*., 2006, **21**, 41–49.

97 C. Zheng, L. Yang, R.S. Sturgeon and X. Hou, UV photochemical vapour generation sample introduction for determination of Ni, Fe, and Se in biological tissue by isotope dilution ICPMS, Anal. Chem., 2010, **82**, 3899-3904.

98 P. Wu, L. He, C. Zheng, X. Hou and R.E. Sturgeon, Application of chemical vapour generation in non-tetrahydroborate media to analytical atomic spectrometry, *J. Anal. At. Spectrom*., 2010, **25**, 1217–1246.

99 Z. Long, Y. Luo, C. Zheng, P. Deng and X. Hou, Recent advance of hydride generation–analytical atomic spectrometry: Part I-technique development, *Appl. Spectrosc. Rev*., 2012, **47**, 382-413.

100 C.J. Park and S.A. Yim, Determination of nickel in water samples by isotope dilution inductively coupled plasma mass spectrometry with sample introduction by carbonyl vapor generation, *J. Anal. At. Spectrom*., 1999, **14**, 1061–1065.

101 J. Davies and R.D. Snook, Low-noise laminar flow torch for inductively coupled plasma atomic-emission spectrometry, *Analyst*, 1985, **110**, 887-888.

102 N.N. Sesi, P.J. Galley and G.M. Hieftje, Evaluation of a linear-flow torch for inductively coupled plasma atomic emission spectrometry, *J. Anal. At. Spectrom.*, 1993, **8**, 65-70.

103 R.H. Wendt and V.A. Fassel, Induction-coupled plasma spectrometric excitation source, *Anal. Chem.*, 1965, **37**, 920-922.

104 I.L. Turner and A. Montaser, Plasma generation in ICPMS, in *Inductively Coupled Plasma Mass Spectrometry*, ed. A. Montaser, Wiley-VCH, New York, 1998, pp. 265-334.

105 N. Furuta, Spatial profile measurement of ionization and excitation temperatures in an inductively coupled plasma, *Spectrochim. Acta, Part B*, 1985, **40**, 1013-1022.

106 A.T. Ince, J.G. Williams and A.L. Gray, Noise in inductively coupled plasma mass spectrometry: some preliminary measurements, *J. Anal. At. Spectrom.*, 1993, **8**, 899-903.

107 F. Vanhaecke, R. Dams and C. Vandecasteele, 'Zone model' as an explanation for signal behaviour and non-spectral interferences in inductively coupled plasma mass spectrometry, *J. Anal. At. Spectrom.*, 1993, **8**, 433-438.

108 L. Flamigni, J.Koch and D. Günther, Experimental and theoretical investigations about the vaporization of laser-produced aerosols and individual particles inside inductively-coupled plasmas - Implications for the extraction efficiency of ions prior to mass spectrometry, *Spectrochim. Acta, Part B,* 2012, **76**, 70-76.

109 M. Aghaei, L. Flamigni, H. Linder, D. Günther and A. Bogaerts, Occurrence of gas flow rotation motion inside the ICP torch: a computational and experimental study, *J. Anal. At. Spectrom.*, 2014, **29**, 249-261.

110 D. Günther, H.P. Longerich, S.E. Jackson and L. Forsythe, Effect of sampler orifice diameter on dry plasma inductively coupled plasma mass spectrometry (ICP-MS) backgrounds, sensitivities, and limits of detection using laser ablation sample introduction, *Fresenius J. Anal. Chem.*, 1996, **355**, 771-773.

111 Solution mode ICPMS, http://www.jsg.utexas.edu/icp-ms/solution, consulted on the 24th of August 2014.

112 N.M. Reed, R.O. Cairns, R.C. Hutton and Y. Takaku, Characterization of polyatomic ion interferences in inductively coupled plasma mass spectrometry using a high resolution mass spectrometer *J. Anal. At. Spectrom.*, 1994, **9**, 881-896.

113 R.K. Winge, D.E. Eckels, E.L. DeKalb and V.A. Fassel, Spatiotemporal characteristcs of the Inductively coupled plasma, *J. Anal. At. Spectrom.*, 1988, **3**, 849-855.

114 D.J. Douglas and S.D. Tanner, Fundamental considerations in ICPMS, in *Inductively Coupled Plasma Mass Spectrometry*, ed. A. Montaser, Wiley-VCH, New York, 1998, pp. 615-679.

115 N. Taylor and P.B. Farnsworth, Experimental characterization of the effect of skimmer cone design on shock formation and ion transmission efficiency in the vacuum interface of an inductively coupled plasma mass spectrometer, *Spectrochim. Acta*, *Part B*, 2012, **69**, 2-8.

116 M.L Larsen and A.B. Kostinski, Simple dead-time corrections for discrete time series of non-Poisson data, *Meas. Sci. Technol.*, 2009, **20**, paper 095101.

117 A. Ulianov, M. Honisch and O. Müntener, Calculating the net activity uncertainty if the background includes a nonstationary component, *Anal. Chem.*, 2013, **85**, 2589-2594.

118 M.J. Chang, J.D. Naworal and C.T. Connell J. Direct introduction of cigarette smoke for puff-by-puff trace metals analysis by inductively coupled plasma mass spectrometry, *J. Anal. At. Spectrom.*, 2006, **21**, 574–581.

119 F.L. King, J. Teng and R.E. Steiner, Glow discharge mass spectrometry: trace element determination in solid samples, *J. Mass. Spectrom.*, 1995, **30**, 1061-1075.

120 H.P. Longerich, S.E. Jackson and D. Günther, Laser ablation inductively coupled plasma mass spectrometric transient signal data acquisition and analyte concentration calculation, *J. Anal. At. Spectrom.*, 1996, **11**, 899-904.

121 A. Benninghoven, F.G. Rüdenauer and H.W. Werner, *Secondary ion mass spectrometry: basic concepts, instrumental aspects, applications and trends*, John Wiley & Sons, New York, 1987, p. 1227.

122 W. Compston, I.S. Williams and C. Meyer, U-Pb geochronology of zircon from lunar breccia 73217 using a sensitive high mass-resolution ion microprobe, *J. Geophys. Res.*, 1984, **89**, B525-B534.

123 J.M. Eiler, C.M. Graham and J.M. Valley, SIMS analysis of oxygen isotopes: matrix effects in complex minerals and glasses, *Chem. Geol.*, 1997, **138**, 221-244.

124 L.R. Riciputi, B.A. Paterson and R.L. Ripperdan, Measurement of light stable isotope ratios by SIMS: matrix effects for oxygen, carbon, and sulphur isotopes in minerals, *Int. J. Mass Spectrom.*, 1998, **178**, 81-112.

125 U. Klötzli, E. Klötzli, Z. Günes and Kosler, J. Accuracy of laser ablation U-Pb zircon dating: Results from a test using five different reference zircons. *Geostand. Geoanal. Res.*, 2009, **33**, 5-15.

126 E. Marillo-Sialer, J. Woodhead, J. Hergt, A. Greig, M. Guillong, A. Gleadow, E. Evans and C. Paton, The zircon ‘matrix effect’: evidence for an ablation rate control on the accuracy of U-Pb age determinations by LA-ICP-MS, *J. Anal. At. Spectrom.*, 2014, **29**, 981–989.

127 W.A. Fuller, *Measurement Error Models.* John Wiley & Sons, New York, 1987, p. 440.

128 D. Gujarati, *Basic Econometrics*, The McGraw-Hill Companies, 4th edn, 2004, p. 1002.

129 J.G. Eisenhauer, Regression through the origin, *Teaching Statistics* 2003, 76-80.

130 J.-M. Mermet, Quality of calibration in inductively coupled plasma atomic emission spectrometry, *Spectrochim. Acta, part B*, 1994, 49, 1313-1324.

131 K. Habfast, Advanced isotope ratio mass spectrometry I: Magnetic isotope ratio mass spectrometers, in *Modern isotope ratio mass spectrometry*, ed. I.T. Platzner, Wiley, New York, 1997, ch. 3, pp. 11-82.

132 R. S. Houk, Mass spectrometry of inductively coupled plasmas, *Anal. Chem.*, 1986, 58, 97A-105A.

133 A.A. Pupyshev, V.N. Muzgin and A.K. Lutsak, Thermochemical processes and ion transport in inductively coupled plasma mass spectrometry: theoretical description and experimental confirmation, *J. Anal. At. Spectrom.*, 1999, **14**, 1485–1492.

134 J.H. Macedone, D.J. Gammon and P.B. Farnsworth, Factors affecting the analyte transfer through the sampling orifice of an inductively coupled plasma mass spectrometer, *Spectrochim. Acta, Part B*, 2001, **56**, 1687-1695.

135 J.W. Müller, Counting statistics of a Poisson process with dead time, BIMP report 111, 1970, 14 p.

136 W.L. Smith, Renewal theory and its ramifications, *J.R. Stat. Soc., Series B*, 1958, **20**, 284-302.
137 G. Vannucci and M.C. Teich, Dead-time-modified photocount mean and variance for chaotic radiation, *J. Opt. Soc. Am.*, 1981, **71**, 164-170.
138 G. Vannucci and M.C. Teich, Effects of rate variations on the counting statistics of dead-time-modified Poisson processes, *Opt. Comm.*, 1978, **25**, 267-272.
139 M.D. Srinivas, Measurements and quantum probabilities, Universities Press (India) Ltd., Hyderabad, 2001, p. 272.
140 A. Held and P.D.P. Taylor, A calculation method based on isotope ratios for the determination of dead time and its uncertainty in ICP-MS and application of the method to investigating some features of a continuous dynode multiplier, *J. Anal. At. Spectrom.*, 1999, **14**, 1075-1079.
141 S.M. Nelms, C.R. Quétel, T. Prohaska, J. Vogl and P.D.P. Taylor, Evaluation of detector dead time calculation models for ICP-MS, *J. Anal. At. Spectrom.*, 2001, **16**, 333-338.
142 H. Rameback, M. Berglund, D. Vendelbo, R. Wellum and P.D.P. Taylor, On the determination of the true dead-time of a pulse-counting system in isotope ratio mass spectrometry, *J. Anal. At. Spectrom.*, 2001, **16**, 1271-1274.
143 J. Vogl, Calibration strategies and quality assurance, in *ICP Mass Spectrometry Handbook*, ed. S.M. Nelms, Blackwell Publishing, Oxford UK, 2005, pp. 147-181.
144 U. Nygren, H. Ramebäck, M. Berglund and D.C. Baxter, The importance of a correct dead time setting in isotope ratio mass spectrometry: implementation of an electronically determined dead time to reduce measurement uncertainty, *Int. J. Mass Spec.*, 2006, **257**, 12-15.
145 D. Frei and A. Gerdes, Precise and accurate *in situ* U–Pb dating of zircon with high sample throughput by automated LA-SF-ICP-MS, *Chem. Geol.*, 2008, **261**, 261-270.

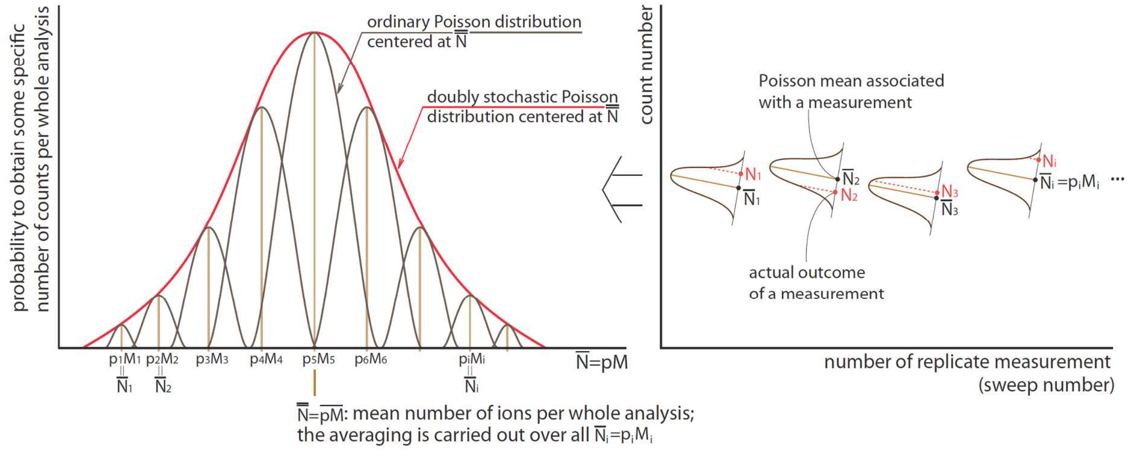

Fig. 1. A schematic probability distribution of a doubly stochastic Poisson process as a blend of many individual Poisson processes, each of them having its own mean $\overline{N_i} = p_iM_i$ and variance $\sqrt{\overline{N}_i}$ and contributing a count number value, randomly positioned around $\overline{N}_i$, to the mixed probability distribution of the doubly stochastic process. Two statistics arise: (i) statistics of the random count number values, as measured; (ii) underlying statistics of the mean count number values, which are not directly accessible. In time-resolved ICPMS applications, this implies that a (hidden) mean count number vs. sweep pattern underlies the observed count number vs. sweep pattern. In strong signals, the two patterns almost coincide: in such signals, the ordinary Poisson scattering is insignificant compared to the scattering of the Poisson means (in other words, compared to the excess variance; see text for further explanations). In weak signals, the mean count number pattern is almost constant; the ordinary Poisson scattering dominates. There are at least two tools to reconstruct the hidden pattern - scaling the observed pattern of a strong signal obtained simultaneously with a weaker signal on a multi-collector spectrometer (to obtain the mean count number pattern of the weaker signal) and using the Kalman filter; discussing these tools in detail lies beyond the scope of this text.

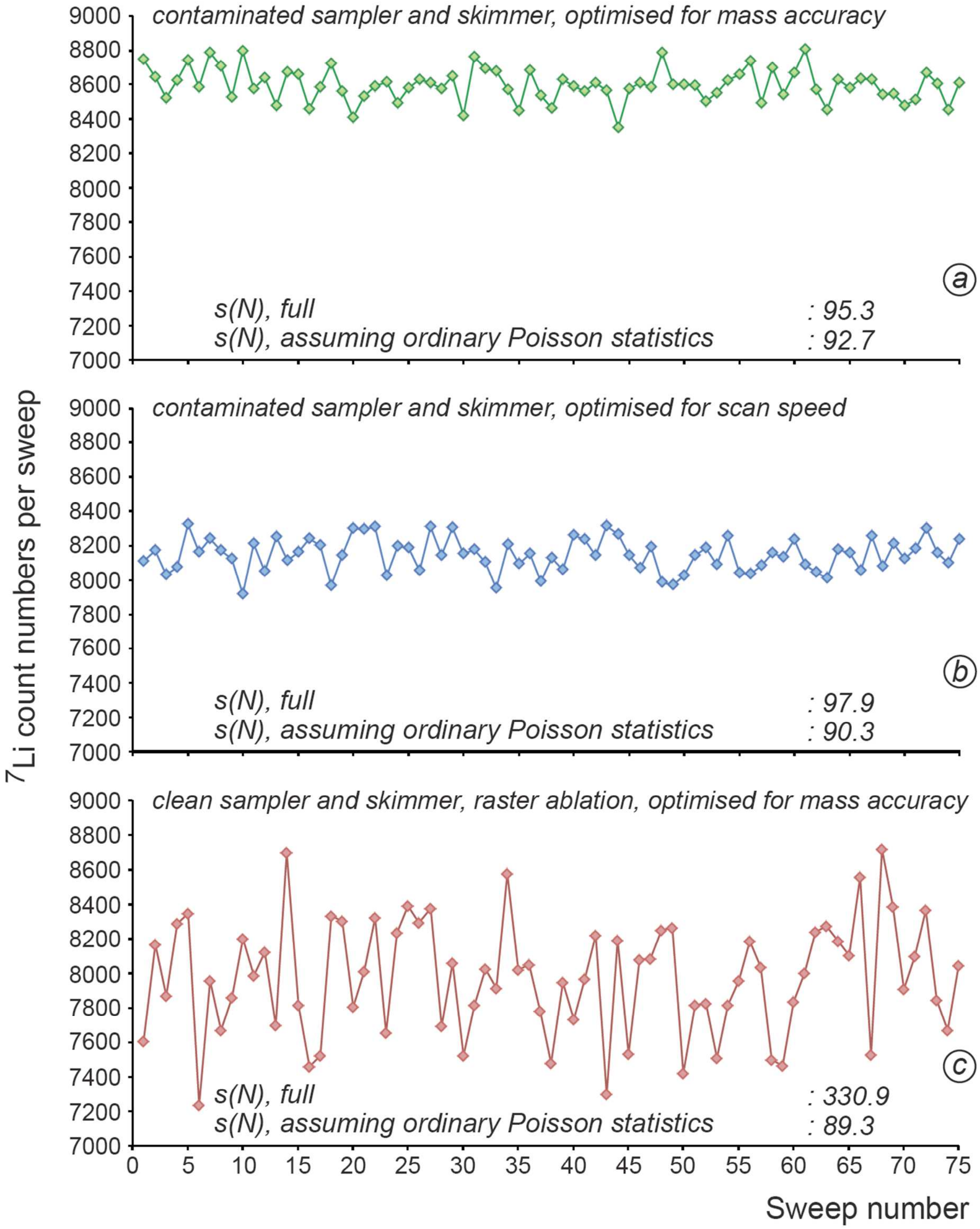

Fig. 2. Count vs. sweep number statistics for lithium. (a-b) ^{7}Li background noise related to the contamination of the sampler and skimmer cones of an Element XR sector-field ICPMS. (c) ^{7}Li signal obtained by the raster laser ablation of a NIST SRM 612 glass using the same ICPMS equipped with clean sampler and skimmer cones [see Electronic Appendix 4 for experimental conditions and section '*Sources of double stochasticity, experimental constraints; Fluctuating p?*' for discussion].

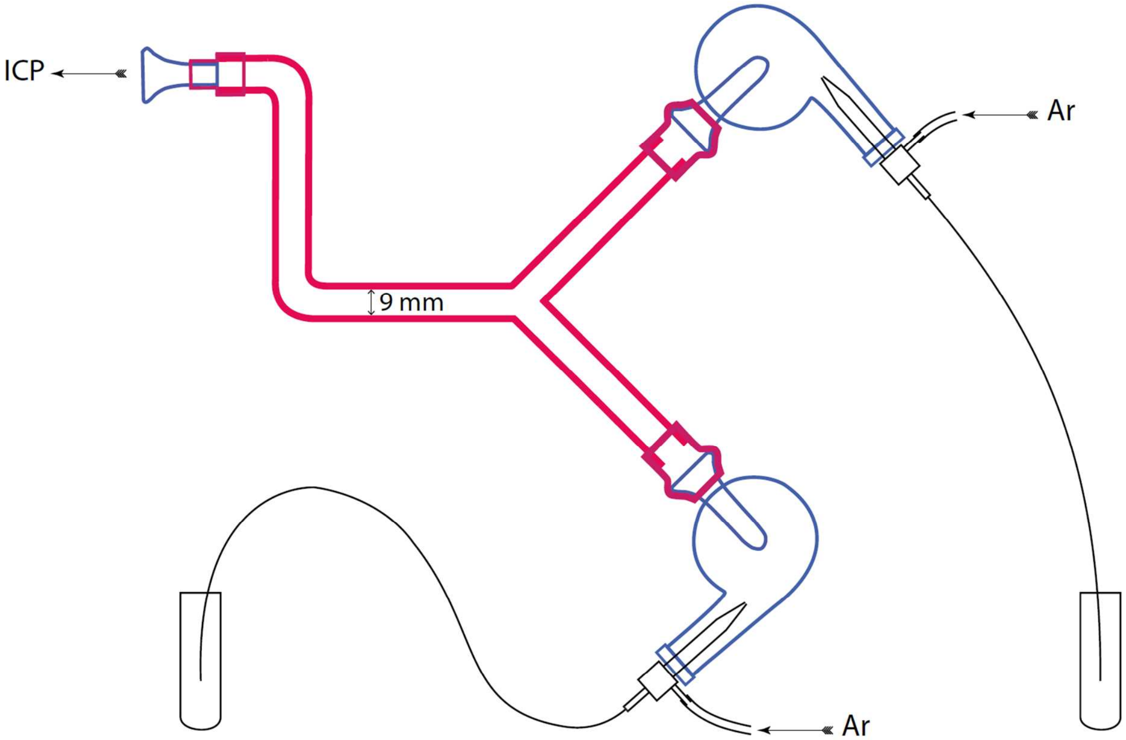

Fig. 3. A schematic arrangement of the test of two independent parallel sample introduction systems; the droplet selection takes plays in the spray chambers only, no precipitates in the connecting tubing were observed [for details, see Table 2 and section ‘*Fluctuating M, sample introduction system*’].

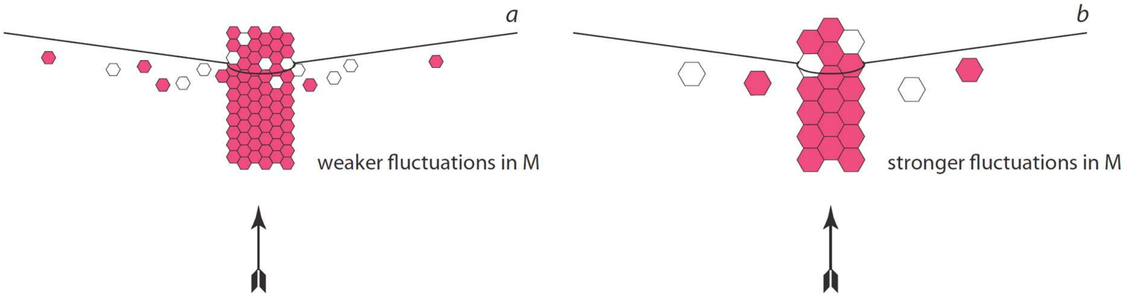

Fig. 4. A schematic illustration of the mixing process in front of the sampler cone [for details, see section ‘*Fluctuating M, transfer of analyte inside the ICP and from the ICP to the mass spectrometer*’].

Table 3. Statistics obtained by the analysis of argon-xenon and argon-neon mixtures using an Element XR sector-field ICPMS. In experiments with xenon, 40 to 160 ml/min of Ar-Xe mixture containing 100 ppb(v) of xenon was added to the sample argon gas. In experiments with neon, pure neon gas was added. For details on experimental conditions and for raw data and calculus, see Electronic Appendix 8.

addition to the sample argon flow, ml/min	mean count number per sweep	ordinary Poisson standard deviation (s(N)=√N)	full standard deviation, as measured
^{129}Xe			
40	14730	121.4	245.5
60	22777	150.9	363.3
80	30733	175.3	502.1
100	39069	197.7	613.2
120	47090	217.0	753.4
140	55127	234.8	870.8
160	62716	250.4	1017.2
^{130}Xe			
40	2294	47.9	63.1
60	3545	59.5	87.3
80	4772	69.1	107.7
100	6067	77.9	128.7
120	7315	85.5	143.7
140	8573	92.6	172.7
160	9775	98.9	186.8
^{132}Xe			
40	15302	123.7	265.3
60	23625	153.7	367.9
80	31833	178.4	524.9
100	40455	201.1	625.9
120	48730	220.7	788.3
140	56961	238.7	917.2
160	64824	254.6	1057.6
^{22}Ne			
40	19417	139.3	297.4
60	30299	174.1	429.4
80	41318	203.3	553.1
100	52756	229.7	623.8
120	64381	253.7	747.6
140	76212	276.1	910.7
160	87857	296.4	964.7

Table 4. Sources of excess variance of the ICPMS signal.

source	anticipated importance	experimental support	theoretical model	selected references
fluctuations of the rate of analyte supply to the ICP related to the operation of the sample introduction system	important, but sample introduction system specific	fluctuations of the aerosol density supplied to the ICP by the sample introduction system, as documented by laser light scattering; fluctuations of the signal intensity associated with the arrival of larger droplets in the ICP	$Var(M^*) = (\bar{c}^*)^2 \overline{N}^* (1-p^*) + \bar{c}^* \overline{N}^*$ $Var(N) = \overline{\overline{N}} + p^2 Var(M)$	[52,64-83]
fluctuation of the analyte (ion) content because of the changes of the ICP temperature during the desolvation of droplets	possibly important, especially for solution nebulisation techniques	correlated response of the ICP signals during the dual nebuliser test at a small distance from the load coil; positive fluctuations of the analyte and H-bearing molecular ions in the presence of a vaporising droplet	$Var(N) = \overline{\overline{N}} + M^2 Var(p)$ as a general model	[70,71]
fluctuations of the analyte content in the ICP channel because of the destabilising action of the surrounding gas	of low importance, or insufficiently studied	less noise in the ICPMS signal observed using laminar flow torches	$Var(M') = (\bar{c}')^2 \overline{N}' (1-p') + \bar{c}' \overline{N}'$ $Var(N) = \overline{\overline{N}} + p^2 Var(M)$	[22,23, 101,102]
fluctuations of the analyte content during the extraction of ions at the boundary between the ICP and interface	possibly important	optical observations showing the instable behaviour of the ICP flame at the boundary with the interface	idem	[23,106]
fluctuations of ion transmission efficiency during the extraction of ions inside the interface, between sampler and skimmer	insufficiently studied	a disturbance, probably - a standing shock wave documented at the tip of the skimmer cone	$Var(N) = \overline{\overline{N}} + M^2 Var(p)$ as a general model	[44,83, 115]
fluctuations of ion transmission efficiency during the extraction of ions from the interface and their transport to the detector	seem to be of low importance, provided a modern instrument is used at low resolution	peak position changing over a series of repetitive measurements	idem	merely a general belief